IMMUNOLOGICAL AND HEMOSTATIC RESPONSES
TO VENTRICULAR ASSIST DEVICE SUPPORT

by

Joshua Ryan Woolley

B.S. Mechanical Engineering, Geneva College, 2003

Submitted to the Graduate Faculty of

Swanson School of Engineering in partial fulfillment

of the requirements for the degree of

Doctor of Philosophy

University of Pittsburgh

2014

UNIVERSITY OF PITTSBURGH

SWANSON SCHOOL OF ENGINEERING

This dissertation was presented

by

Joshua Ryan Woolley

It was defended on

March 20, 2014

and approved by

James Antaki, PhD

Professor, Departments of Biomedical Engineering and Computer Science, Carnegie Mellon University;

Professor, Departments of Bioengineering and Surgery, University of Pittsburgh

Harvey Borovetz, PhD

Robert L. Hardesty Professor, Department of Surgery; Professor, Departments of Bioengineering and

Chemical and Petroleum Engineering, University of Pittsburgh

Robert Kormos, MD, FRCS(C), FACS, FAHA

Professor, Department of Cardiothoracic Surgery, University of Pittsburgh; Director, Artificial Heart

Program, and Co-Director, Heart Transplantation, UPMC

Peter Wearden, MD, PhD

Surgical Director, Pediatric Heart and Lung Transplantation, and Director, Pediatric Mechanical

Cardiopulmonary Support Program, Children's Hospital of Pittsburgh; Assistant Professor, Department of

Cardiothoracic Surgery, University of Pittsburgh

Dissertation Director: William Wagner, PhD,

Professor, Departments of Surgery, Bioengineering and Chemical Engineering, and Director, McGowan

Institute for Regenerative Medicine, University of Pittsburgh

IMMUNOLOGICAL AND HEMOSTATIC RESPONSES

TO VENTRICULAR ASSIST DEVICE SUPPORT

Joshua Ryan Woolley, PhD

University of Pittsburgh, 2014

Ventricular assist devices (VADs) are critical in the treatment of advanced heart failure, but continue to be plagued by infection, bleeding and thrombosis. Immunity may be affected by VADs, though most paradigms were developed in older-generation pumps and may not currently be applicable. Similarly, hemostasis and platelets may be impacted by device type, though the patient's health may also influence outcomes. Temporal immune cell activation and thrombosis biomarkers levels were evaluated across several contemporary pumps. This relationship was further studied in vitro through development of a method for visualizing cellular deposition onto opaque materials. An improved understanding of the cellular effects of VADs was sought through a comparative evaluation of these pumps, and this understanding may aid in the development of predictive indices of adverse events and influence future device design.

Patients implanted with a currently-utilized VAD did not experience changes to adaptive immunity reported with previous-generation devices. However, infection was still an ongoing risk for these patients. Further investigation found the impact of VADs on immunity was greater than that of similar surgeries, especially among innate immunity. Granulocyte activation was elevated following VAD implantation, and was significantly pronounced in one model, suggesting an influence of design on immune cells. Granulocyte activation promotes extravasation and apoptosis, suggesting a pathway for decreased cellular immunity.

Pre-operative hepatic dysfunction had immediate and long lasting hemostatic effects on VAD patients. Model for End-stage Liver Disease (MELD) score was found to be a positive pre-operative predictor of post-implant bleeding, blood product consumption and elevation of thrombosis biomarkers. MELD score was also found to be a stronger predictor of immediate post-operative bleeding than device type, underscoring the importance of patient pre-operative health on post-operative outcomes.

With this difficult hemostatic environment, improvement of the blood-contacting surfaces of rotary VADs may reduce complications. A flow chamber for real-time visualization of platelet deposition onto surfaces of opaque VAD materials under physiologically-relevant conditions was developed. This was accomplished through the novel combination of fluorescently-marked platelet-rich-plasma and translucent hemoglobin-depleted red blood cells. This method enables the hemocompatibility assessment of a wide range of implantable materials.

TABLE OF CONTENTS

LIST OF TABLES

LIST OF FIGURES

PREFACE

The Lord is my strength and my shield;

My heart trusts in him, and I am helped.

My heart leaps for joy, and I will give thanks to him in song.

Psalm 28:7

I received a tremendous amount of help while working on this dissertation research. It is with much gratitude to a great many people that this work was completed. I hope that at some point I may be able to repay even a fraction of the goodwill, kindness and collegiality I experienced during my career in Pittsburgh.

It is with sincere gratitude that I thank Dr. William R. Wagner for his patience and persistence as my dissertation advisor. His casual, constant excellence inspired and motivated me to improve my own work ethic. While many of my graduate courses were excellent for my development as a student, none were as instructive or as lasting as the discussions held in Dr. Wagner's office. His guidance in all aspects of this dissertation research was thorough, thoughtful and abundant.

To my committee members Dr. Harvey Borovetz, Dr. James Antaki, Dr. Robert Kormos and Dr. Peter Wearden, I am tremendously grateful. It was Dr. Borovetz who first encouraged me to enter into this program. He also helped see me through by providing me with wonderful guidance in both academic and professional arenas. I will miss the meetings in Dr. Antaki's office when I would be pleasantly overwhelmed with knowledge and creativity as he provided assistance in overcoming obstacles in my progress. I would often spend days afterwards

processing his ideas and visions. Dr. Kormos was invaluable as a mentor in my clinical research, providing clear and direct analysis of complex clinical situations. His depth and breadth of knowledge of the field was humbling and inspiring. I owe gratitude to Dr. Peter Wearden for his energy and kindness during the many pre-clinical studies in which we participated. His patient instruction helped me to develop the research techniques and analysis that were necessary to complete this work.

Many other professors and academic staff were extremely helpful in assisting me with various aspects of this dissertation research. Dr. Sanjeev Shroff deserves special recognition for allowing me to participate as a trainee in his excellent and prestigious Cardiovascular Bioengineering Training Program, as this program afforded me many opportunities for collaboration and friendship among peers and advisors. I am indebted to Dr. Marina Kamineva for both her very knowledgeable guidance, and for her kindness. She was always a source of encouragement when I needed it most. I owe gratitude to the patient instruction of Dr. Vera Donnenberg, Dr. William Federspiel, and Dr. Richard Koepsel. Daniel McKeel rescued my research with innovative solutions more times than I can list. Sujatha Raghu was extremely helpful in coordinating the patient studies and providing statistical expertise. I am also grateful to the co-authors on my publications for providing their expertise and time, which include Dr. Wagner, Dr. Kormos, Dr. Jeffery Teuteberg, Dr. Christian Bermudez, Dr. Jay Bhama, Kathleen Lockard and Nicole Kunz.

I owe gratitude to the many past and present members of the Wagner Lab. Dr. Trevor Snyder was instrumental in my development early in my graduate career. He patiently taught me how to conduct proper research, and many of his musings during evening experiments were the seeds for future publications and research. Dr. Sang Ho Ye was a great friend, teacher and

and efficient manner. Much of this work would not have been possible without his generous assistance. I also owe gratitude to Kuan-Chieh Chen and Carnegie Mellon University's Center for Bioimage Informatics.

I owe thanks and appreciation to my colleagues and the patients of the Artificial Heart Program (AHP) at UPMC. Stephen Winowich and Dr. Richard Schaub deserve special recognition for their many contributions to my work and to my development as a professional. My interest in ventricular assist device research was a direct result of their involvement and support. Many of my experiences as an engineer at AHP provided the enthusiasm and energy necessary to continue my research in the lab. My participation with AHP was deeply satisfying and rewarding during a period that was often punctuated by difficulty and discouragement. I also owe appreciation to the rest of my colleagues at AHP, including Donald Severyn, Douglas Lohmann, Genevieve O'Shea, and Erin Driggers. The nurses at AHP also deserve gratitude as they were very much involved in my research by providing patient consents, clinical expertise and manuscript preparation, and include Kathleen Lockard, Nicole Kunz, and Ashley Wimer.

I owe gratitude to my family members for all of their support and prayer. To my parents, Ronald and Sally Woolley, I am always indebted. Their constant love, prayers, support and guidance helped me to persevere during challenging times. They instilled in me from an early age the curiosity and appetite for truth that is necessary for research work. I also would not have been able to persevere without support from Dale and Chantal Kennedy. Their prayers on my behalf and words of affirmation were a great encouragement to me. I also owe gratitude for the support and prayers that I received over the years from Jon and Julie Woolley, Ryan and Rachel Ely, Joel Kennedy and Kevin and Rachel Kennedy. Their love and prayers helped sustain me during difficult times.

To my lovely and loving wife, Danila Nadine Woolley, no amount of gratitude is sufficient. This work would not have been possible without her love, support and prayers. Her enthusiasm and interest in my work multiplied times of enjoyment and satisfaction, while her encouragement and steadfastness divided my distress during times of difficulty. I often marveled at her understanding and patience during my frequent late nights and long hours in the lab or at the hospital. I am so very thankful for the many times she offered prayers and petitions of supplication on my behalf. Her tireless work in all other areas of our life provided me with the time and freedom necessary to complete this dissertation research. Thank you for your love, patience and sacrifice. This work is dedicated to you.

1.0   INTRODUCTION

1.1   SIGNIFICANCE

(Note: A majority of this chapter was previously published as: Woolley JR, Kormos RL, Wagner WR. Biologic responses to the interface between device and circulation. In:Kormos RL, Miller LW, editors. Mechanical circulatory support: a companion to Braunwald's heart disease. Philadelphia: Elsevier; 2012. p. 249-257.)

Left Ventricular Assist devices (VADs) present a unique challenge for blood biocompatibility from other medical devices in that blood contacts a large surface area with complex flow fields for an extended period of time. Other chronic devices such as stents or grafts may have surface areas that are orders of magnitude smaller with favorable flow conditions, while similar-sized devices, such as membrane oxygenators, are intended for acute use in the presence of substantial anticoagulation. In contrast, a VAD patient's blood must come in extensive contact with artificial surfaces for months or years while simultaneously being weaned to the lowest allowable levels of anticoagulation preferable for chronic use. In light of these challenging circumstances, it is not surprising that many of the biological complications such as thrombosis, thromboembolism and bleeding encountered with the first implants with this technology are still problematic today. These complications contributed to a dampening of the initial enthusiasm for application of these devices to heart failure patients, and remain problematic for clinicians and device designers.[1,2]

1

The first VADs mimicked the biphasic flow of the natural heart and served as effective bridges to transplant for heart failure patients waiting for donor organs.[3] The volume displacement required for pulsatile flow made these VADs large in size, preventing implant in smaller patients. The introduction of rotary blood pumps decreased the size and power requirements and increased the mechanical life of VADs, expanding the size of eligible patient population and increasing their overall quality of life.[4] The use of sophisticated computational fluid dynamic modeling programs and the utilization of magnetic levitation to eliminate bearings improved the blood path through the pumps, helping to improve hemocompatibility. However, even with these technological advancements, all VAD patients are still vulnerable to hemostasis problems such as thrombosis, thromboemboli, and bleeding.[5,6]

1.2   SURVEY OF THROMBOSIS AND BLEEDING COMPLICATIONS IN THE SETTING OF VENTRICULAR ASSIST DEVICES

Thromboembolic rates in VAD patients can be difficult to define and compare, with reported rates varying substantially between specific VADs and institutions. Early reports and investigational device studies may have different levels of reporting that could distort cross-comparisons. For example, Goldstein et al combined "embolic stroke, transient ischemic attack, and peripheral embolism" into one parameter of "thromboembolic event"[7]; in contrast, Miller et al report separately on ischemic stroke, hemorrhagic stroke, transient ischemic attack, "other neurologic" and "peripheral nonneurologic thromboembolic event".[4] The combination of careful assessment of potential thromboembolic events together with standardization of these methods and reporting across centers was needed to provide a better framework for comparative

studies between devices and patient management protocols. A related situation was found in the reporting of bleeding rates.[4,8]

Given this need, the Interagency Registry for Mechanically Assisted Circulatory Support (INTERMACS©), a voluntary national patient registry for FDA-approved devices, was formed as a centralized source for various VAD implant information including detailed adverse event definitions and rates. INTERMACS also provides standardized definitions for suspected neurological or bleeding events.[9] (**Figure 1.1**) In addition to reporting each adverse event, institutions participating in INTERMACS must provide information on aspects surrounding the event, such as date and location of patient during onset, contributing factors, event type and severity, anticoagulation therapy, and mortality, among other details.[9] Based on these definitions, INTERMACS investigators reported in 2008 that 18% of VAD patients experience neurologic dysfunction and 35% have bleeding complications (420 patients).[10] An update of this report reveals actuarial freedom from stroke to be 89%, 83% and 81% for implant years 1, 2 and 3 respectively (N=5366; continuous flow VADs only). When the rate of neurologic dysfunction was separated by pulsatile and continuous flow devices, pulsatile LVAD patients experienced a significantly higher adverse event rate of 3.81 compared to continuous flow patients at 1.83 (events/100 patient-months in the first 12 months of implantation; pulsatile LVAD N = 594, continuous flow LVAD N = 5358). The same comparison of patients found bleeding adverse event rates were higher in pulsatile LVAD patients than continuous flow LVADs (17.28 v 9.45, respectively).[6] Additionally, biventricular support presents an especially challenging situation as twice the artificial surface is implanted into typically the sickest of VAD patients. INTERMACS reported in 2009 substantially higher bleeding rates for pulsatile biventricular support compared to only LVAD support (55% vs. 35%); interestingly, neurologic

complications are slightly lower for biventricular support (16% vs. 18%), illustrating the challenge clinicians face in attempting to predict risk factors for adverse events (465 LVADs, 128 BiVADs).[11] Recent data reveals that actuarial freedom from infection, bleeding event, stroke, device malfunction or death to be much lower in BiVAD patients compared to continuous flow LVADs (14 vs 30% respectively at 12 months of support; BiVAD N = 145, LVAD N = 5291).[6]

Major Bleeding

An episode of <u>SUSPECTED INTERNAL OR EXTERNAL BLEEDING</u> that results in one or more of the following:

    a. Death,
    b. Re-operation,
    c. Hospitalization,
    d. Transfusion of red blood cells as follows:

If transfusion is selected, then apply the following rules:

During first 7 days post implant
- <u>Adults ($\geq$ 50 kg)</u>: $\geq$ 4U packed red blood cells (PRBC) within any 24 hour period during first 7 days post implant.
- <u>Pediatrics (< 50 kg)</u>: $\geq$ 20 cc/kg packed red blood cells (PRBC) within any 24 hour period during first 7 days post implant.

After 7 days post implant
- Any transfusion of packed red blood cells (PRBC) after 7 days following implant with the investigator recording the number of units given. (record number of units given per 24 hour period).

Note: Hemorrhagic stroke is considered a neurological event and not as a separate bleeding event.

Neurological Dysfunction

Any new, temporary or permanent, focal or global neurological deficit ascertained by a standard neurological examination (administered by a neurologist or other qualified physician and documented with appropriate diagnostic tests and consultation note). The examining physician will distinguish between a transient ischemic attack (TIA), which is fully reversible within 24 hours (and without evidence of infarction), and a stroke, which lasts longer than 24 hours (or less than 24 hours if there is evidence of infarction). Each neurological event must be subcategorized as:

1) Transient Ischemic Attack (acute event that resolves completely within 24 hours with no evidence of infarction)
2) Ischemic or Hemorrhagic Cerebral Accident/CVA (event that persists beyond 24 hours or less than 24 hours associated with infarction on an imaging study.

In addition, to above, for patients < 6 months of age, any of the following:
3) New abnormality of head ultrasound

    4) EEG POSITIVE FOR SEIZURE ACTIVITY WITH OR WITHOUT CLINICAL SEIZURE

Figure 1.1: INTERMACS definitions for Major Bleeding and Neurological Dysfunction. Note: hemorrhagic stroke is considered a neurological event and not a separate bleeding event. From INTERMACS Manual of Operations, version 3.0.[9]

Outside of INTERMACS, other researchers and institutions have reported bleeding and thrombotic adverse event rates in the literature. Given the different flow fields and shear stresses in each type of pump, one would expect that pulsatile and rotary pumps may have different rates of adverse events. The Thoratec pulsatile internal pneumatic VAD (IVAD) was reported to have stroke rate of 8% and bleeding rate of 46% (33% requiring re-operation)(39 patients in the study).[12] Miller et al reported on the HeartMate II rotary VAD bridge to transplantation (BTT) trial in which 11% of patients experienced hemorrhagic or ischemic strokes (0.18 events/patient year), 2% pump thrombosis and 41% of patients had bleeding requiring re-operation (a slight increase in thromboembolic complications over the pulsatile Thoratec IVAD) (133 patients).[4] An update on this report by Pagani et al through the BTT trial's continued access protocol revealed that 53% of HeartMate II patients experienced a bleeding event, with 26% requiring re-operation (1.67 and 0.45 events/patient year, repectively).[13] Embolic stroke afflicted 5% of the patients (0.09 events/patient year) and another 1% had primary device thrombosis requiring surgical intervention (0.04 events/patient year; 281 patients). Starling et al reported on the HeartMate II BTT post-approval trial in which 44% of HeartMate II patients experienced a bleeding event (1.44 events/patient year) and 4.7% experience an embolic stroke event (0.06 events/patient year; 169 patients).[14] In destination therapy (DT) patients, Slaughter et al reported on 81% of HeartMate II patients that experienced a bleeding event (1.66 events/patient year) with another 30% requiring reoperation for bleeding (0.23 events/patient year).[15] Similar to the BTT trials, Slaughter et al reported that 8% DT patients experienced thromboembolic stroke and another 4% had pump thrombosis (0.06 and 0.02 events/patient year, respectively; 134 patients). Furthermore, in an illustration of differences between implant centers, John et al reported on the HeartMate II but in a single-center setting; of these patients, only 3%

experienced stroke and 15% had bleeding that required re-operation (a significant reduction in adverse event rates compared to previous reports) (47 patients).[16]

Recently, a report from Starling et al discussed a troubling and sudden increase in pump thrombosis across three major HeartMate II implant centers.[17] The Cleveland Clinic, Washington University Barnes-Jewish Hospital, and Duke University combined to form a single report on patients implanted with the HeartMate II from 2004 to 2012. The report found that prior to 2011 only 2.2% of patients experienced pump thrombosis within 3 months of support, while 8.4% of patients implanted from 2011 to 2013 had pump thrombosis, a four-fold increase (837 patients). (**Figure 1.2**) Of those patients that were not able to be transplanted and experienced pump thrombosis, mortality was 48.2%. Although the authors could not identify a single cause for this observed increase, the authors suggested that modifications to the outflow graft and bend relief as well as modifications to the inflow conduit, perturbations that affected flow around the bearing, and changes to the anticoagulation regimen may have been contributing factors, Additionally, the authors noted that any perturbations that affected flow around the blood-lubricated bearing (such as aortic regurgitation, cannula kinking, and arrhythmias) could have decreased heat dissipation and increased protein deposition around the bearing. Interestingly, the target INR recommendation during this period was reduced due to an increase in bleeding complications from acquired Type 2 von Willebrand Syndrome that has been associated with implantation of this pump.[18] However, the authors were not able to prove correlation of thrombosis with these changes.
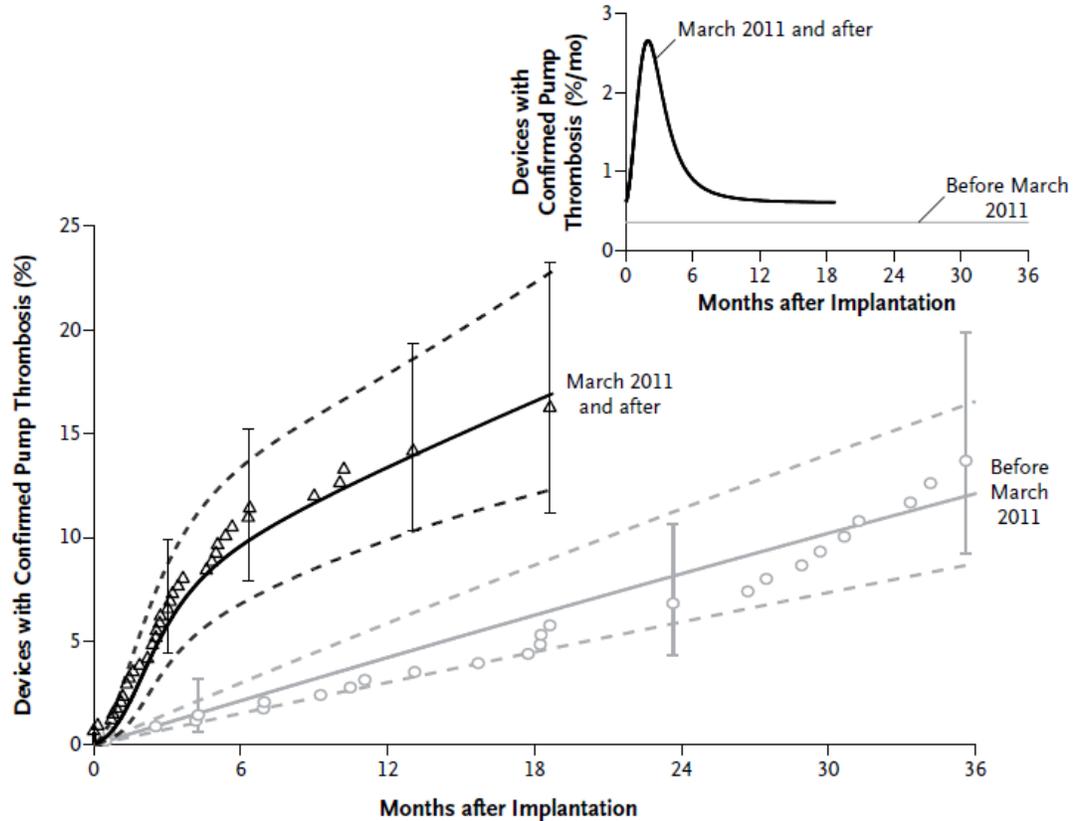
Figure 1.2: Increase in confirmed HeartMate II pump thrombosis at three active implanting institutions after March 2011. This trend was surprising and unexpected by the authors as all three institutions had been regularly implanting HeartMate II LVADs since 2004. From Starling et al. [17]

The introduction of impeller-levitation technology (no internal bearings; single moving part) and improved fluid dynamics design on VADs have not been able to eliminate these complications. One such pump (Ventracor LVAD) reported stroke in 24% of patients (0.48 events/patient year), 15% thrombosis and/or thromboembolism, and 24% hemorrhage (0.48 events/patient year) (33 patients).[19] The European clinical trial for the HeartWare HVAD reported bleeding events in 24% of patients and ischemic stroke in 4% (0.27 and 0.04 events/patient year, respectively; 50 patients).[20] The US clinical trial for the HeartWare

HVAD exhibited slightly different event rates, with 15% of patients experiencing bleeding that necessitated reoperation and 7.5% experiencing embolic stroke with another 4% needing pump exchange due to thrombus formation (0.19, 0.09 and 0.05 events/patient year, respectively; 332 patients).[21] (**Figure 1.3**) A single-center report on HeartWare patients by Wu et al revealed bleeding events in 23% of patients, with 84% of the events requiring reoperation.[22] Wu et al also reported 7% of the patients died due to a central nervous system event, with another 1% of patients requiring pump exchange for pump thrombosis (141 patients). A similar single-center report revealed that 26% of patients implanted with the HeartWare HVAD had an ischemic stroke (50 patients).[23]
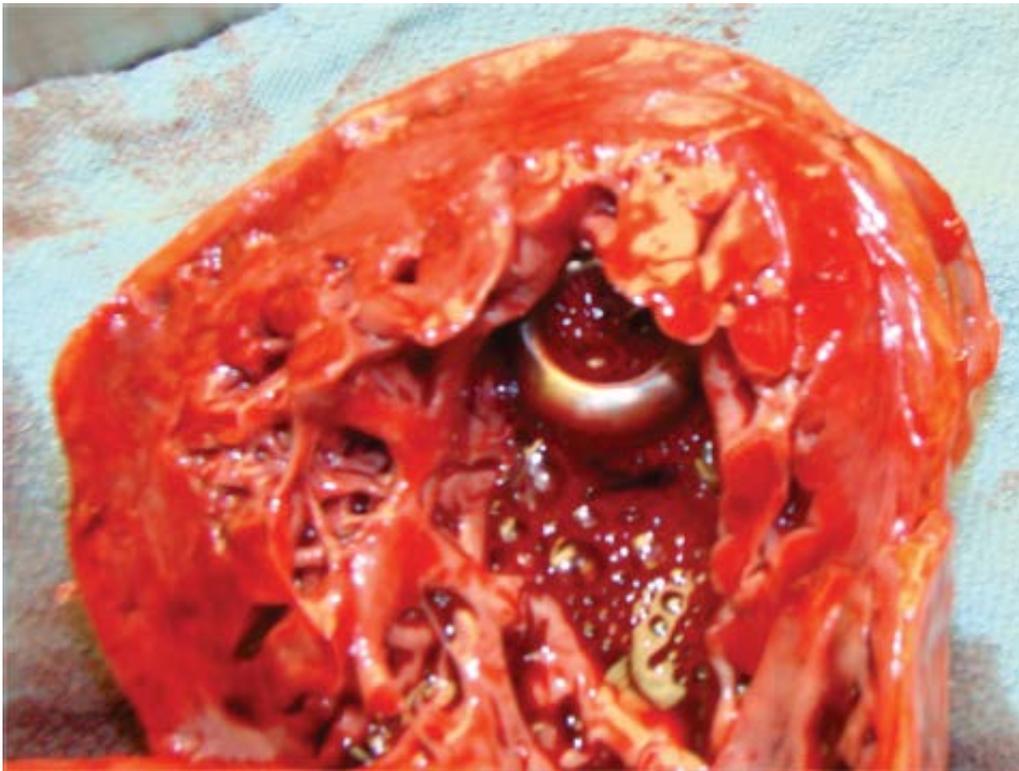
Figure 1.3: Device thrombosis in the inflow cannula of a continuous flow ventricular assist device. From Eckman et al. [24]

8

As clinicians become more familiar with these patients and devices, improvements in event rates due to progress in patient anticoagulant management have also been reported in the literature. Long et al demonstrated decreases in adverse event rates through refined patient management and pre-implant screening; a new patient management protocol provided by the manufacturer addressed patient selection, wound care, nutrition and perioperative and postoperative care. Long continued to show that for patients implanted with the pulsatile HeartMate XVE, neurologic dysfunction (0.15 vs. 0.39 events/patient year) and bleeding (0.15 vs. 0.46 events/patient year) were reduced under the new protocol when compared to previously published values that were collected during early use of this device (42 patients).[8,25] Similarly, the HeartWare HVAD BTT trial revealed an improvement in ischemic cerebrovascular accident rates following a change to the anticoagulation protocol during the study (0.11 events/patient year, N = 253 v 0.07 events/patient year, N = 211).[21]

These relatively high complication rates remain troubling for clinicians, especially when compared to similar heart failure populations that do not receive VAD support but remain on optimal medical therapy (OMT). Rogers et al followed OMT patients for a comparable length of time as VAD implantation and found that 11% experience stroke while 0% experienced bleeding (18 patients).[26] Similarly, Rose et al found neurological dysfunction at a rate of 0.09 events/patient year and no bleeding events (61 patients).[8] A meta-analysis by Witt et al found that only 5% of heart failure patients experience ischemic stroke within the first 5 years of diagnosis.[27]

Regardless of the pump or institution, studies suggest that patients are most at risk for thromboembolism and bleeding events during the first 30 days of VAD implantation.[4,7,8,17,28,29] **(Figure 1.4)** Refinement of anticoagulation protocols and

increased experience with this patient population has helped to reduce the quantity and severity of these events, but they are still high enough to give pause to referring clinicians on the effectiveness of this technology. Additionally, thromboembolic events causing neurological damage are frequently seen as especially pernicious complications due to their often sudden onset and debilitating nature. Previous INTERMACS data shows that neurologic adverse events are the primary cause in 18% of deaths while on device, while surgical bleeding accounts for only 3%.[10] Clearly more investigation into changes in the hemostatic state of these unique patients post-implantation is warranted, and may enable clinicians to advance the management of this population and improve outcomes of morbidity and mortality.[30,31]
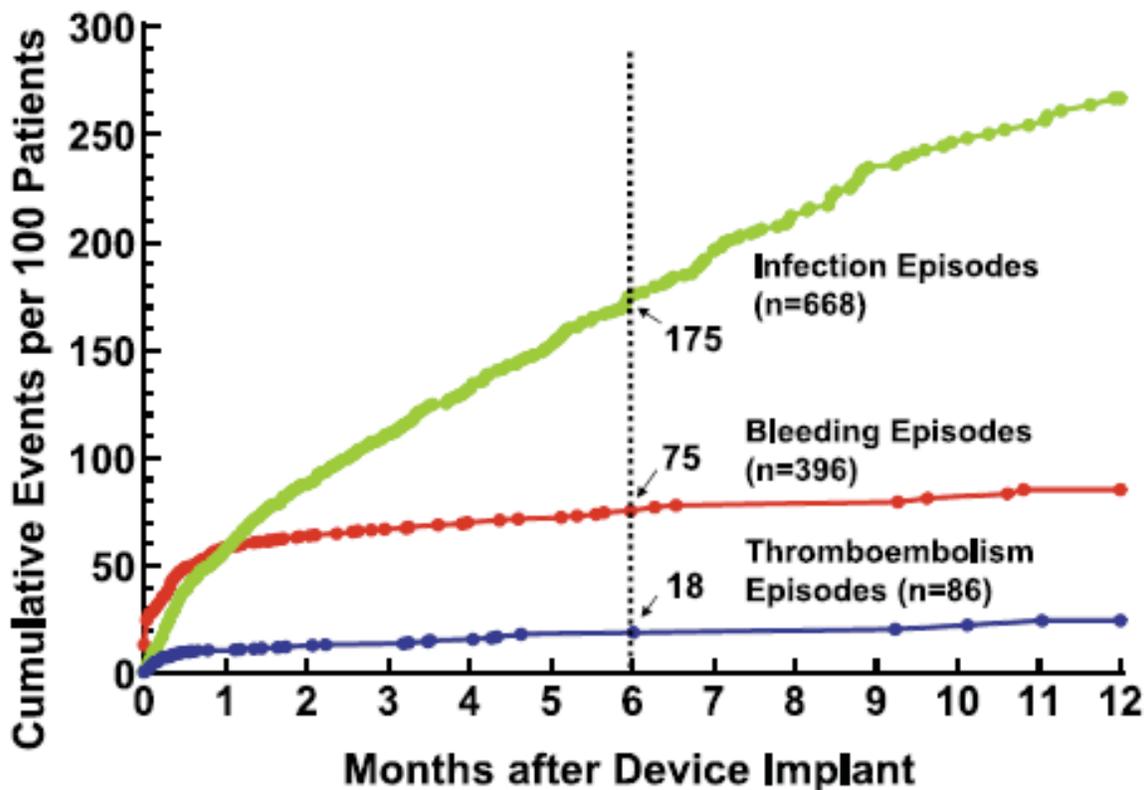
Figure 1.4: Neurological, bleeding and infection adverse events from a report on the Mechanical Circulatory Device Database. Notice the preponderance of thromboembolism and bleeding incidents in the first 30 days of support, as well as the continued risk for infection throughout the implant period. From Deng et al. [29]

1.3   VIRCHOW'S TRIAD APPLIED TO VENTRICULAR ASSIST DEVICES

Thrombogenicity is a material characteristic that may be used interchangeably to describe the localized formation of blood clots, the systemic damage inflicted by embolization of a clot, or the destruction or consumption of blood components resulting in a relative reduction in the ability of blood to function normally.[32] Each of these facets of thrombogenicity may contribute to the failure of a medical device to function properly with the host. A device may trigger a "stabilized" local thrombus formation that is well-anchored to the substrate; however, it is difficult to accurately predict the location and size of adherent thrombus and an ill-placed clot may completely undermine the function of the device (e.g. incomplete valve seal; stent occlusion). Additionally, a material may resist thrombus adherence but still cause embolism through transient clot formation; hence, there are reports of *in vivo* material evaluations demonstrating "clean" surfaces but producing end-organ infarcts.[33] Furthermore, some devices exhibit a continual destruction or removal of blood cells or proteins resulting in a hemostatic imbalance that may contribute to adverse events (e.g. consumptive coagulopathy from oxygenator circuits; anemia from hemolysis). Often times a device will present a combination of these problems, confounding attempts to improve the device or even to properly isolate the offending processes. Notice though that a thrombogenic device may cause seemingly opposite adverse events within the same host; namely, unregulated clot formation and uncontrolled bleeding.

In a healthy individual free from implant, a balance is maintained between the coagulation and fibrinolytic systems to prevent severe blood loss during vessel puncture while also re-establishing normal blood flow to the vessel following repair.[34] In 1856 Rudolph Virchow proposed that the interaction of the constitution of the blood, interrupted blood flow,

and irritation of the blood vessel contributed to the phenomena of venous thrombosis (Virchow's Triad).[35] His insight helped to qualitatively describe the underlying processes responsible for thrombus formation and helped to isolate key variables that could be optimized by researchers to minimize thrombogenicity in medical procedures. However, when artificial surfaces are introduced, this balance may be disrupted by the body's interaction with the foreign matter resulting in unregulated reactions that may be difficult to remedy.[36-39] Virchow's Triad still provides the framework for medical device design and assessment, with an expansion on the composition of the blood and subtle changes to the other variables to reflect a more general application to artificial and organic surfaces. Blood coagulation in the setting of artificial surfaces involves three areas of interdependency: the blood (platelets, the coagulation cascade, fibrinolysis), the flow over the material, and the blood-contacting material.[34] Below is a brief discussion of each variable as it relates to VAD thrombosis and hemostasis.

1.3.1   Blood: the delicate balance

When first contacted with blood, artificial surfaces very quickly undergo protein adsorption, forming a layer over the material almost instantly. This dynamic protein layer is thermodynamically driven by the Vroman effect, where smaller, diffusible proteins initially adsorb to the material surface and are gradually displaced by less diffusible proteins with higher affinity for the surface.[40] All subsequent blood interactions with the device then involve the plasma proteins with the most affinity for the material and not the material surface itself. The shear forces of the flowing blood on the surface will further influence the Vroman effect; a high shear stress setting (e.g. arterial flow) may remove all low-affinity proteins that may be present

on the same material in a low shear milieu (e.g. venous flow; recirculation zones). This adds substantial complexity to predicting device thrombogenicity since the same material may have different adsorbed proteins depending on the flow through the device.[36]

Platelets adhere to artificial surfaces through the binding of platelet surface receptors with adsorbed plasma proteins; in particular, glycoprotein Ib (GP Ib) adheres to adsorbed von Willebrand factor (vWF) while glycoprotein IIb/IIIa (GP IIb/IIIa) adheres to adsorbed fibrinogen, fibronectin and vWF.[41,42] This process is driven by the shear force of the blood such that at lower wall shear rates (<1000 s^{-1}), binding is dependent on GP IIb/IIIa, while at higher shear rates the tethering shifts to GP Ib.[41] Adherent platelets become activated resulting in the release of the contents of internal vesicles (α- and dense granules) into the extracellular environment, formation of pseudopodia, exposure of phosphatidylserine (a negatively-charged phospholipid) and binding with other platelets to form aggregates. Dense granules contain platelet activation agonists such as adenosine diphosphate (ADP), calcium ions and serotonin that help to recruit passing platelets to the site of injury and solidify the platelet aggregate. The phospholipid surface of the deposited platelet mass provides a catalytic surface for the cleavage of prothrombin to thrombin; thrombin then is a potent platelet activator and serves as a positive feedback agent for the growing thrombus. Additionally, there is a growing body of literature suggesting that high shear stress regions may induce low-level activation in the platelet, causing the formation of tendrils that then bind to adsorbed proteins or adherent platelets to form aggregates.[43]

Blood coagulation involves the serial proteolytic cleavage of circulating plasma proteins converging in the activation of prothrombin to thrombin. Of particular importance for artificial materials is the intrinsic system of the coagulation cascade leading to the common

13

pathway. The negatively charged surface of the deposited platelets provides a favorable environment for the anchoring of plasma proteins involved in the initial steps of the intrinsic system. The formation of the platelet plug may help to reduce the flow of blood through the area of insult, allowing the coagulation proteins to form a local gradient to aid in the rapid development of the thrombus.

The fibrinolytic system regulates the clot formation through the degradation of excess fibrin mesh, allowing flow to return to normal to the region of insult after healing. Plasminogen is the principle fibrinolytic agent and is incorporated into the fibrin mesh during clot formation. During healing, plasminogen activators are released by cells near the injury (such as tissue plasminogen activator and urokinase) and the fibrin mesh is disassembled.[34]

Not only are VADs ambitious for the amount of surface area exposed to the blood and the length of time implanted, but these devices are reserved for implant into some of the very sickest patients. VAD patients often have conditions that predispose them to blood clots (such as coagulopathies, fibrillation, ischemia, etc) before VAD placement and the artificial device may unfortunately serve to aggravate the issue. Additionally, 44% of patients are implanted following critical cardiogenic shock which characteristically magnifies extreme inflammation and hypercoagulation.[10] Post-operative patient management is difficult and frequently includes administration of blood products and varying levels of anticoagulation. The effects of surgery and post-operative care on the blood cells can last for weeks before reaching steady state. In short, the hemostatic state VAD patients represent one of the most challenging environments in which to place a medical device.

As stated previously, post-operative bleeding and adverse neurological events are more prevalent during the first month of implantation. Bleeding may be broadly defined by a

14

combination of chest tube drainage, blood products required and re-operation for hemorrhage. A number of mechanisms contribute to difficulties in patient management during this early post-operative period. The highly invasive surgical procedure is associated with blood loss, hemodilution, coagulation protein consumption and platelet activation.[44] The dynamic hemostatic state of these patients immediately after implant often drives clinicians to delicately balance the anticoagulation regimen to ensure proper inhibition of thrombosis while preventing over-anticoagulation (and associated bleeding).[45-47]

Some reports have shown that the traditional measures of anticoagulation such as aPTT and INR are not predictive of observed thromboembolic events.[48] Difficulties with keeping a patient's INR in range while on warfarin (and the poor outcomes associated with highly variable INR values) have been studied.[49] (**Figure 1.5**) In an effort to find more descriptive indices of a patient's hemostatic state (and possibly predictors of adverse events), researchers and clinicians have investigated circulating biomarkers of thrombosis and fibrinolysis. Joshi et al measured INR, aPTT and prothrombin fragment F1.2 (F1.2; a protein cleaved when prothrombin is converted to thrombin) in VAD patients daily before discharge, then weekly thereafter. The investigators found that an elevation of F1.2 was a significant predictor of neurological events while INR and aPTT were not.[48] Additionally, Wilhelm et al found increasing levels of plasma F1.2 coincided with an increase in cranial microembolic signals measured using transcranial doppler.[50] Global platelet activation has been investigated through measurement of plasma levels of proteins released from platelet alpha granules (platelet factor 4 and beta-thromboglobulin).[51,52] Individual interrogation of platelet activation state has been performed by flow cytometry through measurement of surface expression of CD62P and CD63 (both cell receptors are found in platelet alpha granules and are expressed upon activation).[50,53] These

reports suggest that platelet activation levels in VAD patients rise after implant and continue to be elevated through the duration of support. D-dimer has been targeted as a potential indicator of thrombus formation as it is a by-product of fibrin degradation.[51,54] Platelet response to stimulation[55,56], circulating thrombin-antithrombin III complex[52], plasminogen activator inhibitor-1[56], monocyte-platelet aggregates[50], and monocyte expression of tissue factor[57], among others, have also been targeted to help assess the patient's coagulation state as well as predict adverse events.
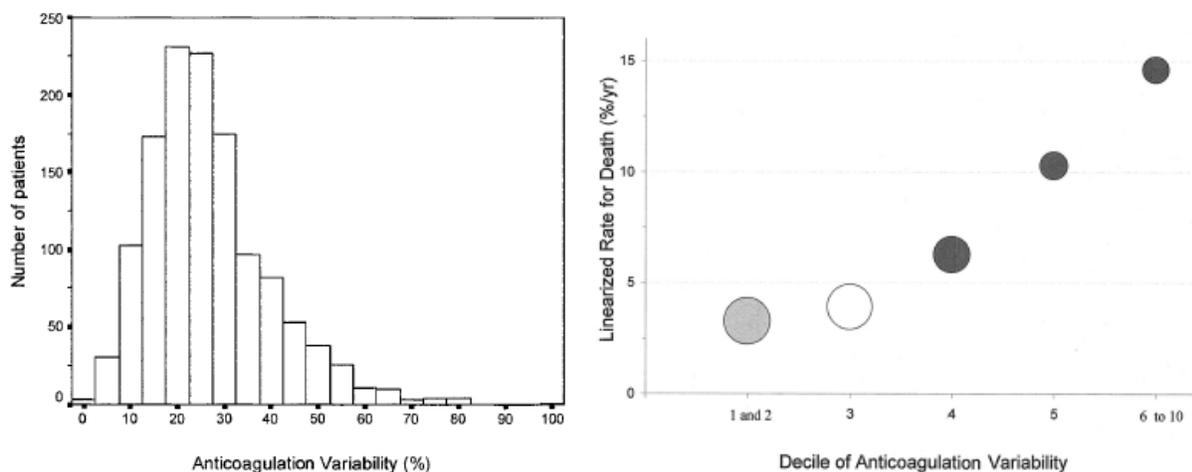
Figure 1.5: (Left) Percentage of INR values outside of the therapeutic range (2-4) for 1272 heart valve patients. (Right) Linearized Death Rate for mitral valve replacement patients outside of the therapeutic INR range of 2-4 (647 patients). From Butchart et al. [49]

While the hemostatic state of VAD patients is often varied and dynamic, anticoagulation protocols are surprisingly uniform across institutions and devices, based upon heparin in the perioperative and immediate post-operative period, and chronic warfarin administration supplemented with ASA and/or dipyridamole as additional anti-platelet agents.[4,12,17,19,26,51,58,59] Advancements in individualized therapy may help to significantly reduce the occurrence of adverse events through patient-specific regimens. Platelet

16

genotyping and platelet function testing for detection of hyper- or hypo-responsiveness to anticoagulation or anti-platelet agents have been increasingly employed for other cardiac procedures (such as stent and valve placements)[60,61]; however, consensus on the utility and robustness of this approach has not yet been achieved.[62] Another approach to tailored medicine is systems biology modeling of patient-specific blood response to activating factors and pharmaceutical agents. Several complex coagulation models are being developed (reviewed by Diamond[63]) that allow for user-input of values such as coagulation factor concentrations and platelet response to known agonist concentrations. Patient-specific data may be obtained (for individualization of the model) by high-throughput blood screening using microfluidics blood analysis. The result is a powerful tool that may be able to diagnose blood defects or predict the effectiveness of anticoagulant and anti-platelet agents. However, further progress needs to be made regarding robustness of the models, computational capabilities and clinical implementation before the potential of this technology is realized.[64,65]

1.3.2   Flow: complex flow fields with a non-Newtonian fluid

As described earlier, blood flow controls the rate of incidence of blood cells and proteins contacting the device wall through diffusion and convection.[66] Flow fields and shear stresses in VADs vary dramatically between different types of pumps and even in different regions within the same pump. The shear forces of the blood help to determine the composition of adsorbed proteins and resultant thrombus. Areas of recirculation within a pump may trap platelets, increasing their exposure time to the artificial surface while also increasing the local concentrations of agonists released from previously adherent platelets. High-shear regions within

17

a pump may become problematic as passing platelets are transiently activated by the shear and deposit on pump seams and bearings that under low shear flow may have been clean of thrombus. In contrast, areas of uninterrupted laminar flow at moderate shear stresses may increase the hemocompatibility of the device by reducing platelet exposure time to artificial surfaces and rapidly removing or diluting agonists from previously adherent platelets. Thus the flow conditions within the VAD may enhance or exasperate the hemocompatibility of the pump surface, undermining even the best attempts at presenting an optimal surface to prevent platelet adhesion and activation.

Shear forces are substantially different between different VAD models depending on a myriad of factors, not the least of which includes if the pump is pulsatile or rotary. Pulsatile pumps are generally characterized as low-shear flow due to the slow filling of a large blood sac and then the gradual increase in pressure to dispel the fluid. However, this is only true when the shear stresses are averaged over an entire pump cycle; the biphasic nature of pulsatile pumps causes changing conditions that may result in transiently sub-optimal flow conditions at localized regions in the pump. For example, shear stresses at the valves during systole will initially be very severe (a high-velocity nozzle during the opening of the valve) and then decrease greatly (fully open valve becomes a large-diameter tube), even resulting in recirculation and stasis zones near the valves once they close during diastole.[67,68] Pulsatile pumps often operate with a "residual volume" of blood that is unable to be completely dispelled from the blood sac during diastole due to geometric constrains of the pump. This residual volume of blood is inevitably exposed to the pump surface for a relatively long time and may become a nidus for platelet deposition or bulk phase aggregate formation. Though most pulsatile pumps are designed such that the fluid rotationally fills the pump sac (to discourage stasis in the pump during the transition from

diastole to systole), this phenomenon is imperfect and unable to completely remove the flow disturbances that occur during transitions in biphasic flow conditions.[67] **(Figure 1.6)** These disturbances in flow may dislodge adherent thrombi or break off aggregates sending emboli downstream with possibly catastrophic results.
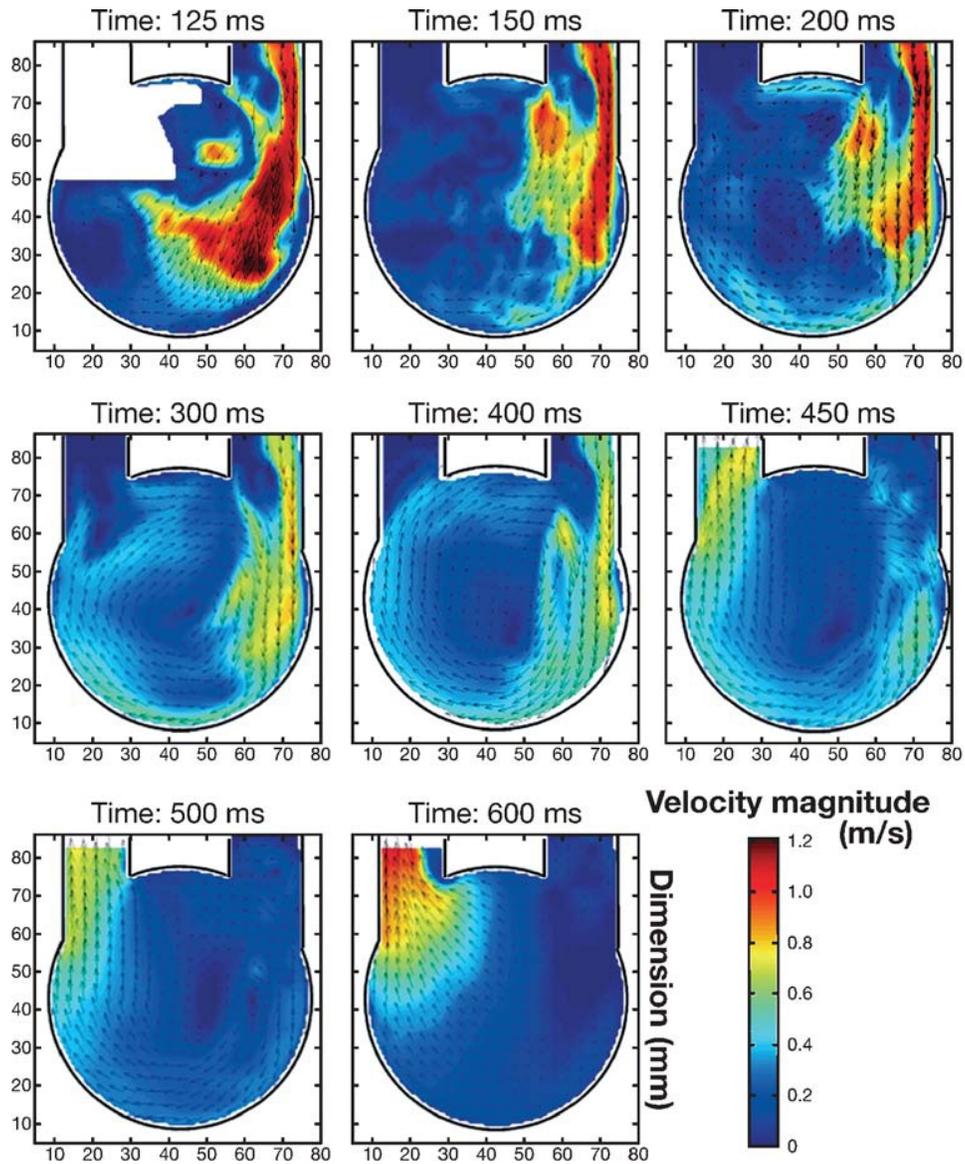
Figure 1.6: Particle image velocimetry of a pulsatile VAD at the onset of pump systole. Notice the initial high velocity at the opening of each valve followed by low velocity caused by recirculation and stasis. From Hochareon et al. [68]

Rotary VADs are different from pulsatile pumps in that the blood continuously flows through the pump at a relatively constant rate. Rotary VADs employ the use of a spinning impeller to move the blood forward; depending on the VAD, this impeller may be supported by bearings in the flow field or magnetic suspension. The blade tips of the spinning impeller in rotary VADs presents regions of consistently high-shear stress that gradually decrease towards the center of the flow field. These high-shear regions vary between pumps (often depending on the width of the gap between the impeller blades and pump housing, among other factors) but are usually supraphysiological.[69] Leverett et al described a relationship between cell exposure time and shear stress which helps to define the hemolysis threshold for blood cells **(Figure 1.7)**; as such, many researchers attempt to design pump operation within this limit but this is often not possible.[70] However, despite continuously exposing blood to high shear regions, these pumps have not experienced the hemolysis that was a concern during development.[71] Studies have suggested that laminar flow through the pump allows a cell-free boundary layer to form, which then experiences most of the high-shear regions while pushing the cells toward the lower shear regions, effectively excluding the cells from the high shear stresses. For pumps that require bearings, this area has typically required special design to limit stasis at the bearing site and reduce blood damage from friction leading to crushing of cells and local heat generation. Thrombus forming at the bearings of pumps has been especially problematic as it not only poses a biological threat of embolization, but a mechanical threat to the pump due to abnormal bearing wear and/or unexpected power consumption (limiting the accuracy of flow estimation and reducing battery life). Magnetically levitated impellers are not unaffected by problems though, as the slightest thrombus formation on an impeller blade may disrupt the delicate magnetic balance and cause the impeller to crash into the pump housing.
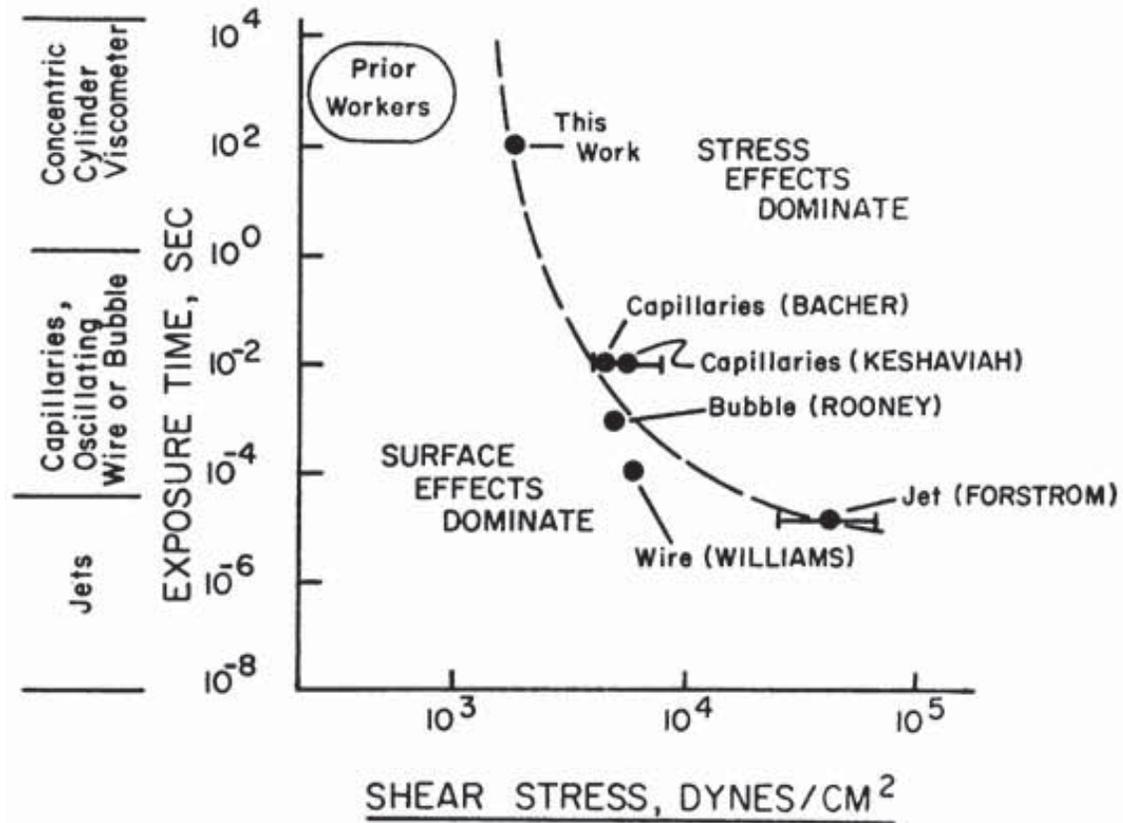
Figure 1.7: Original curve from Leverett et al suggesting the shear stress limits to red blood cells before lysis. The "safe zone" for red blood cells is beneath the curve. From Leverett et al. [70]

Computational fluid dynamics (CFD) is the mathematical simulation of fluid flow in which a programmer is able to import a technical drawing of a VAD and model varying conditions of blood flow.[72] CFD has emerged as a powerful tool for designers to visualize the effects of pump changes during development and identify potentially problematic flow fields *in silico.*[73] CFD allows for the *in silico* manipulation of design of the pump in order to optimize targeted design parameters and predict pump performance prior to fabrication.[74,75] However, the non-Newtonian nature of blood increases the difficulty of predicting flow through even the simplest medical devices, while VADs present some of the most complex flow geometries in

21

medicine. Additionally, research is still ongoing concerning which parameters in the pump design are most important during optimization.[76]

1.3.3 Material surface: where body and machine interface

In addition to differing fluid dynamics, pulsatile and rotary VADs usually contain different blood contacting surfaces due to the material design requirements specific to each pump. Despite these differences the various materials are selected for relative blood biocompatibility, meaning relative resistance to thrombotic deposition and a lack of hemolytic activity. The blood sac in many pulsatile VADs is composed of a durable elastomer incorporating a manufacturer-specific non-thrombogenic molecular component at the surface. For example, the Thoratec pneumatic VAD contains an inflow cannula and blood sac composed of a proprietary polymer consisting of polyurethane blended with a biocompatible surface modifier (Thoralon) intended to reduce thrombogenicity.[77]

The biocompatibility strategy pursued by the HeartMate XVE VAD is in stark contrast to other pulsatile and rotary VADs. Rather than utilizing blood contacting surfaces that do not support platelet deposition, the inside of the HeartMate XVE contains on one side a stationary titanium wall covered in sintered 50-75 µm titanium microspheres and on the other side a pusher-plate covered by a roughly textured Biomer polyurethane diaphragm.[78] These thrombogenic surfaces encourage the formation of a highly organized clot that firmly anchors and matures into a "pseudointima" composed of platelets, monocytes, lymphocytes, fibroblasts and in some cases endothelial cells.[79,80] This biological blood interface has allowed many patients to be effectively weaned from all anticoagulant medications except aspirin with few

22

thromboembolic events.[81] While mechanical problems and size considerations have caused reductions in patient volume, the challenge to traditional paradigms by the HeartMate XVE will continue to be studied by researchers for application in future medical devices. Interestingly, this technology has not been successfully translated to rotary VADs, possibly due to the low tolerances and clearance requirements that are not compatible with the inability to control the thickness of the pseudointima layer.

The pump housing and impeller found in rotary VADs require hard materials that may be easily manufactured and able to withstand mechanical wear. Some manufactures are able to use hard polymers (e.g. polycarbonate in the Levitronix Centrimag) or coatings (e.g. diamond – like carbon coating (DLC) on the Ventracor Ventrassist[82]) to improve thrombogenicity, but most rotary VADs use a highly polished titanium alloy ($TiAl_6V_4$) as the blood – contacting material (e.g. Thoratec Heartmate II, Jarvik 2000, HeartWare HVAD).[82] $TiAl_6V_4$ excels at the material properties described above; it also is non-magnetic which allows it to be incorporated into pumps that are magnetically suspended and/or controlled.

$TiAl_6V_4$ produces an oxide layer which helps to make this material relatively inert to thrombus formation. However, the tolerance of blood to this material appears to be proportional to the width of the oxide layer, which may vary *in vivo*; additionally, titanium without the oxide layer is relatively thrombogenic and has exhibited problems with general biocompatibility compared to other surfaces.[83] One area of improvement being explored by researchers is the development of long-lasting coatings applied to the blood – contacting surfaces within the pumps. Synthetic phospholipid polymers have been studied extensively for their ability to mimic cell surfaces to prevent platelet activation and adhesion.[84,85] Polymers containing phosphorylcholine groups appear to be especially promising for reducing thrombogenicity, in

particular the covalent attachment of 2- methacryloyloxyethylphosphorylcholine (MPC) to titanium alloys.[86-88] **(Figure 1.8)** Polyethylene glycol (PEG) coatings have also been extensively studied due to the remarkable resistance of PEG to protein adsorption (and hence platelet adhesion).[89] However, PEG is typically adsorbed onto the titanium surface resulting in a weak coating; the flow rates experienced under normal pump operation may lead to a relatively quick removal of the coating, exposing the thrombogenic titanium. Another limiting factor with the application of this technology is the prohibitive costs for FDA approval (if necessary) or third-party licensing (if patented by other manufacturers). Regardless, the shortcomings and uniform use of titanium as the primary blood contacting material in rotary VADs provides an opportunity for great strides to be made in reducing thrombotic events through investment in this area of research.
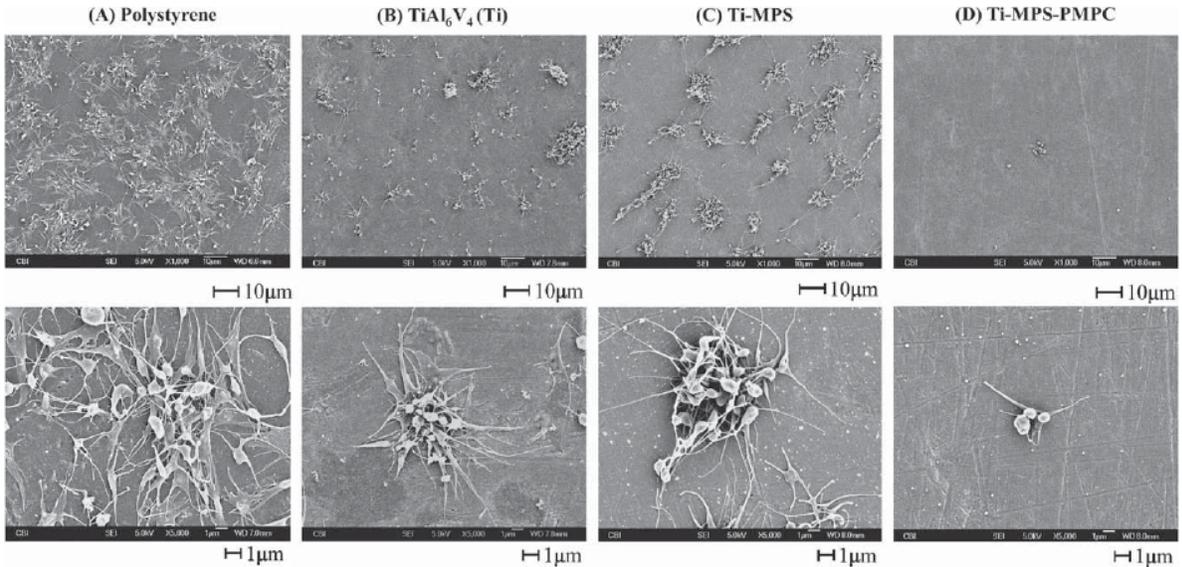
Figure 1.8: Reduction of platelet adhesion to a titanium substrate after application of a phosphorycholine polymer (MPC) as shown by scanning electron micrographs of the surface following contact with sheep blood. (A) polystyrene positive control. (B) TiAl$_6$V$_4$. (C) TiAl$_6$V$_4$ just prior to attachment of MPC (as a control surface). (D) MPC coated titanium. From Ye et al. [88]

1.3.4 Thrombosis modeling: application of Virchow's Triad to predict device performance

Advancements in computing power and mathematical modeling have allowed for recent attempts by researchers to develop a tool for predicting thrombus formation *in silico* during the design of medical devices.[90-92] Complex modeling of the interaction between blood constituents, flow fields and blood-contacting surfaces involves a concerted balanced effort to advance both the accuracy of the numerical simulations and the experimental methods necessary for providing input values and validating outcomes.[93] The success of such a tool could greatly reduce the cost of developing a VAD while possibly improving the performance of the device. VAD design typically consists of a trial and error methodology to reduce the thrombogenicity of the pump; often many design generations are produced due to the discovery of unforeseen thrombogenic areas revealed with each consecutive round of testing, driving up the cost of the product. Even after multiple design iterations and expensive pre-clinical animal testing, clinical trials free of thrombotic events are not assured.[94,95] As discussed above, progress in VAD CFD research has helped to elucidate some of the nonphysiological flow fields presented in mechanical valves and rotating impellers; combined with experimental determinations of protein and platelet interactions with given materials, a predictive numerical relationship may be able to be defined between the flowing blood and the VAD.[96,97] One form the mathematical model may take is that of a map of the probability and location of thrombus formation within the VAD.[90] Researchers could then use this information to design out the "hot spots" predicted in the model, optimizing the pump *in silico* for a fraction of the cost of previous design methods.[98] Though the accuracy of the current models still needs to be refined, this area of research will be vital to

decreasing adverse events and improving outcomes as the future of VAD technology continues to evolve.

1.4   SUMMARY OF INTRODUCTION

Technological innovation in mechanical circulatory support has greatly improved the lives of people afflicted with end-stage heart failure. New devices and advancements in peripheral equipment have expanded the eligible patient population, making this therapy now routine in some institutions. Despite the mechanical progress, some of the same problems experienced with the first implants are still confounding clinicians today. Thrombosis, thromboembolism and bleeding remain major complications plaguing VAD patients and are persistent partly because of their multi-factorial nature. Tools such as blood biomarkers, individualized anticoagulation therapy, CFD, platelet-resistant coatings and thrombosis modeling may help to decrease the amount of adverse events experienced with this technology while positioning it at the forefront of heart failure support and transplant medicine.

1.5   OBJECTIVES

As has been discussed above, VAD support is challenging due to a number of factors including the intended duration of support, the health of the population expected to receive the device and the surface area of the materials exposed to blood. It is not surprising then that cellular immunity of VAD patients has been shown to be compromised and changed compared to heart failure

control patients. Theories regarding cellular impact have ranged from immune cell interactions with proteins adherent to the surface of the pump to the influence of super-physiological shear stresses on immune cell function. These same factors have also been shown to influence hemostasis as platelets interact with both adsorbed proteins on the surface of pumps and are subjected to high shear fields in current rotary VADs. This interaction of platelets with VAD surfaces at high shear rates have been studied in vitro, but typically only use end-point analysis. These previous studies became the foundation on which this current work was built. The main goal of this research was to investigate the response of immune cells and platelets to circulatory support with continuous flow ventricular assist devices. This was accomplished through a combination of clinical research and in vitro studies composed of the following objectives:

1.5.1   Objective #1: Investigate the validity of immune cell paradigms developed with the HeartMate XVE LVAD in a current-generation device.

Paradigms of selective T cell reduction and subsequent immunological imbalance were developed in a the now-obsolete HeartMate XVE LVAD. This paradigm has not been examined in patients implanted with a current-generation rotary device, and alternative paradigms have not been expressed. This objective will challenge one of the primary studies that inspired the body of literature outlining the selective T cell reduction hypothesis.

1.5.2 Objective #2: Investigate temporal leukocyte values, granulocyte activation and infection among several different contemporary VADs.

Most contemporary studies investigating the near-constant risk of infection experienced by VAD patients focus the post-operative surgical wounds or the presence of a percutaneous driveline. Several in vitro studies have shown that innate immune cells may be susceptible to activation through interactions with artificial surfaces at elevated shear rates. This objective will investigate the influence of current VAD technology on patient granulocyte activation, alterations in leukocyte enumeration and infection.

1.5.3 Objective #3: Investigate the effects of VAD support on hemostasis and thrombosis based on pre-operative liver dysfunction as well as between VAD types.

This objective will challenge and enlarge the current body of knowledge available to the VAD clinical community through the investigation of hemostatic and thrombotic alterations in heart failure patients after implantation with contemporary rotary or pulsatile VADs. Cellular level effects as well as adverse event rates will be compared based on measures of patient pre-operative hepatic dysfunction as well as between the type of device implanted.

1.5.4 Objective #4: Develop a method for real-time visualization of platelet deposition onto opaque surfaces under physiologically-relevant flow conditions.

Previous experiments of platelet deposition onto opaque surfaces used either non-physiologic platelet rich plasma as the perfusion fluid or relied on discreet timepoint observations to analyze

the performance of the material. This objective will develop a method for real-time visualization of platelet deposition onto opaque surfaces under physiologically-relevant flow conditions. These in vitro experiments will serve as the foundation for evaluating alternative materials to titanium as the blood contacting surface in rotary VADs.

2.0   LYMPHOCYTE PROFILES AND ALLOSENSITIZATION IN PATIENTS IMPLANTED WITH THE HEARTMATE II LEFT VENTRICULAR ASSIST DEVICE

2.1   INTRODUCTION

The utilization of ventricular assist devices (VADs) to prolong life in advanced heart failure patients is established and expanding.[6] While many of the mechanical problems experienced during the procedure's infancy have been greatly reduced, biologic complications continue to be seen. Among these complications, risk of infection may be the most troubling due to its prevalence throughout the implant period. VAD patients typically experience a greater number of infections than patients undergoing similar surgical procedures, with a resultant increase in infection-related mortality. Additionally, infection events may increase the risk of thromboembolic events, complicating anticoagulation monitoring and effectiveness.[99]

The research community has recognized that cellular immunity in VAD patients is compromised, exhibiting an atypical and suboptimal immune response.[31] Several reports by Ankersmit et al outlined the effect of implantation of the HeartMate® XVE (HM XVE) VAD on T cell activation and apoptosis.[100-102] Early reports suggested that the CD4+ T cells of HM XVE patients had an increased susceptibility to activation-induced cell death.[100] This was later confirmed for HM XVE patients through a longitudinal study of differential lymphocyte counts which showed a significant selective reduction in CD4+ T cells over the first 2 months of

implantation (**Figure 2.1**).[101] Further studies showed the CD4+ T cell reduction may contribute to B cell hyperactivity and sensitization.[102] Few adaptive immune – cell studies have been conducted in contemporary rotary blood pumps. This study sought to re-examine some of the early T cell reports from Ankersmit et al in the currently – utilized rotary Heartmate II® (HMII) VAD in a comparably sized patient group.
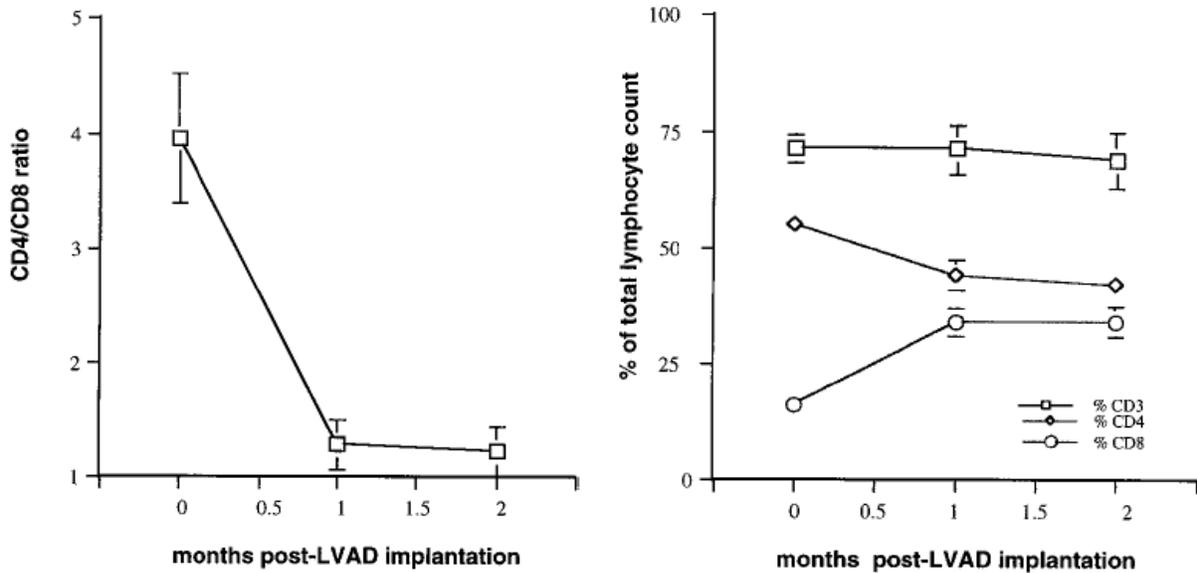
Figure 2.1: (Left) Progressive decline in CD4/CD8 T cell ratio following HeartMate XVE LVAD implantation. (Right) Decline of CD4 T cells and not CD8 T cells, with a relatively unchanged overall number of lymphocytes in patients implanted with the HeartMate XVE LVAD. From Ankersmit et al. [101]

2.2 PATIENTS AND METHODS

2.2.1 Patient selection

All study procedures and consent forms for data collection, blood collection and data analysis for this investigation were approved by the University of Pittsburgh's Institutional Review Board (IRB).

This study was a single-center investigation of patients implanted with the Thoratec® HeartMate II® LVAD (Thoratec Corp, Pleasanton, CA) at the University of Pittsburgh Medical Center (UPMC) Presbyterian Hospital between May 1, 2009 and January 1, 2010. Patient medical history, infection events, human leukocyte antigen (HLA) Class I and II levels, blood product administration and laboratory test values were gathered from an IRB-approved database at UPMC (Transplant Patient Management System). Additionally, patients consented to periodic blood draws for lymphocyte counts. Infection event determination followed the Interagency Registry of Mechanically Assisted Circulatory Support (INTERMACS) definitions.[9] HLA levels were determined by enzyme-linked immunosorbent assay, with allosensitization defined as >10% at any time up to 1 year post-implantation.[103] Blood product exposure was measure for the first 48 h post-implant, with total blood product units (TBPU) equal to the sum of red blood cell (RBC), platelet, frozen plasma and cryoprecipitate units.

2.2.2 Flow cytometric enumeration of circulating CD4+ and CD8+ T cells

Enumeration of circulating T and B cells was performed according to established protocols using commercially available counting beads.[104] The antibodies used in this study were R.

Phycoerythrin-Cyanine 5 (RPE-Cy5)-conjugated CD45, fluorescein isothiocyanate isomer 1 (FITC)-conjugated CD3 and either R. Phycoerythrin (RPE) – conjugated CD4 or CD8 (volumes per manufacturer's specifications; all mouse anti-human; clones HI30, UCTH1, RPA-T4, and LT8, respectively; all from Abd Serotec, Raleigh, NC). Cal – Lyse Whole Blood Lysing Solution and PCB-100 Counting Beads were used per manufacturer's instructions for the wash no – lyse cell counting technique (both from Invitrogen, Grand Island, NY). The cells were immediately analyzed with a 3-color FACScan (BD, Pleasanton, CA) and processed with WINList software (Verity Software House, Topsham, ME) per the counting bead manufacturer's instructions for data collection and analysis.

2.2.3 Statistical Analyses

All data are presented as mean ± standard error of the mean unless noted. Paired-sample T-tests were used for comparison of pre-operative and 30-day variables, and independent T-tests were used for comparison of these same variables to historical means from Ankersmit et al.[101] Friedman's ANOVA was used for non-normally distributed temporal data, with Wilcoxon post hoc analyses using Bonferroni corrections. Sensitization and blood product exposure were analyzed by Mann-Whitney U test. Statistical significance was assumed at $P<0.05$. All statistical tests were performed with SPSS v16.0 (IBM Corp, Armonk, NY).

2.3 RESULTS

2.3.1 Patient demographics

A total of 8 patients were followed for this study; however, only 2 were available for the pre-implant and 30 day timepoints. The pre-operative characteristics for these 8 patients are presented in **Table 2.A**.

Table 2.A: Patient demographics and heart failure information for lymphocyte studies

Demographics	
Implant Age (yr)	47 ± 5
Sex (% male)	88 %
Destination Therapy (Y)	63 %
Diabetes %	40 %
Smoker %	80 %
Hemodynamics	
BSA (m^2)	2.3 ± 0.1
CO (L/min)	4.6 ± 0.4
CI (L/min/m^2)	2.0 ± 0.1
LVEF %	12.9 ± 1.9
BP Mean	80 ± 3
PAP Mean	34 ± 2
CVP	10 ± 2
Pre-op and Concomitant Support	
Milrinone (mg)	0.3 ± 0.1
IABP %	50 %
IABP (avg days)	4.5 ± 1.3
ECMO %	13 %
ECMO (days)	5
RVAD %	0 %
Pre-operative Diagnosis	
Dilated Myopathy: Idiopathic	50 %
Dilated Myopathy: Ischemic	50 %

Average ± Standard Error of the Mean, or Percent

BP=Blood Pressure   BSA=Body Surface Area   CI=Cardiac Index
CO=Cardiac Output   CVP=Central Venous Pressure
DT=Destination Therapy   ECMO=Extracorporeal Membrane Oxygenation
IABP=Intra-Aortic Balloon Pump   LVEF=Left Ventricular Ejection Fraction
PAP=Pulmonary Artery Pressure   RVAD=Right Ventricular Assist Device

2.3.2 Leukocyte and T cell population changes following HeartMate II implantation

Data from a study by Ankersmit et al. that compared T cell populations between a heart failure control group and patients implanted with the HM XVE at post-operative day (POD) 30 are reproduced in **Table 2.B**.[101] A similar analysis was performed for the HMII patients in the current study pre-operatively (serving as internal controls) and at POD 30. The mean historical values from Ankersmit et al. were then compared to patients in the current study at the same timepoints. While Ankersmit et al. found that patients implanted with the HM XVE exhibited relative lymphopenia (P=0.043) and a selective decrease in CD4+ T cells (P=0.009) resulting in a decrease in the CD4/CD8 T cell ratio (P=0.0008), the HMII patients in the current study showed no significant changes in any of these parameters. Comparing the data from Ankersmit et al. groups to the patients in this study, we found no differences between the groups except that HM XVE patients had significantly lower CD4+ T cell counts than the HMII patients at POD 30 (P=0.001).

Table 2.B: Comparison of T cell populations in HMII and HeartMate XVE patients (Ankersmit et al [98])

	HeartMate XVE (Ankersmit et al)			HeartMate II			HeartMate XVE v HeartMate II				
	NYHA Class IV Controls (N=20)	HeartMate XVE Patients (N=12)	P	Pre-Implant Controls (N=8)	HeartMate II Patients (N=8)	P	Controls		VAD Support		
							P	95% CI		P	95% CI	
Lymphocytes (%)	17.0 ± 2.0	9.6 ± 2.4	0.043	17.6 ± 4.5	13.3 ± 2.5	0.250	**0.888**	-8.1	9.3	**0.312**	-3.8	11.3
CD4/CD8 Ratio	4.1 ± 0.4	2.0 ± 0.3	<0.001	2.8 ± 0.4	2.5 ± 0.3	0.945	**0.060**	-2.6	0.1	**0.209**	-0.3	1.3
CD4 Levels (n/µL)	624 ± 59	374 ± 6	0.009	744 ± 204	628 ± 82	0.945	**0.453**	-203	442	**0.001**	114	393
CD8 Levels (n/µL)	194 ± 32	230 ± 93	0.260	272 ± 58	290 ± 60	>0.999	**0.224**	-51	206	**0.638**	-202	322

Values are Mean ± SEM

2.3.3 Temporal T cell changes following HeartMate II implantation

When these observations were examined at POD 120, no difference was found in CD4/CD8 T cell ratio, CD4+ or CD8+ T cell counts, or lymphocyte composition in HMII patients (**Figure 2.2 A, B, C**). There was a slight decrease in CD4+ T cell counts at POD 30 and 60, but the difference was not significant compared to pre-operative levels and was normalized by POD 90 (**Figure 2.2 B**). The CD8+ T cell count was nearly constant during the study period with little variation among timepoints (**Figure 2.2 B**). As a result, the slight changes in CD4+ T cell counts were reflected in the CD4/CD8 T cell ratio, which was also not significantly different over the study period (**Figure 2.2 A**).
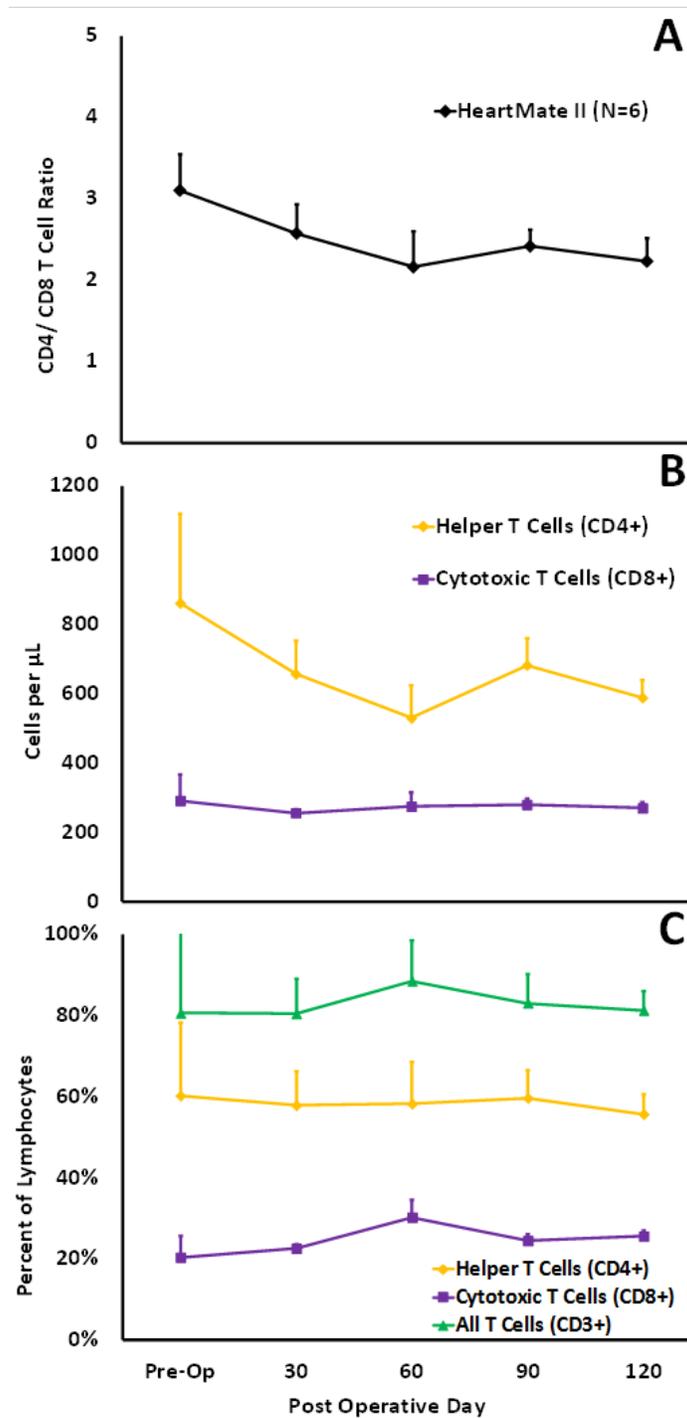
Figure 2.2: Changes in lymphocyte populations following HMII implantation. A) Ratio of circulating CD4+ T cells and CD8+ T cells. B) Absolute cell counts of circulating CD4+ T cells and CD8+ T cells. C) Percentage of circulating lymphocytes consisting of CD4+ T cells, CD8+ T cells and all T cells. Mean plus standard error of the mean for all values. N=8 for all data points.

2.3.4 Infection and sensitization rates in patients implanted with the HeartMate II

No patients had an active infection at the time of implantation. Following device placement, seven infection events were reported during the study period. During the first 30 days of support there were two incidents of sepsis and one localized non-device related event (pneumonia). The next 30 days had one incidence of pneumonia and one localized non-device related (infected sacral decubitus wound) event. During the intervals of POD 61 to 90 and POD 91 to 120 there was one reported incidence of sepsis. Of the 6 patients followed out to POD 120, 3 had at least one reported infection during the study period.

HLA levels were available for 7 patients, of which 29% were sensitized (Patient 1: Class I > 60%, Class II > 30%; Patient 2: Class I > 90%, Class II > 75%; no other patients > 6%). Average blood product exposure was 3.1 ± 1.4 units RBCs, 5.6 ± 3.7 units platelets, and 15.0 ± 7.4 TBPU. When grouped according to sensitization, the sensitized patients had significantly more platelet exposure (19.5 ± 3.5 vs 0.0; P = 0.048) but not RBC (8.5 ± 0.5 vs 1.0 ± 0.4; P = 0.095) or TBPU (39.5 ± 11.5 vs 5.2 ± 3.0; P = 0.095).

2.4 DISCUSSION

The proposed mechanisms for VAD patient vulnerability to infectious agents have spanned from simple barrier breakdown at the driveline interface to complex hemodynamic shear forces affecting viability among circulating monocytes and granulocytes.[105-107] A series of studies with HM XVE patients focused on selective reductions in T cell populations. Ankersmit et al found a significant decrease in CD4+ T cells, possibly from CD95 (Fas) - mediated

apoptosis.[100,101] Subsequent reports revealed that the CD4+ T cell depletion may have caused non-specific B cell hyperactivity in these patients.[102] One study concluded that with the simultaneous combination of increased risk of infection and increased allo-sensitization, the closest disease models to HM XVE implantation are systemic lupus erythematotus and human immunodeficiency virus type 1.[101] The effects of this immune state in HM XVE patients have also been studied, revealing longer transplant wait times and hospital stays, both of which increase health risks and costs to the patient.[108,109]

However, the HM XVE has been replaced by the HMII rotary VAD. Device size, driveline diameter, battery charge time and mechanical lifespan were all improved through the rotary design. Despite this change, no studies on adaptive immune response following rotary VAD implantation have been performed.

This study attempted to replicate the initial reports from Ankersmit et al. in HMII rotary VAD patients.[100,101] **Table 2.B** shows that we were able to confirm much of the information presented by Ankersmit et al. The control and pre-operative values between each study are not different, suggesting that similar populations were represented in each. The implanted cohorts in each study were also not different in almost all of the parameters followed, including percent lymphocytes, CD8+ T cell count and CD4/CD8 ration. However, we were not able to confirm the main thesis of the Ankersmit et al. studies of the selective reduction of CD4+ T cells.[101] CD4+ T cell counts in HMII patients did not change following device placement (P=0.945), while HM XVE patients exhibited a significant decrease (P<0.001). Additionally, HMII and HM XVE patients had similar pre-operative CD4+ T cell counts (P=0.453) but HMII patients had higher counts following implantation (P=0.001). When followed to POD 120, HMII patients continued to exhibit no difference in CD4+ T cells compared to pre-operative values (**Figure 2.2**

39

B). Given this finding, it is not surprising that HMII patients also failed to exhibit the significant drop in CD4/CD8 ratio following VAD implantation found in the Ankersmit study (**Table 2.B, Figure 2.2 A**). The control and pre-operative T cell counts and CD4/CD8 ratio from Ankersmit et al. and this study were similar to other descriptions of patients undergoing cardiac surgery but were markedly lower than reports of healthy adults or general surgery patients.[110-113]

These results are not unexpected as the surfaces of the HM XVE and the HMII were designed to interact differently with the blood of the implanted patient.[114] The pulsatile HM XVE had rough surface textures throughout the device which promoted endothelial deposition. (**Figure 2.3 A, B**) While this unique approach allowed for an aspirin-only anti-thrombotic regimen, the biologic mechanisms involved were complex.[47] Additionally, residual volumes between beats and recirculation zones common in pulsatile pumps may have contributed to leukocyte entrapment and adhesion. The surfaces of explanted pumps were found to contain activated cells from macrophage and dendritic lineages, as well as endothelialization.[79,115] (**Figure 2.3 C**) Overstimulation of CD4+ T cells from these antigen presenting cells on the HM XVE surface may have helped to trigger the apoptotic response found by Ankersmit et al.
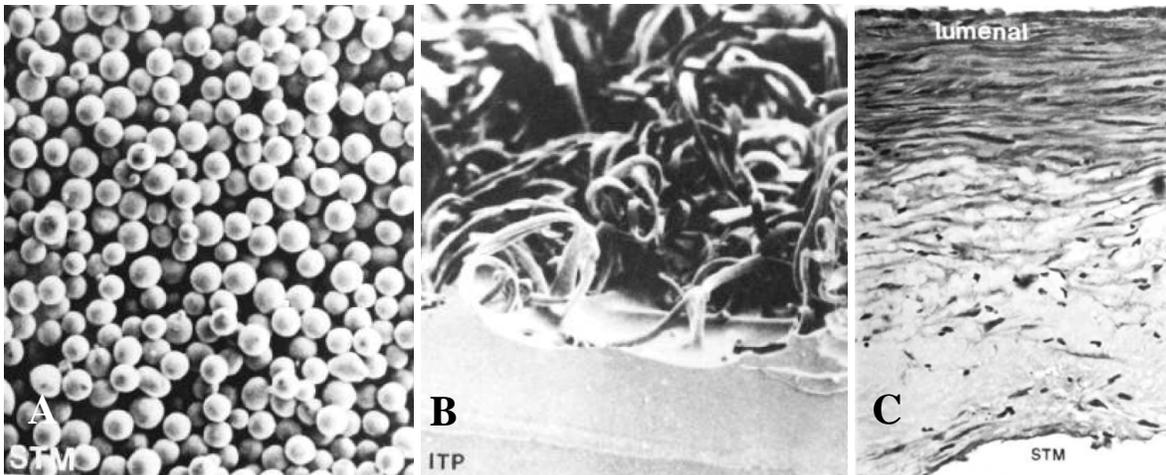
Figure 2.3: SEM micrographs of the textured blood contacting surfaces of the HeartMate XVE LVAD. (A) Sintered titanium. (B) Textured flexible polyurethane. (C) Histological cross section of the organized biological material found on the sintered titanium portion of the LVAD after 41 days of implantation. Mononucleated cells were apparent on the upper luminal side of the cross section. STM, Sintered Titanium Microspheres; ITP, Integrally Textured Polyurethane. From Dasse et al. [116]

In contrast, the HMII is polished over the majority of the flow path to minimize cellular adhesion, with sintered titanium surfaces limited to the inflow cannula and the bends leading into and out of the pump. The continuous flow profile of this pump may reduce the time of contact between circulating leukocytes and the textured segments, limiting the quantity of leukocytes on the device surface. The high shear stresses found in the blood flow path of the HMII may also prevent leukocyte adhesion and motility on the surface. When compared to the HM XVE, the HMII environment may reduce the potential for accumulation and interaction of antigen presenting cells and CD4+ T cells.

Despite no changes in adaptive immune cell profiles, the occurrence of infection among HMII patients continues to be seen. Half of the patients within 120 days of implant had an infection event, usually resulting in longer hospitalization time and increased risk to the patient.

Of particular concern were two incidences of sepsis after POD 60, occurring past the usual surgical recovery period and in the absence of other procedures.

One consequence suggested in the Ankersmit et al study of the selective decrease of CD4+ T cells in HM XVE patients was allosensitization from hyperresponsive B cells.[102] Schuster et al reported that in HM XVE patients, 43% were sensitized to Class I antibodies and 33% were sensitized to Class II antibodies, which was higher than seen in heart failure control patients.[102] Other similar reports for HM XVE patients reported sensitization rates post-implantation to be between 28 and 63%.[117-119] In contrast, two studies comparing sensitization of HM XVE and HMII patients found that HMII patients were significantly less likely to become sensitized (8% and 9% for HMII v 28% and 45% for HM XVE) while a third found virtually no difference in sensitization rates or in post-transplant rejection outcomes.[103,120,121] Some attribute this difference to the presence of the HM XVE device, while others have suggested that blood product exposure (specifically platelet administration) from the procedure may be a confounding factor.[119,122] Even though HMII patients in this study did not exhibit the same pattern of T cell reduction found in reports of HM XVE patients, the rate of sensitization was still relatively high. However, examination of blood product exposure in the two sensitized patients suggests this may have been a contributing factor as both received $\geq$ 28 units of platelets compared to no platelet administration in the other 5 patients.

2.5   LIMITATIONS

A primary limitation of this study is that it was performed at a single institution study and consisted of a relatively small number of patients; as such, the hypothesis tests have an increased

susceptibility to type II errors. While the inclusion of more patients is warranted to confirm our results, the design of this study was guided by the reports by Ankersmit et al. and our methodology and study size does not represent a major deviation from the previous work.[100,101] A simultaneous comparison of the two devices would have been ideal, but the historical comparison was necessary as the HM XVE is no longer available for implantation. The pre-operative values from the patients in our study were not different from the Ankersmit et al. control subjects, suggesting similar populations were examined in both studies.[101] Additionally, the sharp and sustained decline in CD4+ T cells exhibited by the HM XVE cohort would be difficult to hide if this effect was indeed present in the HMII patients followed. Selection bias could also have been present in this study, although none of the patients presented with conditions known to influence T cell counts other than heart failure. Further investigation of the influence of HMII implantation on immune cells may help our understanding of the challenges faced by these patients, although this report and reports from others suggest that the focus may need to turn towards the innate immune cells.[106,107]

2.6   CONCLUSIONS

HMII patients do not exhibit the selective CD4+ T cell reduction or a reduction in the CD4/CD8 T cell ratio previously reported in HM XVE patients. Despite these improvements in T cell profiles, infection was still a substantial risk during the study period, particularly sepsis. Sensitization was also problematic, though the cause in this instance may have been from donor platelet exposure. Thus, despite increased experience with VADs and technological advances

afforded by rotary VADs, HMII patients may continue to be at risk to the same immunological

adverse events as previous-generation devices.

3.0 TEMPORAL LEUKOCYTE NUMBERS AND GRANULOCYTE ACTIVATION IN PULSATILE AND ROTARY VENTRICULAR ASSIST DEVICE PATIENTS

3.1 INTRODUCTION

(Note: a majority of this chapter was previously published as: Woolley JR, Teuteberg JJ, Bermudez CA, Bhama JK, Lockard KL, Kormos RL, Wagner WR. Temporal leukocyte numbers and granulocyte activation in pulsatile and rotary ventricular assist device patients. Artif Organs 2014; in press.)

Ventricular Assist Devices (VADs) have become an established treatment for advanced heart failure, prolonging the life of patients when used as a bridge to transplantation or as destination therapy. Despite technological advances and increased experience, VAD patients are still vulnerable to infection and hemostatic complications such as bleeding and thromboembolism. While the mortality from bleeding or thromboembolism has been shown to decrease substantially after the first 30 days of support, infection is an ongoing risk while on mechanical support.[123-125] The speculated causes for the occurrence of infection range from the existence of a percutaneous line providing a pathway for infectious agent migration, to impaired leukocyte function from interactions with the foreign surfaces of some VADs.[100,124]

Most previous VAD immunological studies included patients with prior generations of pulsatile pumps, many of which are no longer available, rather than continuous flow pumps,

45

which are currently the dominant technology. This is significant in that the design of contemporary rotary VADs is considerably different than pulsatile VADs and may lead to a different leukocyte response from that reported in previous studies.[106,107] Additionally, few studies have presented temporal leukocyte counts [126], as most investigators report leukocyte counts at a specific post-operative time point where they are incorporated as risk factors in outcome scores.[127] The effects of VAD support on granulocytes have also been studied, but only one study followed granulocyte populations over time [126] and no studies have reported the degree of granulocyte activation through the expression of macrophage antigen-1 (MAC-1). The objective of this study was to investigate the influence of current VAD technology on patient granulocyte activation, leukocyte counts and infection.

3.2   PATIENTS AND METHODS

3.2.1   Patients and devices

All study procedures and consent forms for data collection, blood collection and data analysis for this investigation were approved by the University of Pittsburgh's Institutional Review Board (IRB).

This study was a single-center investigation which consisted of patients who underwent placement of a long-term left ventricular assist device (LVAD) (intended length of support >14 d) at the University of Pittsburgh Medical Center (UPMC) Presbyterian Hospital between 1999 and 2011. Patients were excluded if they had a temporary LVAD, had a long-term right ventricular assist device implanted, or were supported < 30 d by the device. Three different

46

devices were included in this study: the Thoratec® PVAD™ pneumatic device (PVAD; Thoratec Corp, Pleasanton, CA), and the Thoratec® HeartMate II® (HMII; Thoratec) and HeartWare® HVAD ® (HW; HeartWare Inc, Framingham, MA) rotary blood pumps. All patients had traditional driveline tunneling with partial velour exposure. Patient medical history, infection events and hospital or outpatient laboratory test values were collected from the IRB-approved Transplant Patient Management System database at UPMC. A subset of these patients that were implanted between 2009 and 2011 were included in an investigation of granulocyte activation levels and consented to providing blood samples pre-operatively and throughout device support. Data from this subset is presented to POD 30 and POD 120 to present short- and long-term perspectives; whereas data were available for all patients in the subset to at least POD 30, some lab values were unavailable when followed to POD 120 and these patients were not included in the long-term analysis. The Interagency Registry of Mechanically Assisted Circulatory Support (INTERMACS) definition for an infection event was used to determine the occurrence of infections.[9]

3.2.2   Flow cytometric determination of MAC-1 expression on circulating granulocytes

Flow cytometry was performed by a modified method from *Donnenberg et al*.[128] Within 4 hr of collection 100 mL citrated (Vacutainer, BD, Pleasanton CA) whole blood was placed in polystyrene tubes and lysed by the addition of 2 mL ammonium chloride lysis buffer. The lysed solution was centrifuged at 400xg for 10 min and, following removal of supernatant, the cells were washed with 1 mL Dulbecco's Phosphate-Buffered Saline without Ca++ or Mg++ with 4% calf bovine serum (Staining Buffer; MP Biomedicals LLC, Solon, OH) and centrifuged again at 400xg for 10 min. The leukocyte pellets were decanted dry and then stained with 2 µL

fluorescein isothiocyanate isomer 1-conjugated mouse anti-human CD15 (clone MEM-158) and 2 µL either R. Phycoerythrin-conjugated mouse anti-human MAC-1 (CD11b, clone ICRF44) or a R. Phycoerythrin-conjugated mouse IgG1 isotype control (all from Abd Serotec, Raleigh, NC), incubated for 20 min in the dark and washed with 1 mL Staining Buffer. Following centrifugation at 400xg for 10 min, the cells were resuspended in 500 µL 1% paraformaldehyde (Sigma, St. Louis, MO) and stored at 4°C (<36 hr) until analyzed. At least 4000 CD15+ events were collected on a 3-color FACScan (BD) and analyzed with WINList flow cytometry software (Verity Software House, Topsham, ME). Granulocytes expressing MAC-1 were defined as CD15+ cells, exhibiting the characteristic granulocyte forward- and side-scatter values, that had displayed MAC-1 binding higher than 98% of the isotype control as measured through fluorescence intensity.

3.2.3 Infection events and peak granulocyte MAC-1 expression

The influence of infections as a confounding factor on peak granulocyte MAC-1 expression in HMII patients was investigated by comparing the average pre-operative MAC-1 expression levels to average values during an infection and average peak levels which were not during an infection. The 3 groups in this comparison are "Mean Pre-operative Value", "Mean Infection Value" and "Mean Peak Noninfection Value". "Mean Pre-operative Value" is defined as blood samples that were collected and analyzed within 5 days prior to implantation. No patients exhibited signs of infection prior to device placement. "Mean Infection Value" were from blood samples withdrawn an average of 3.9 days after a confirmed infection event and before the apparent resolution of the event. Blood samples for the "Mean Peak Noninfection Value" were

collected during periods when the patient was not actively infected (at least 14 days before a confirmed event).

3.2.4   Statistical analyses

All continuous data is mean ± standard error of the mean. All continuous data were analyzed by ANOVA with Bonferroni *post hoc* tests or Kruskal-Wallis test with Mann-Whitney *U post hoc* analysis (and Bonferroni correction). Categorical data was tested with Chi-square (using the Likelihood Ratio statistic). Temporal studies were analyzed by repeated measures ANOVA with Bonferroni *post hoc* testing. The analysis of infection events on granulocyte MAC-1 expression in HMII patients contained 5 patients that experienced at least one infection during implantation; however, 3 of the 5 patients experienced two infections. In instances of two infection events, the second infection event was used in the comparison to allow for repeated measures ANOVA tests without affecting the average for the group. Statistical significance was assumed at $P<0.05$. All statistical tests were performed with SPSS v16.0 (IBM Corp, Armonk, NY).

3.3   RESULTS

3.3.1   Patient demographics, bypass time, chest tube output and blood product exposure

A total of 56 patients were followed for this study, with a subset of 20 patients that had additional blood collected for granulocyte activation determination. Most patients were male (77%) with a mean age of 55 and a pre-operative diagnosis of ischemic cardiomyopathy (46%).

The only significant pre-operative differences between the patients implanted with each device were implant age, pre-operative diabetes, and mean blood pressure (**Table 3.A**). The operation rates for all pumps were within each manufacturer's suggested range, and did not vary greatly over the course of the study. For the HMII cohort, the median rotations per minute (RPM) was 9400 at POD 14 and POD 120, with a maximum of 10,200 and a minimum of 8800. HW patients had median RPMs of 2800 at POD 14 and 2880 at POD 120, with a maximum of 3160 and a minimum of 2500. PVAD patients had a median beats per minute rate of 82 at POD 14 and POD 120, with a maximum of 99 and minimum of 64. No differences were found between any group for cardiopulmonary bypass (CPB) time, chest tube output during the first 24 h post-implant, or blood product exposure during the first 48 h post-operation (**Table 3.B**).

Table 3.A: Macrophage antigen-1 (MAC-1) study patient demographics and heart failure information

	HMII ($n = 32$)	HW ($n = 12$)	PVAD ($n = 12$)	P
Demographics				
Implant age (years), mean ± SEM	56 ± 3	64 ± 2	42 ± 3	0.008*
Male (%)	84	75	58	0.246
Destination therapy (%)	59	NA	NA	—
Diabetic (%)	38	67	17	0.049†
Smoker (%)	59	67	67	0.808
Hemodynamics				
Body surface area (m²), mean ± SEM	2.1 ± 0.1	2.0 ± 0.1	1.8 ± 0.1	0.054
Cardiac output (L/min), mean ± SEM	4.3 ± 0.2	4.6 ± 0.5	3.6 ± 0.3	0.180
Cardiac index (L/min/m²), mean ± SEM	2.1 ± 0.1	2.2 ± 0.2	1.9 ± 0.1	0.406
LVEF (%), mean ± SEM	13.8 ± 1.0	15.8 ± 1.6	14.8 ± 1.5	0.552
Blood pressure (mm Hg), mean ± SEM	83 ± 2	78 ± 3	74 ± 2	0.033‡
PAP (mm Hg), mean ± SEM	38 ± 2	39 ± 2	40 ± 3	0.899
Central venous pressure (mm Hg), mean ± SEM	12 ± 1	11 ± 1	16 ± 2	0.128
Preoperative support				
Milrinone dosage (mg), mean ± SEM	0.5 ± 0.2	0.6 ± 0.2	0.3 ± 0.1	0.510
IABP (%)	56	42	75	0.265
IABP (days), mean ± SEM	4 ± 1	3 ± 1	3 ± 1	0.508
ECMO (%)	3	0	0	>0.999
ECMO (days)	5	NA	NA	—
Concomitant support				
Temporary RVAD (%)	16	17	25	0.889
RVAD (days), mean ± SEM	8 ± 2	9 ± 2	12 ± 5	0.889
Preoperative diagnosis (%)				0.688
Ischemic	50	42	42	—
Nonischemic	44	50	33	—
Other	6	8	25	—

*HMII vs. HW $P = 0.330$, HMII vs. PVAD $P = 0.006$, HW vs. PVAD $P = 0.001$.
†HMII vs. HW $P = 0.306$, HMII vs. PVAD $P = 0.646$, HW vs. PVAD $P = 0.108$.
‡HMII vs. HW $P = 0.419$, HMII vs. PVAD $P = 0.039$, HW vs. PVAD $P > 0.999$.
ECMO, extracorporeal membrane oxygenation; HMII, HeartMate II; HW, HeartWare; IABP, intra-aortic balloon pump; LVEF, left ventricular ejection fraction; NA, not applicable; PAP, pulmonary artery pressure; PVAD, Thoratec pneumatic VAD; RVAD, right ventricular assist device.

Table 3.B: Cardiopulmonary bypass support, postoperative bleeding, and blood product exposure*

	HMII ($n = 32$)	HW ($n = 12$)	PVAD ($n = 12$)	P
Cardiopulmonary bypass support (min)	107 ± 6	110 ± 12	124 ± 14	0.466
Chest tube drainage (mL)*	2484 ± 291	1641 ± 381	1744 ± 243	0.144
Total blood products (units)[†]	14 ± 3	11 ± 4	10 ± 3	0.697
Red blood cells (units)[†]	5 ± 1	4 ± 1	3 ± 1	0.504
Platelets (units)[†]	4 ± 1	3 ± 1	2 ± 1	0.560

Data presented as mean ± SEM.
* During first 24 h post-implantation.
[†] During first 48 h post-implantation.
HMII, HeartMate II; HW, HeartWare; PVAD, Thoratec pneumatic VAD.

3.3.2 Temporal leukocyte numbers and infection events

PVAD patients had significantly different temporal trend of white blood cell counts than HW patients (P=0.036) (**Figure 3.1 A**). Each group of patients significantly peaked on POD 14 above all other timepoints (P<0.001) and above the intra-hospital normal range. By POD 60, white blood cell counts in patients from each group had decreased significantly below the pre-operative counts. The percentage of leukocytes consisting of granulocytes in each group exhibited a slight peak at POD 14 but remained relatively flat for the study period (**Figure 3.1 B**). Hematocrit significantly dropped below all other timepoints at POD 14 (P<0.006) and remained lower than pre-operative levels to 60 (P<0.012) (**Figure 3.1 C**).

Infection events per patient-day were concentrated in the first 30 days of device support, though the PVAD patients exhibited a biphasic trend (**Figure 3.1 D**). The HW group experienced a significantly lower number of infection events per patient during the study period than the HMII and PVAD groups (**Table 3.C**). The HMII and HW VAD patients were then combined to form a continuous flow VAD group, and infection events for this group were compared to the pulsatile flow PVAD patients. The continuous flow VAD patients (N=44) did not experience a different number of infections per patient during the study versus the pulsatile PVAD patients

(N=12) (0.98±0.25 versus 1.42±0.36, P=0.099). The continuous flow patients also did not experience a different number of sepsis events or localized non-device infections than the pulsatile group (respectively: 0.27±0.09 versus 0.17±0.11, P>0.999; 0.64±0.18 versus 0.75±0.28, P=0.770). However, the number of driveline infections per patient were significantly lower for continuous flow patients than for pulsatile patients (0.05±0.03 versus 0.42±0.23, P=0.007).
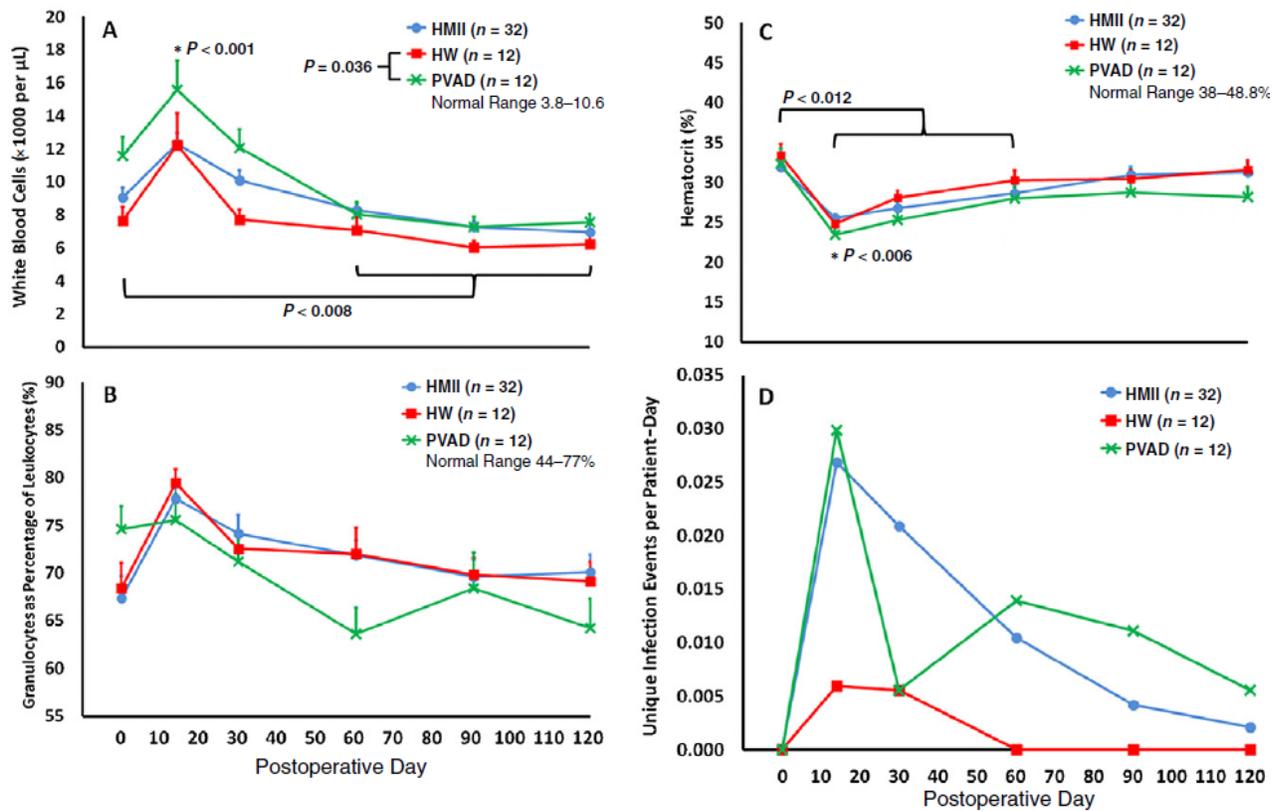
Figure 3.1: Leukocyte and hematocrit changes and incidence of infection events in HMII, HW and PVAD patients following implantation of the device. (A) White blood cell numbers. (B) The percentage of white blood cells consisting of granulocytes. (C) Total hematocrit. (D) Infection events per day of patient support. Mean plus standard error of the mean for continuous data. Normal ranges are intrahospital values. The "0" on the abscissa indicates preoperative values. HMII, HeartMate II; HW, HeartWare; PVAD, Thoratec pneumatic VAD.

Table 3.C: Infection events in ventricular assist device patients to postoperative day 120

	HMII ($n = 32$)	HW ($n = 12$)	PVAD ($n = 12$)	P
Infection adverse events	1.28 ± 0.32 (53)	0.17 ± 0.11 (17)	1.42 ± 0.36 (75)	0.009*
INTERMACS categories				
Sepsis	0.38 ± 0.13 (28)	0.08 ± 0.08 (8)	0.25 ± 0.13 (25)	0.411
Percutaneous site and/or pocket	0.06 ± 0.04 (6)	0.00 (0)	0.50 ± 0.23 (33)	0.012†
Localized nondevice	0.84 ± 0.23 (47)	0.08 ± 0.08 (8)	0.67 ± 0.28 (42)	0.057

Data presented as mean ± standard error of the mean, with percentage of patients who experienced at least one event during the study in parentheses.
* HMII vs. HW $P = 0.039$, HMII vs. PVAD $P > 0.999$, HW vs. PVAD $P = 0.012$.
† HMII vs. PVAD $P = 0.036$, HW vs. PVAD $P = 0.186$.
HMII, HeartMate II; HW, HeartWare; INTERMACS, Interagency Registry of Mechanically Assisted Circulatory Support; PVAD, Thoratec pneumatic VAD.

3.3.3 Granulocyte MAC-1 expression and infection events in a subset of patients

MAC-1 expression on circulating granulocytes had significantly different trend in HMII patients than HW or PVAD patients when evaluated to POD 30 ($P<0.035$) and HW patients to POD 120 ($P=0.014$) (**Figure 3.2 A, B**). The HMII patients exhibited a 2.3 fold increase in MAC-1 expression on POD 14 over pre-operative levels and stayed elevated to POD 30 (**Figure 3.2 A**). When followed to POD 120, the HMII patients had a 2.5 fold increase (from pre-operative levels) in MAC-1 expression on POD 14 and remained elevated to POD 60 (**Figure 3.2 B**).
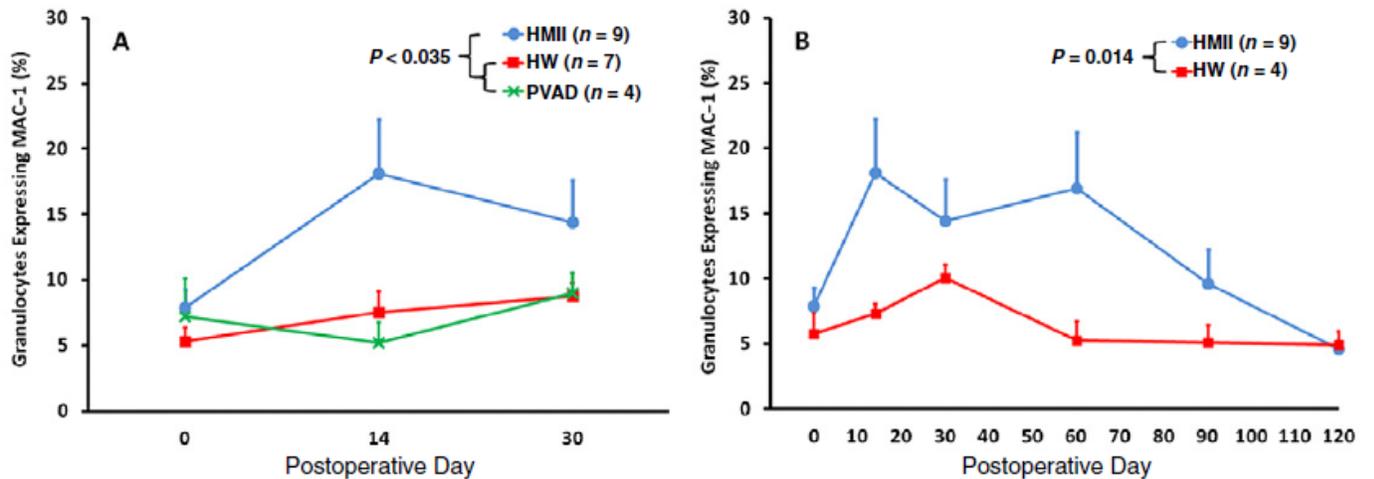
Figure 3.2: Macrophage antigen-1 (MAC-1) expression on circulating granulocytes in a subset of ventricular assist device patients following implantation. (A) MAC-1 expression in all three devices evaluated to 1 month post-implant. (B) MAC-1 expression in HMII and HW patients to postoperative day 120. Data presented as mean plus standard error of the mean. The "0" on the abscissa indicates preoperative values. HMII, HeartMate II; HW, HeartWare; PVAD, Thoratec pneumatic VAD.

HMII patients that experienced an infection over the course of study enrollment were examined to determine the effect of infection events on granulocyte MAC-1 expression (**Figure 3.3**). MAC-1 expression during an infection event exhibited almost no increase over pre-operative values (9.6% to 9.0%, respectively); however, these same patients had peak granulocyte MAC-1 expression at levels >2.5 fold higher than those pre-operatively or during an infection (24.2%; P<0.015). The average POD of infection for these patients was 54 ± 22 d.
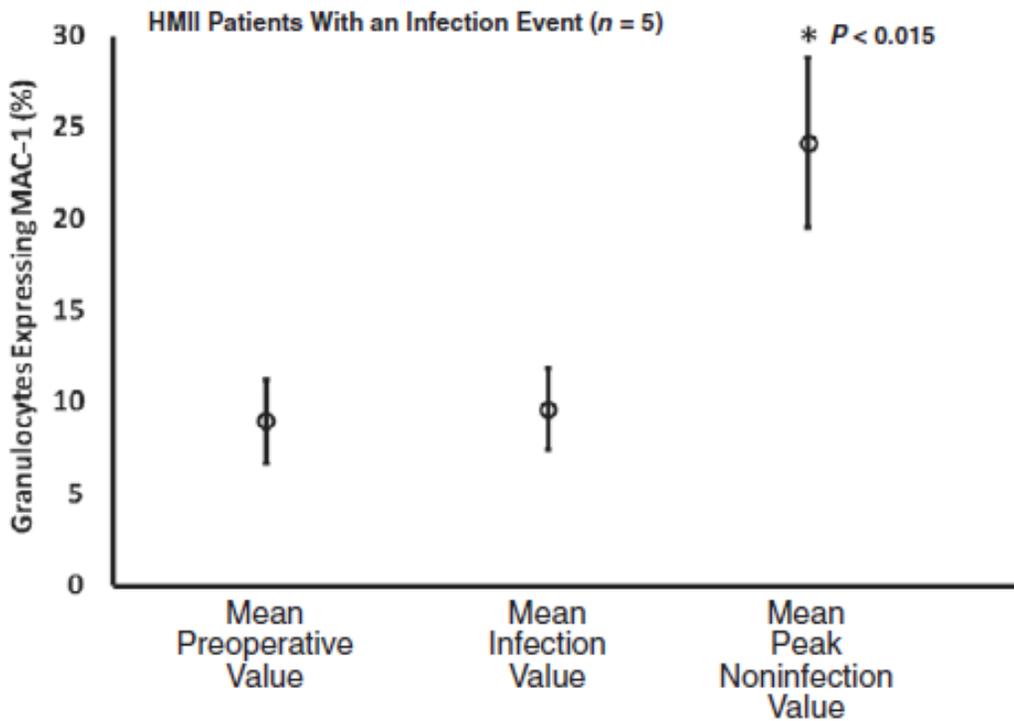
Figure 3.3: Granulocytes expressing macrophage antigen-1 (MAC-1) in HMII patients who experienced as least one infection event during study enrollment. Data presented as mean ± standard error of the mean. HMII, HeartMate II.

3.4   DISCUSSION

This study presents a window into the leukocyte and infection profiles of pulsatile and rotary VAD patients out to 120 days post-implantation, providing a few notable findings. First, white blood cell counts increased significantly in the early post-operative period, despite a simultaneous decrease in hematocrit (**Figure 3.1 A, C**). While other authors have found similar trends with patients having undergone coronary artery bypass graft or heart valve surgeries [110,111], both the white blood cell and hematocrit effects described in these studies returned to normal or pre-operative values by POD 5 and were not as pronounced as was found for patients

in this report. This suggests that the surgery- and device- induced systemic response may be substantial, as post-operative bleeding and reduction of the inflammatory response would be expected to reduce circulating leukocytes by this timepoint. Second, HMII patients experienced a similar rate of infection to the Thoratec PVAD to POD 120, despite a greatly reduced percutaneous driveline exit area (and significantly less driveline infections) (**Table 3.C**). In contrast, HW patients had significantly fewer infection events than either the HMII or the PVAD patients, and the post-operative increase in white blood cell counts was lower than the PVAD group. In the PVAD and HMII patients, most infections occurred during the first 30 days of support, but they continued to be susceptible throughout the study (**Figure 3.1 D**). The peak rates of infection for all VAD patients coincided with significant increases in white blood cell counts (above the normal range) and an upward trend in relative granulocyte concentration (**Figure 3.1 A, B**). This result is in line with the observation that leukocyte proliferation is a hallmark of infection. In this setting, infectious agents are presented with increased opportunities to find safe harbor and flourish on devitalized tissues and along the synthetic surfaces of the percutaneous driveline and indwelling catheters in the peri-operative period. The concentration of infections during the first 30 days of support agrees with reports [123,129] and hazard models [130,131] seen in studies with other devices.

Granulocytes are an important first line of defense against infection, migrating from the vasculature to sites of injury to combat infectious agents. MAC-1 is an adhesion molecule expressed on stimulated granulocytes that mediates migration of the cell from the circulation into inflamed tissue. Upregulation of granulocyte MAC-1 expression in cardiovascular interventions is commonly associated with CPB circuit perfusion and sepsis as a biomarker for systemic inflammation.[132,133] Extravasated granulocytes (following MAC-1 expression) release

enzymes and reactive oxygen species that damage tissue and have been linked to increased edema and organ damage following surgery.[134,135]

Despite growing evidence of altered immune cell function in VAD patients, there is a paucity of information on granulocyte activation and the few papers that discuss it are incomplete or inconclusive. Diehl et al investigated the prevalence of leukocyte-derived microparticles in several rotary or pulsatile VADs at 144 days post-implantation compared to a historical control population.[136] Although the authors found that VAD patients had significantly elevated levels of circulating microparticles expressing MAC-1, the cellular origins of the microparticles were not reported. The authors discussed the possibility of increased microparticles caused by elevated wall shear stresses in various VADs disrupting the immune system but did not distinguish the results by type of circulatory support or provide information on infections for these patients.

Loebe et al reported elevated circulating levels of various inflammatory biomarkers such as complement anaphylatoxins, cytokines and polymorphonuclear leukocyte elastase (PMNE, an indicator of granulocyte activation) compared to normal values for patients implanted with the pulsatile Novacor® or the rotary MicroMed DeBakey® VAD.[137] While these investigators found that C5a and interleukin-6 were significantly increased in the rotary VAD population compared to the pulsatile cohort, PMNE values were nearly identical between the two groups. Additionally, each variable was condensed from 3 months of timepoints into a single averaged post-operative value and not compared to pre-operative levels, limiting the usefulness of this information.

In this study, HMII patients exhibited a rise in granulocyte MAC-1 expression on POD 14 which remained elevated to POD 60 (**Figure 3.2 B**). Similarities among temporal trends for

MAC-1 expression, white blood cell counts and infection events in HMII patients initially suggested that the elevated MAC-1 expression may be the result of blood samples withdrawn during active infections (**Figures 3.1 A, D and 3.2 A, B**). However, closer inspection of HMII patients that experienced at least one infection event revealed that peak MAC-1 expression occurred in the absence of infection (**Figure 3.3**).

Studies involving patients exposed to CPB circuits report only short-term leukocyte activation, with most subjects returning to pre-operative levels within 48 hours.[138,139] The current study reveals that HMII patients experienced granulocyte MAC-1 expression elevated to levels comparable to that with CPB patients, but these findings continued to 60 days post-procedure. To the authors' knowledge, this is the first report demonstrating persistent circulating activated granulocytes this long after the early post-operative period. This study also suggests that the extended MAC-1 elevation phenomenon for the group of VADs studied was specific to the HMII pump and not attributable to differences in CPB time or blood product exposure (**Figure 3.2 A, B; Table 3.B**). The MAC-1 data presented in this study does not appear to be predictive of infection events (**Figure 3.3**), but rather offers some insight into the underlying cellular immunological health of the patient. The prolonged expression of MAC-1 on circulating granulocytes has been shown by others to be detrimental to patients. The potential impact of ongoing and elevated granulocyte extravasation could help to explain prolonged tissue edema and organ dysfunction sometimes seen in patients supported by the HMII (such as pulmonary edema and kidney insufficiency). Expression of MAC-1 has been reported to be a modulator of granulocyte apoptosis, shortening lifespan and facilitating sequestration and clearance in the spleen.[140] Similarly, Shive et al found increased neutrophil apoptosis following exposure to high fluid shear stresses, such as those assumed to be experienced in a continuous flow

pump.[107] While higher rotational speeds within an individual device is related to shear stress, comparisons of shear forces between devices based on pump speed was not considered in this study as differences in pump architecture is a critical variable in the estimation of fluid shear stress, and the local shear profiles at varying speeds in blood for each pump design were not available.

The similar occurrence of infection events between the HMII and PVAD patients might be unexpected considering the substantially smaller exit site of the HMII driveline (**Table 3.C**). The increased levels of granulocyte MAC-1 expression found in HMII patients may have negatively affected granulocyte reactivity and responsiveness in these patients. MAC-1 induced apoptosis of granulocytes could help to explain the relatively high incidence of infection among HMII patients during the first 60 days of implantation. In contrast, the HW device may have advantages over the other devices in that it has a smaller percutaneous exit site than the PVAD, and its patients had significantly lower levels of granulocyte MAC-1 expression than those of the HMII. Both of these factors could contribute to HW patients experiencing significantly less infection events than either the PVAD or HMII patients. It appears that there may be VAD design factors other than driveline exit site contributing to a risk of infection.

3.5   LIMITATIONS

This was a single institution study consisting of a relatively small number of patients; a larger multi-center study is warranted. The methodology of this study focused on assessing the prolonged effects of VAD implantation on circulating immune cells. Only patients supported for > 30 d were included in the study, which may have contributed to some selection bias. However,

recent INTERMACS data suggest this still represents > 85% of all VAD patients.[6] Another limitation with this study was that only bridge-to-transplant patients could be implanted with the HW or PVAD pumps, which resulted in shorter enrollment periods in the prospective study due to pump explant or transplantation. Additionally, the PVAD was rarely utilized as an LVAD-only device, decreasing the number of available patients that were included in this cohort. All of these factors contributed to a smaller statistical power for the subset of patient whose granulocyte activation levels were followed, especially when evaluated to POD 120. Infectious event data was also limited by the size of the study, and confirmation of differences in infection rates between devices would require more patients followed for a longer period of time. Only driveline tunneling with partial velour exposure was used during the study. Other techniques have been described that may improve infection rates [141]; however, the presence of infection did not contribute to the increased MAC-1 levels in HMII patients (**Figure 3.3**). Another study limitation was that other parameters, such as markers of inflammation or granulocyte apoptosis were not measured. Simultaneous measurement of tissue edema as well as plasma interleukin-2, interleukin-6, complement anaphylatoxins and tissue necrosis factor-α along with granulocyte MAC-1 expression would be of interest in future studies.

3.6   CONCLUSIONS

Alterations in leukocyte numbers and granulocyte activation experienced by VAD patients may be device-specific. HMII patients experienced a significantly different trend of circulating granulocyte MAC-1 expression compared to PVAD and HW patients to POD 30, and HW patients to POD 120, as well as substantially longer elevation than was reported in temporal

studies involving CPB circuits. Extravasation and apoptosis of activated granulocytes may contribute to persistent edema and continued infection risk among HMII patients. In contrast, HW patients exhibited little granulocyte activation and significantly less infection events. VAD design may thus influence circulating immune cell activation and infection risk, although the specific relationship between this activation and infection is not known.

4.0   PRE-OPERATIVE LIVER DYSFUNCTION INFLUENCES BLOOD PRODUCT ADMINISTRATION AND ALTERATIONS IN CIRCULATING HEMOSTATIC MARKERS FOLLOWING VENTRICULAR ASSIST DEVICE IMPLANTATION

4.1   INTRODUCTION

(Note: a majority of this chapter was previously published as: Woolley JR, Kormos RL, Teuteberg JJ, Bermudez CA, Bhama JK, Lockard KL, Wagner WR. Pre-operative liver dysfunction influences blood product administration and alterations in circulating hemostatic markers following ventricular assist device implantation. Eur J Cardiothorac Surg 2014; in press.)

The use of ventricular assist devices (VADs) to treat end-stage heart failure is widespread and continues to grow.[6] Bleeding complications in the peri-operative period following VAD placement are still common, due in part to prior operations, pre-implant coagulation status, chronic hepatic congestion and the need for anticoagulation and anti-platelet agents post-implantation.[6] Bleeding events may also have far reaching effects as some studies have linked blood product consumption to a variety of complications such as increased risk of mortality, acute lung injury, concomitant right ventricle dysfunction and allosensitization.[24,142]

Recent publications have demonstrated a correlation between the Model for End-Stage Liver Disease (MELD) score with peri-operative bleeding and post-operative morbidity and

mortality.[143-145] High MELD scores may predict the development of multi-organ failure and hepatic congestion, leading to hemostatic imbalance and disregulation.[145,146] The objective of this study was to investigate the utility of MELD scores to predict post-implant circulating hemostatic markers, blood product consumption and bleeding events in contemporary VAD patients.

4.2   PATIENTS AND METHODS

4.2.1   Patient selection and devices

The University of Pittsburgh's Institutional Review Board (IRB) approved all study procedures and consent forms for data collection, blood collection and data analysis for this investigation. Written consent for this study was obtained from all participants.

This study was a single-center investigation which consisted of patients who underwent placement of a long-term LVAD (intended length of support >14 d) at the University of Pittsburgh Medical Center (UPMC) Presbyterian Hospital between January 2001 and November 2011. Patients were excluded if they were implanted with a temporary LVAD, implanted with a long-term right ventricular assist device, or were supported less than 2 months with the device. Three different devices were included in this study: the Thoratec® HeartMate II® (HMII; Thoratec; N=31) and HeartWare® HVAD ® (HW; HeartWare Inc, Framingham, MA; N=15) rotary blood pumps, and the Thoratec® PVAD™ pneumatic device (PVAD; Thoratec Corp, Pleasanton, CA; N=17). Medical history, post-operative complications and laboratory test values were collected from the IRB-approved Transplant Patient Management System database at

UPMC. MELD score was calculated within 5 days of implantation by previously described methods.[143,145] Interagency Registry of Mechanically Assisted Circulatory Support (INTERMACS) definitions were used to determine the occurrence of bleeding adverse events.[9] Similar to a report by Goldstein et al, neurological deficits (i.e. transient ischemic attacks, cerebrovascular accidents) suspected to be caused by emboli and thromboectomy procedures were combined into the thromboembolism adverse events category.[7] A subset of patients (N=21) were included in an investigation of circulating sub-clinical biomarkers of hemostasis and consented to providing blood samples throughout device support.

All patients followed the same anticoagulation guidelines. Surgical implantation was performed with cardio-pulmonary bypass (CPB) using systemic anticoagulation with heparin (target partial thromboplastin time (PTT) >480 s). Protamine was administered following CPB wean for full anticoagulation reversal. The sternum was closed unless there were indications of possible right ventricular dysfunction. Normal hemostasis was encouraged in the early post-operative period. Following a reduction in chest tube drainage, patients were anticoagulated with heparin (target PTT = 1.5 to 2.5 times institutional normal) as a bridge to Warfarin therapy. Per clinical discretion, 81 mg aspirin was administered daily and increased to 325 mg through thrombelastography monitoring (target platelet arachidonic acid inhibition >70%). Warfarin was initiated within 7 days of surgery, with a target INR that was determined by device used (target INR vaules: HMII = 2.2 - 2.8, HW = 2.5 - 3.0, PVAD = 2.5 - 3.5).

4.2.2 Determination of biomarker activation levels

Circulating levels of activated platelets and platelet-platelet microaggregates were measured using previously established protocols.[147,148] Briefly, whole blood was added to Dulbecco's

phosphate-buffered saline without Ca++ or Mg++ (DPBS; MP Biomedicals LLC, Solon, OH) with appropriate concentrations of recombinant phycoerythrin-conjugated mouse anti-human CD42b (Abd Serotec, Raleigh, NC), and either PE-Cy^{TM}5-conjugated mouse anti-human CD62P (p-selectin) or matched isotype control (both from BD, San Diego, CA) and incubated in the dark for 20 min. The cells were washed with DPBS, centrifuged, and the pellet isolated. The cells were re-suspended in 1% paraformaldehyde and stored at 4°C (<24 hr) until analyzed. CD42b+ events (>5000) were collected on a 3-color FACScan (BD) and analyzed with WINList software (Verity Software House, Topsham, ME). Flow cytometry size calibration beads (3.4 µm diameter, Spherotec Inc., Lake Forrest, IL) were analyzed weekly to provide the basis for distinguishing single platelets from platelet microaggregates. Single platelets expressing p-selectin were defined as appropriately sized CD42b+ cells exhibiting anti-CD62P binding higher than 98% of isotype control. Platelet-platelet microaggregates were defined as being larger than single platelets and exhibiting simultaneous increase in CD42b expression and forward scatter intensity. The percentages of p-selectin positive single platelets and platelet-platelet microaggregates were combined to produce the index of total circulating platelet activation.

Plasma levels of D-dimer and prothrombin fragment F1+2 (F1+2) were determined using commercially available enzyme linked immunosorbent assays according to the manufacturer's instructions (D-dimer: American Diagnostica, Stamford, CT; F1+2: Siemens Healthcare Diagnostics, Deerfield, IL).

4.2.3 Statistical analyses

All values are presented as mean and standard error of the mean (SEM) unless specified. Pre-operative patient characteristics were analyzed using ANOVA with Bonferroni *post hoc* tests for

normally distributed continuous data, Mann-Whitney non-parametric tests for ordinal or non-normally distributed data and Chi-square (using the Likelihood Ratio statistic) analyses for categorical data. Temporal studies were analyzed by repeated measures ANOVA with Bonferroni post hoc testing between variables. Univariate linear regression analysis was used to investigate the utility of MELD scores to predict peri-operative blood product consumption, chest tube drainage and cardio-pulmonary bypass (CPB) time. Univariate linear regression was also performed with several pre-operative variables for the prediction of post-operative total blood product consumption. Variables that predicted total blood product consumption with $P<0.25$ were included in a multivariate linear regression. Step-wise backward linear regression was used, with entry and exit criterion set at $P<0.25$ and $P<0.05$, respectively. Statistical significance was assumed at $P<0.05$ for all tests. All statistics were performed with SPSS v16.0 (IBM Corp, Armonk, NY).

4.3   RESULTS

4.3.1   Patient demographics

A total of 63 patients were followed for the first two months of VAD support. PVAD patients were significantly younger than the other two devices ($P=0.002$) and had a lower body surface area ($P=0.034$) (**Table 4.A**). The overall average MELD score of this study was 14.9 ± 0.1, which is similar to other reports.[144,146] There were no significant differences in mean MELD scores between type of LVAD (mean $\pm$ standard error of the mean: HMII=15.1 ± 0.9, HW=13.0

± 1.0, PVAD=15.7 ± 1.4) (P=0.34). Following the methodology of similar investigations which utilized quartiles to separate patients into high and low MELD score cohorts, the patients in this study were separated *a priori* by the 75% quartile, resulting in a cut-point of 18.0.[143,145] Patients with a MELD score above the 75% quartile (high MELD group) were significantly more likely to have been supported pre-operatively with an intra-aortic balloon pump (P=0.019) (**Table 4.A**). There was a similar distribution of devices between the high MELD score cohort (HMII=10, HW=2, PVAD=4) and the low MELD cohort (HMII=21, HW=13, PVAD=13) (P=0.418).

Table 4.A: MELD Score patient demographics and heart failure information

	Device Group				MELD Cut-point Group		
	HMII (N=31)	HW (N=15)	PVAD (N=17)		>18.0 (N=16)	<18.0 (N=47)	
Demographics							
Implant Age (yr)	56 ± 14	57 ± 16	42 ± 14	a	57 ± 14	51 ± 16	
Sex (% male)	84 %	67 %	53 %		88 %	66 %	
Survive to Transplant/Explant	74 %	67 %	88 %		75 %	77 %	
Diabetes %	32 %	53 %	18 %		38 %	32 %	
Smoker %	68 %	67 %	65 %		75 %	64 %	
Pre-op Hemodynamics							
BSA (m^2)	2.1 ± 0.3	1.9 ± 0.3	1.8 ± 0.2	b	2.0 ± 0.3	1.9 ± 0.3	
CO (L/min)	4.3 ± 1.1	4.4 ± 1.6	3.9 ± 1.3		4.1 ± 1.4	4.2 ± 1.3	
CI (L/min/m^2)	2.1 ± 0.5	2.2 ± 0.7	2.1 ± 0.6		2.0 ± 0.6	2.1 ± 0.6	
LVEF %	14 ± 5	18 ± 7	15 ± 5		15 ± 6	15 ± 6	
BP Mean	85 ± 11	77 ± 11	77 ± 8	c	84 ± 12	80 ± 11	
PAP Mean	37 ± 10	38 ± 9	38 ± 11		39 ± 9	37 ± 10	
CVP	11 ± 7	13 ± 5	15 ± 7		14 ± 6	12 ± 7	
Pre-op Support							
Milrinone (mg)	0.5 ± 0.9	0.4 ± 0.2	0.3 ± 0.2		0.4 ± 0.2	0.4 ± 0.7	
IABP %	52 %	33 %	53 %		75 %	38 %	d
IABP (avg days)	4.7 ± 2.0	4.0 ± 1.9	4.1 ± 2.5		4 ± 2	4 ± 2	
ECMO %	3 %	0 %	6 %		6 %	2 %	
ECMO (days)	5	0	6		5	6	
Pre-operative Diagnosis							
Ischemic	48 %	33 %	41 %		38 %	45 %	
Non-ischemic	45 %	47 %	41 %		56 %	43 %	
Other	6 %	20 %	18 %		6 %	13 %	
Concomitant Support							
RVAD %	16 %	20 %	29 %		19 %	21 %	
RVAD (avg days)	14 ± 10	9 ± 4	7 ± 3		7 ± 2	11 ± 8	

Average ± Standard Deviation where applicable

a: HMII vs HW *P>0.99*, HMII vs PVAD *P*=0.004, HW vs PVAD *P*=0.011.
b: HMII vs HW *P*=0.29, HMII vs PVAD *P*=0.032, HW vs PVAD *P>0.99*.
c: HMII vs HW *P*=0.085, HMII vs PVAD *P*=0.041, HW vs PVAD *P>0.99*.
d: *P*=0.019
BP=Blood Pressure   BSA=Body Surface Area   CI=Cardiac Index   CO=Cardiac Output   CVP=Central Venous Pressure
DT=Destination Therapy   ECMO=Extracorporeal Membrane Oxygenation   HMII=HeartMate II   HW=HeartWare
IABP=Intra-Aortic Balloon Pump   LVEF=Left Ventricular Ejection Fraction   PAP=Pulmonary Artery Pressure
PVAD=Thoratec PVAD pneumatic   RVAD=Right Ventricular Assist Device

A subset of 21 patients had biomarker studies performed (HMII = 10, HW = 7, PVAD = 4). In this subset, the PVAD patients were significantly more likely to have a temporary RVAD placed during implantation (PVAD N=3, HMII N=1, HW N=1) (P=0.048) than the other pumps,

but the duration of RVAD support if needed was similar to that found in the other pumps (PVAD=7±1.7 vs. HMII=5 and HW=6 d). The same MELD threshold of 18.0 was applied to this subset; the resultant high MELD score cohort consisted of 7 patients (HMII=5, HW=1 and PVAD=1) and the low MELD score cohort consisted of 14 patients (HMII=5, HW=6, PVAD=3). There were no other significant pre-operative differences between the high and low MELD score subset groups (**Table 4.B**).

Table 4.B: MELD score subgroup patient demographics and heart failure information

	Device Biomarkers Group			MELD Biomarkers Group	
	HMII (N=10)	HW (N=7)	PVAD (N=4)	>18.0 (N=7)	<18.0 (N=14)
Demographics					
Implant Age (yr)	52 ± 15	51 ± 18	37 ± 15	56 ± 13	45 ± 17
Sex (% male)	80 %	86 %	25 %	100 %	43 %
Survive to Transplant/Explant	70 %	57 %	100 %	57 %	79 %
Diabetes %	30 %	29 %	0 %	43 %	14 %
Smoker %	70 %	57 %	75 %	71 %	64 %
Hemodynamics					
BSA (m^2)	2.2 ± 0.4	2.0 ± 0.3	1.8 ± 0.1	2.1 ± 0.4	2.0 ± 0.4
CO (L/min)	4.4 ± 1.2	5.0 ± 2.2	4.2 ± 1.6	4.8 ± 1.6	4.4 ± 1.6
CI (L/min/m^2)	2.0 ± 0.4	2.5 ± 0.8	2.4 ± 0.7	2.3 ± 0.5	2.2 ± 0.7
LVEF %	14 ± 6	19 ± 7	16 ± 6	16 ± 7	16 ± 7
BP Mean	80 ± 11	77 ± 13	76 ± 9	81 ± 10	77 ± 12
PAP Mean	34 ± 6	39 ± 10	34 ± 10	34 ± 6	37 ± 9
CVP	9 ± 5	15 ± 6	14 ± 4	11 ± 5	12 ± 5
Pre-op Support					
Milrinone (mg)	0.3 ± 0.2	0.5 ± 0.2	0.4 ± 0.1	0.3 ± 0.2	0.4 ± 0.2
IABP %	50 %	57 %	50 %	71 %	43 %
IABP (avg days)	5.3 ± 3.0	3.8 ± 2.1	4.5 ± 0.7	4.0 ± 3.0	4.8 ± 2.2
ECMO %	10 %	0 %	0 %	14 %	0 %
ECMO (days)	5	0	0	5	0
Concomitant Support					
RVAD %	10 %	14 %	75 % a	14 %	29 %
RVAD (avg days)	5	6	7 ± 1.7	5	7 ± 1.7
Pre-operative Diagnosis					
Dilated Myopathy: Idiopathic	50 %	0 %	25 %	29 %	29 %
Dilated Myopathy: Ischemic	40 %	57 %	25 %	43 %	43 %
Dilated Myopathy: Adriamycin	0 %	14 %	0 %	0 %	7 %
Dilated Myopathy: Postpartum	0 %	14 %	0 %	0 %	7 %
Dilated Myopathy: Other	0 %	0 %	25 %	0 %	7 %
Myocardial Infarction	10 %	0 %	0 %	14 %	0 %
Congestive Heart Failure	0 %	14 %	0 %	14 %	0 %
Chemotherapy Induced	0 %	0 %	25 %	0 %	7 %

Average ± Standard Deviation where applicable   * P<0.05

a: HMII vs HW *P>0.99*, HMII vs PVAD *P=0.041*, HW vs PVAD *P=0.088*.

BP=Blood Pressure   BSA=Body Surface Area   CI=Cardiac Index   CO=Cardiac Output   CVP=Central Venous Pressure
DT=Destination Therapy   ECMO=Extracorporeal Membrane Oxygenation   HMII=HeartMate II   HW=HeartWare
IABP=Intra-Aortic Balloon Pump   LVEF=Left Ventricular Ejection Fraction   PAP=Pulmonary Artery Pressure
PVAD=Thoratec PVAD pneumatic   RVAD=Right Ventricular Assist Device

4.3.2 Blood product transfusion and bleeding adverse events

Blood products transfused within the first 48 h post-implant, chest tube drainage within the first 24 h post-implant and CPB time during the implant surgery were each regressed on MELD score, resulting in a significant positive relationship for each variable tested (**Table 4.C, Figure 4.1**).

Table 4.C: Peri-operative outcomes regressed onto MELD score (N=63)

Peri-Operative Outcomes	R	R^2	P	Coefficient β	Standard Error β
Total Blood Products (Units)	0.37	0.13	0.003	1.02	0.33
Packed Red Blood Cells (Units)	0.30	0.07	0.018	0.21	0.09
Packed Platelets (Units)	0.41	0.15	0.001	0.50	0.14
Cryoprecipitate (Units)	0.20	0.02	0.121	0.06	0.04
Fresh Frozen Plasma (Units)	0.26	0.05	0.043	0.25	0.12
Chest Tube Drainage per 48 h (mL)	0.28	0.06	0.026	70.75	30.92
Cardiopulmonary Bypass Time (min)	0.25	0.05	0.048	1.85	0.92
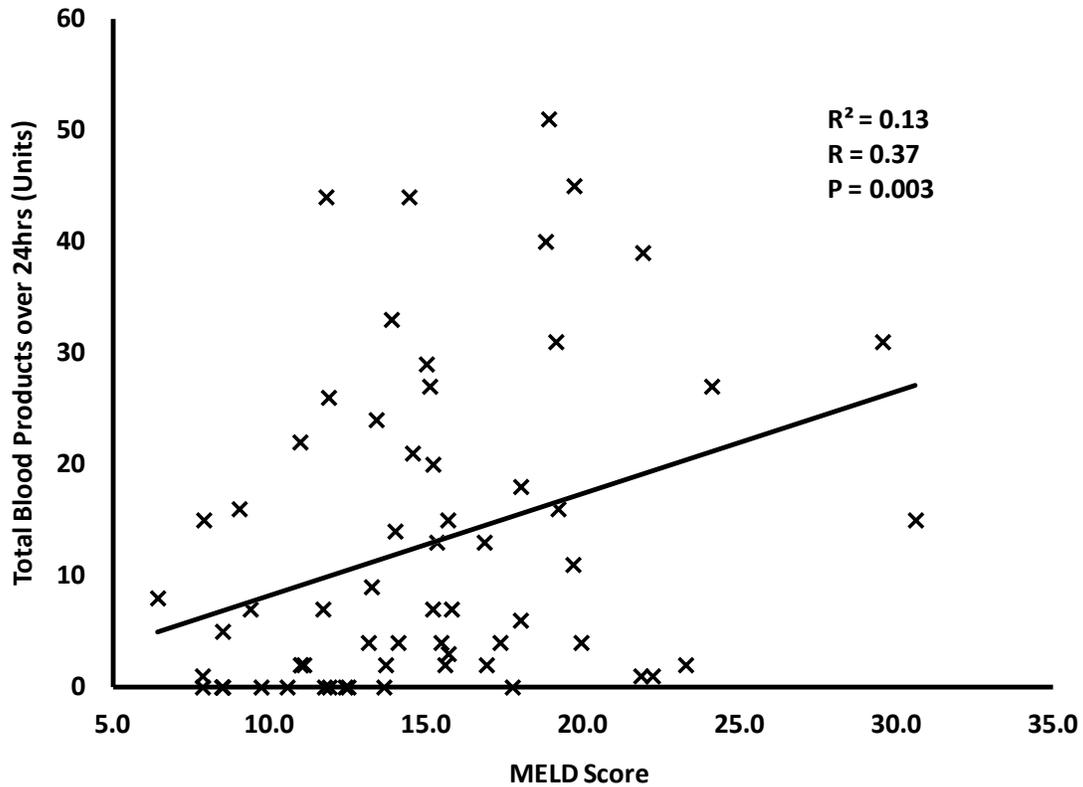
Figure 4.1: Linear regression example for total blood products regressed onto MELD score (N=63).

Predictors of total blood product usage (TBPU) during the first 48 h of VAD support were first analyzed by univariate linear regression analysis (**Table 4.D**). Variables having P > 0.25 were then entered into a multivariate linear regression analysis (**Table 4.E**). Contributors to the final model were MELD score, age, mean pulmonary artery pressure and body surface area, with MELD score (P = 0.004; standardized β = 0.35) and age (P = 0.016; standardized β = 0.28) exhibiting the strongest predictive value.

Table 4.D: Pre-operative univariate predictors in VAD patients of peri-operative total blood product requirements (N=63)

	R	R^2	P
Age (yr)	0.357	0.128	0.004
MELD Score	0.321	0.103	0.010
Body Surface Area (mm^3)	0.223	0.050	0.078
Left Ventricular Ejection Fraction (%)	0.166	0.027	0.195
Mean Pulmonary Artery Pressure (mmHg)	0.160	0.026	0.210
Platelet Count (x10^9/dL)	0.149	0.022	0.244
Sex	0.143	0.020	0.264
Cardiac Index	0.073	0.005	0.572
Central Venous Pressure (mmHg)	0.070	0.005	0.587
Pre-operative ECMO Support	0.070	0.005	0.588
Pre-operative IABP Support	0.054	0.003	0.674
Smoker	0.035	0.001	0.786
Mean Blood Pressure (mmHg)	0.021	0.001	0.873
Diabetes	0.004	0.001	0.975

Table 4.E: Multivariate predictors of total blood product requirements post-VAD implantation*

	P	Coefficient β	Standard Error β	Standardized β
MELD Score	0.004	0.98	0.32	0.35
Age (yr)	0.016	0.25	0.10	0.28
Mean Pulmonary Artery Pressure (mmHg)	0.095	-0.29	0.17	-0.20
Body Surface Area (mm^3)	0.107	-8.99	5.50	-0.19
Left Ventricular Ejection Fraction (%)	0.442			
Platelet Count (x10^9/dL)	0.931			

*Final Model Statistics: R = 0.54, R^2 = 0.29, P = 0.001

When patients were grouped by high and low MELD scores, the high MELD patients had significantly higher TBPU, packed red blood cell (PRBC) units, and packed platelet units during the first 48 h post-implantation. The high MELD group also and had more chest tube drainage during the first 24 h of support (**Table 4.F**).

Table 4.F: Differences in intra- and peri-operative variables by MELD score cut-point

	MELD > 18.0 (N=16)		MELD < 18.0 (N=47)			All Patients (N=63)	
	Mean	SEM	Mean	SEM	P	Mean	SEM
Chest Tube Drainage (24hr)	2583	429	1607	146	0.045	1855	161
Total Blood Products (Units)	21	4	10	2	0.021	13	2
Red Blood Cells (Units)	5	1	3	0	0.050	4	1
Packed Platelets (Units)	8	2	3	1	0.015	4	1
Cryoprecipitate (Units)	1	0	1	0	0.135	1	0
Fresh Frozen Plasma (ml)	7	2	3	1	0.078	4	1
CPB Time (min)	123	11	106	5	0.118	110	5

CPB = Cardio-pulmonary Bypass; SEM = Standard Error of the Mean

VAD patients with high pre-operative MELD scores exhibited significantly lower platelet counts to post-operative day (POD) 55 than patients with low MELD scores (P = 0.006, **Figure 4.2**). All patients had a drop in platelet count at POD 2 (P<0.001) which then recovered and were then above pre-operative levels by POD 12 (**Figure 4.2**). Though the high MELD score patients had lower pre-operative platelet counts compared to low MELD patients (150 ± 18 vs. 191 ± 9 $x10^9$/dL), this difference became much more pronounced at POD 6 and continued to POD 26 (with differences of 88, 73 and 52 $x10^9$/dL for POD 6, POD 12 and POD 26, respectively).
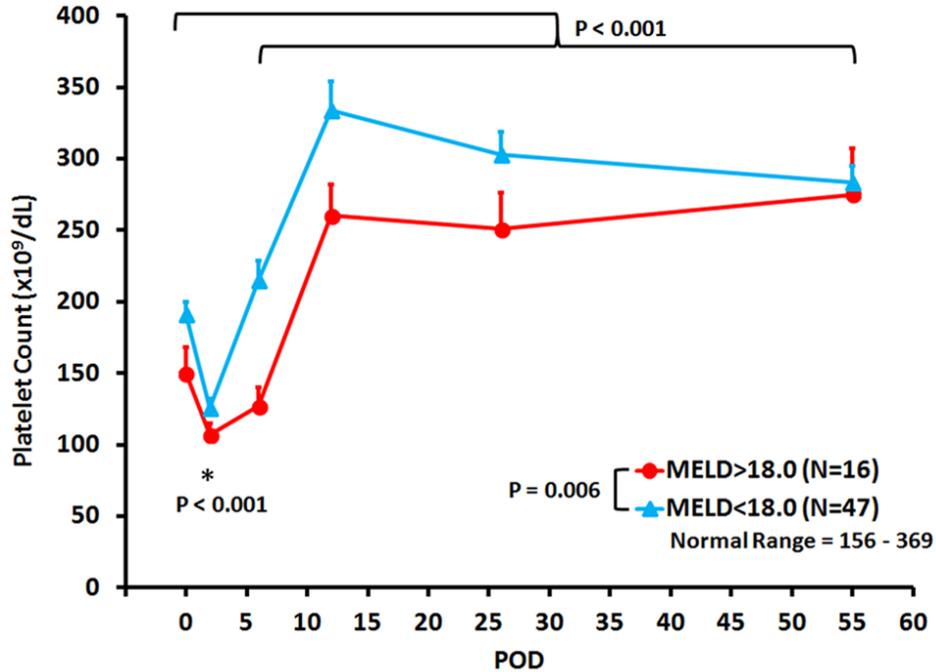
Figure 4.2: Temporal differences in platelet counts between VAD patients with high and low pre-operative MELD scores. Data are presented as mean plus standard error of the mean. The "0" on the abscissa indicates preoperative values. MELD, Model for End-stage Liver Disease.

Although the rates of bleeding and thromboembolism for the high MELD patients were consistently higher than those found in the low MELD groups, this difference was not statistically significant for the time-periods examined. However, the percentage of patients that experienced at least one bleeding event over the course of the study was significantly higher in the high MELD group than the low MELD group (High MELD: 13 of 16 patients vs. Low MELD: 24 of 47, P=0.043; **Table 4.G**).

Table 4.G: Unique adverse events experienced by an implanted patient per patient-day of support

	Bleeding				Thromboembolic			
	Implant to POD 2	POD 3 to POD 30	POD 31 to POD 60	Event Experienced*	Implant to POD 2	POD 3 to POD 30	POD 31 to POD 60	Event Experienced*
MELD > 18 (N=16)	0.344	0.049	0.015	81%	0.031	0.007	0.000	19%
MELD < 18 (N=47)	0.223	0.017	0.004	51%	0.011	0.004	0.002	17%
P	0.268	0.211	>0.999	0.043	>0.999	0.762	0.564	>0.999

*The precentage of patients that experienced the indicated adverse event at least once during the first 60 days of support

4.3.3 Circulating hemostatic biomarkers

High and low MELD score patients had significantly different plasma F1+2 concentration trends with respect to time over the length of the study (P=0.033, **Figure 4.3 A**). While F1+2 concentrations in the high MELD score patients were typically higher than the low MELD patients (P=0.010 at POD 2), the high MELD patients briefly dropped below the levels found in the low MELD patients on PODs 6 and 12 before returning to elevated levels for the remainder of the study. High and low MELD score patients also exhibited plasma F1+2 levels elevated far above the manufacturer's suggested normal median value of 115 pmol/L (95th percentile = 229 pmol/L) throughout the study (**Figure 4.3 A**).

Patients with high MELD scores had a greater degree of circulating platelet activation throughout the study but was only significantly elevated above low MELD score patients on POD 6 (P=0.001, **Figure 4.3 B**). Patients in the high and low MELD score groups exhibited similar trends regarding plasma D-dimer levels, with a significant drop immediately following VAD implantation (P<0.035), followed by a significant rise over pre-operative levels to POD 26 (P<0.010, **Figure 4.3 C**). Though both groups of patients had very similar post-operative D-dimer levels to POD 26, patients with high MELD scores had significantly higher elevations of D-dimer at POD 55 while low MELD score patients dropped to near pre-operative values. D-

dimer levels in both groups of patients were substantially elevated over the manufacturer's suggested normal concentration of <400 ng/mL, with the lowest concentration being 1607 ng/mL by the low MELD group on POD 2.
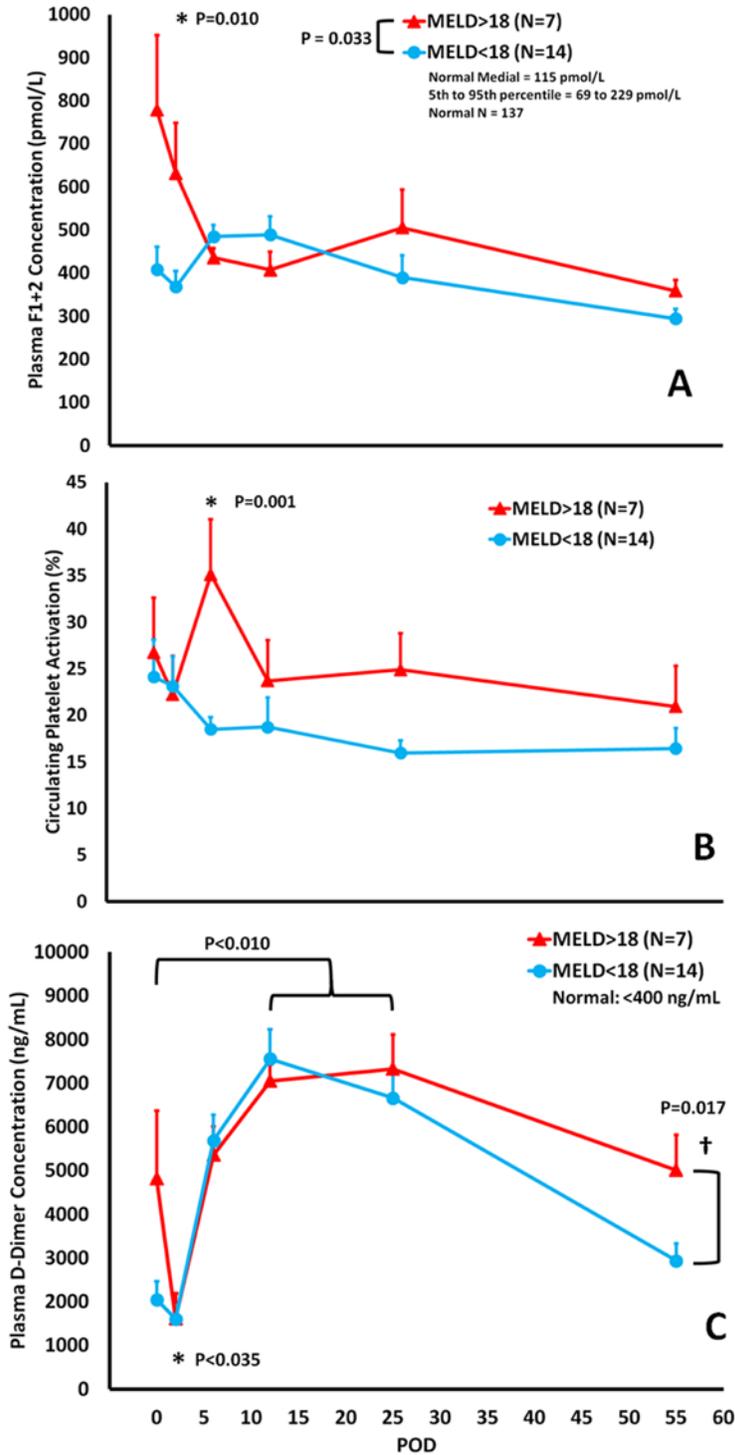
Figure 4.3: Temporal differences in circulating sub-clinical thrombosis markers between VAD patients with high and low pre-operative MELD scores as measured by: (A) Plasma concentration of prothrombin fragment F1+2. (B) Percent of circulating platelets expressing P-selectin or involved in microaggregates. (C) Plasma concentration of D-dimer. Data presented as mean plus standard error of the mean. The "0" on the abscissa indicates preoperative values. MELD, Model for End-stage Liver Disease.

4.3.4 Differences in circulating hemostatic markers between devices

There were no differences between the 3 devices for F1+2 or circulating platelet activation at any timepoint examined (**Figure 4.4 A, B**). When stratified by type of VAD implanted, each VAD patient cohort exhibited circulating D-dimer trends similar to the high and low MELD comparison (**Figure 4.3 C** vs **Figure 4.4 C**). All 3 VAD groups have similar concentrations of D-dimer to POD 14, but the HMII patients remained significantly elevated over the PVAD and HW patients on POD 26 (7943 vs. 6096 and 4984, respectively) and POD 55 (5391 vs. 2748 and 1944, respectively; **Figure 4.4 C**).
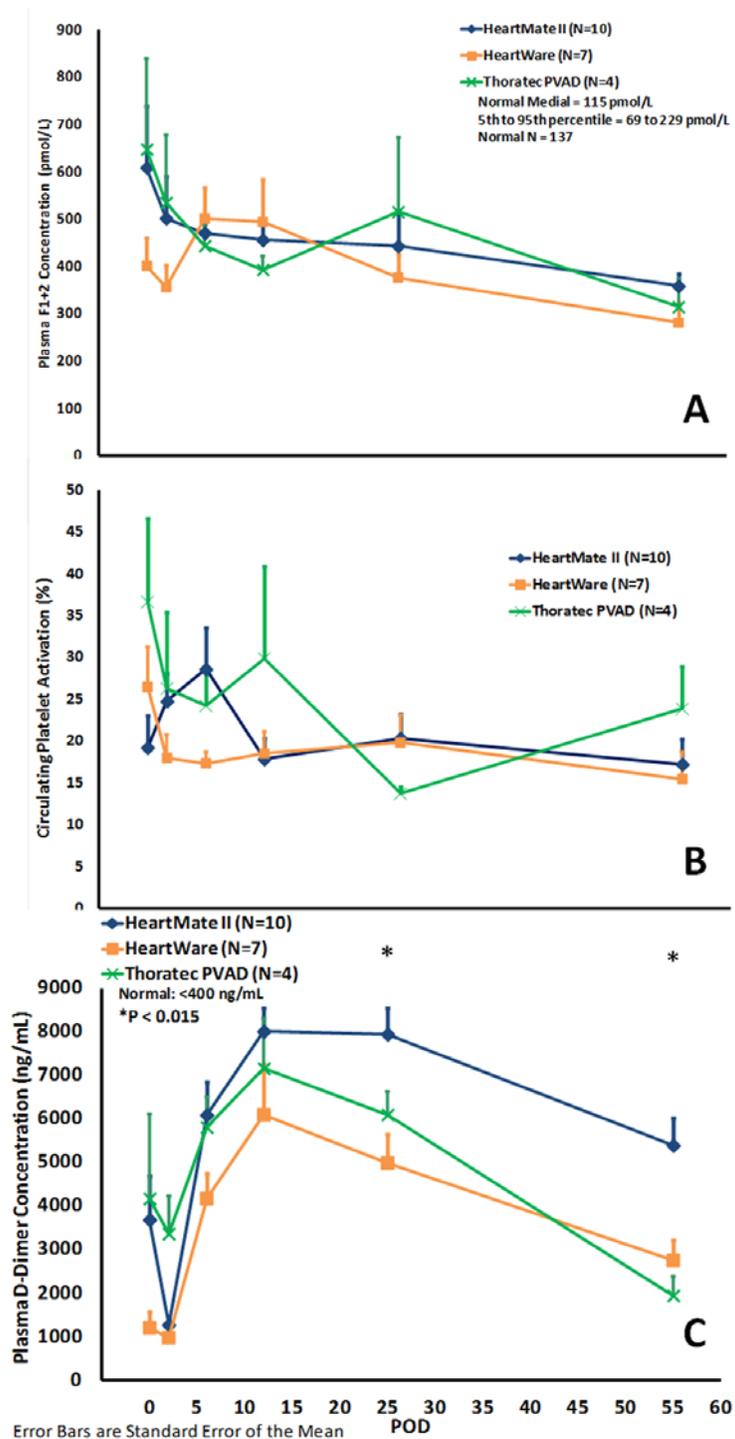
Figure 4.4: Temporal differences in circulating sub-clinical thrombosis markers between VAD patients separated by device implanted as measured by: (A) Plasma concentration of prothrombin fragment F1+2. (B) Percent of circulating platelets expressing P-selectin or involved in microaggregates. (C) Plasma concentration of D-dimer. Data presented as mean plus standard error of the mean. The "0" on the abscissa indicates preoperative values. HMII, HeartMate II; HW, HeartWare; PVAD, Thoratec pneumatic VAD.

When patients were separated by type of LVAD implanted (regardless of MELD score), no significant differences were found between the 3 VADs regarding chest tube drainage or blood product consumption. However, the PVAD cohort had a significantly longer duration of intra-operative bypass than either the HMII or the HW patients (P=0.010, **Table 4.H**).

Table 4.H: Differences in intra- and peri-opeative variables by device implanted

	HMII (N=31)		HW (N=15)		PVAD (N=17)		
	Mean	SEM	Mean	SEM	Mean	SEM	P
Chest Tube Drainage (24hr)	2079	255	1578	311	1689	254	0.387
Total Blood Products (Units)	13	3	11	3	13	2	0.877
Red Blood Cells (Units)	4	1	4	1	4	1	0.959
Packed Platelets (Units)	5	1	3	1	4	1	0.665
Cryoprecipitate (Units)	1	0	1	1	1	0	0.988
Fresh Frozen Plasma (ml)	5	1	4	1	4	1	0.843
CPB Time (min)	101	3	103	11	133	12	0.010

CPB = Cardio-pulmonary Bypass; SEM = Standard Error of the Mean

4.4   DISCUSSION

Pre-operative prediction of hemostatic complications following VAD implantation would be of great benefit in enabling physicians to more effectively manage patients in the peri-operative and early post-operative periods. Previous studies suggest that VAD patients are most at risk for bleeding and thromboembolic events during the first 30 days of support, with a concomitant increased risk of 1 year morbidity and mortality.[6,24,142] Administration of blood products has been associated with increased allosensitization of VAD patients, increasing transplant waiting periods and risk of post-transplant cellular rejection.[119]

81

The MELD score was originally developed as a predictor of mortality and morbidity in patients undergoing transjugular, intrahepatic portosystemic shunts, and has since been utilized in a similar manner for general non-cardiac and cardiac surgeries, including VAD implantation.[144,149-153] While other studies have shown the utility of MELD scores to predict post-operative bleeding, the relationship between high pre-operative MELD scores and increased bleeding is not completely understood. Some have speculated that plasma coagulation proteins may become imbalanced from cardiac hepatopathy due to congestion from right ventricular failure as well as poor hepatic perfusion from left ventricular failure.[146,154]

Recently, MELD scores have been positively correlated with peri-operative bleeding and blood product consumption. Matthews et al found that pre-operative MELD score significantly predicted TBPU as well as individual product components such as RBCs, platelets, plasma and cryoprecipitate.[143] Matthews also found MELD score to be a significant predictor of TPBU in multivariate analysis. However, 80% of the 211 VAD patients analyzed in the study were implanted with now-obsolete pumps. Similarly, Deo et al reported a positive correlation with pre-operative MELD score and both TBPU and platelets in 126 HMII patients.[145] Deo also found a positive correlation between pre-operative MELD score and TBPU in first-time cardiac surgery VAD patients but not in re-operative cardiac surgery VAD patients.

Our study confirmed these reports and expanded upon them by the inclusion of several current devices in the patient selection and the addition of chest tube drainage and CPB time as peri-operative variables. All blood products examined had a significant, positive correlation to pre-operative MELD score except cryoprecipitate (**Table 4.C**). None of the correlations were especially strong, and were similar to those found by Matthews et al.[143] Peri-operative chest tube drainage and CPB time were also significantly correlated to pre-operative MELD score

82

(**Table 4.C**). Separation into high and low MELD score cohorts by 75% quartile yielded similar results except for cryoprecipitate, plasma and CPB time (**Table 4.F**). Not surprisingly, a significantly larger percentage of the high MELD cohort experienced at least one bleeding adverse event during the first 60 days of support (**Table 4.G**). When multivariate linear regression analysis was performed on TPBU, MELD score was a significant predictor along with age and mean pulmonary artery pressure (**Table 4.E**). A recent report by Solomon et al suggests that perioperative administration of fibrinogen concentrate can reduce transfusions during thoracic surgery.[155] The low concentration of fibrinogen in cryoprecipitate may have contributed to cryoprecipitate's relatively reduced administration in these patients. Utilization of fibrinogen concentrate may prove to be useful in high MELD score patients.

Hemostatic monitoring of VAD patients in the immediate post-operative period continues to be challenging. Underlying hemostatic problems may not be apparent until challenged by major cardiothoracic surgery procedures. Previous studies have shown the utility of circulating hemostatic markers such as F1+2 and D-dimer to be sensitive indicators of sub-clinical hemostatic imbalance.[5,48,50,156] The temporal trends of F1+2 and D-dimer in the low MELD score group in this study were similar to trends reported by Wagner et al and the post-operative time course of platelet counts in the low MELD score group were similar to a study by John et al.[5,156] However, the high MELD score patients had a different post-operative F1+2 trend than the low MELD score patients, with significantly higher levels on POD 2 (**Figure 4.3 A**). Differences in circulating D-dimer levels between the two groups also became significant later in the implant period, as the high MELD score patients experienced elevated levels on POD 55 (**Figure 4.3 C**). Furthermore, among the larger population of patients in this study, the high MELD score group exhibited a significantly different temporal trend of platelet counts than the

low MELD group, with lower platelet counts for the first month of VAD support (**Figure 4.2**).[156] High MELD score patients exhibited increased thrombin generation in the early post-operative period, and decreased platelet counts and prolonged fibrinolysis during recovery. Differences in device hemodynamics or surgical procedure might not sufficiently explain the differences found in this study as the three VAD types were evenly distributed among the low and high MELD groups. Instead, the patient's pre-operative condition may have a persistent influence on sub-clinical hemostasis, though the manifestation of this influence is still to be determined.

In this study the type of VAD implanted was not a significant factor in any of the peri-operative bleeding measurements despite very different surgical implantation techniques and VAD hemodynamic profiles. The PVAD required a significantly longer period of time on CPB than either the HMII or the HW, which may reflect the PVAD requirement of tunneling an extra cannula through the skin. Neither the presence of two large exit sites for the PVAD nor the sub-diaphragm pump pocket of the HMII were associated with increased blood product usage or chest tube output (**Table 4.H**). Patients on all 3 devices had similar temporal F1+2, circulating platelet activation and D-dimer responses, which were greatly increased over the reported normal ranges for all time points, and were similar to other reports on VAD patients (**Figure 4.4**).[5,48,156] D-dimer concentrations in HMII patients became significantly higher at 1 and 2 months, which may reflect ongoing fibrinolysis at the textured inflow cannula, which is unique to this pump (**Figure 4.4 C**).

4.5   LIMITATIONS

This was a single institution study consisting of a relatively small number of patients; a larger multi-center study is warranted. The methodology of this study focused on assessing the immediate and prolonged effect of pre-operative MELD scores on hemostasis in VAD patients. Only patients that were supported for at least 55 days post-operatively were included in the study, which may result in some selection bias. However, recent INTERMACs data suggest this still represents >90% of all VAD patients implanted.[6] This bias also prevented mortality prediction with MELD scores, as the results would have been skewed, although this association has already been extensively reported. Additionally, only patients implanted during the last 2 years of the study were followed for investigation of biomarkers of hemostasis, which could contribute to a bias towards healthier patients due to better patient management from increased institutional experience. However, this effect should be limited as all biomarker patients were enrolled during the same period, limiting differences between eras in surgical techniques and patient management. Inclusion of the pulsatile PVAD could be a limitation due to differences in flow patterns and wall shear stresses compared to the rotary HMII and HW. However, part of this study was designed as an assessment of bleeding outcomes and hemostatic markers between pulsatile and rotary VADs. The combination of this evaluation of the three devices with an investigation of the influence of pre-operative liver dysfunction revealed that liver dysfunction strongly affected hemostasis for several weeks after implantation, while the type of VAD had little impact. This does not suggest that VAD design is negligible, and the authors suspect that differences in VAD design may have an increased influence on bleeding and thrombosis further from the time of implantation. However, this was not investigated. At the time of enrollment for this study, implantation of the HW VAD was governed by a clinical trial protocol that may have

biased patients towards a healthier pre-operative condition, yet this bias was not apparent in pre-operative patient characteristics (**Tables 4.A and 4.B**), nor in the pre-operative measurement of any of the indices included in this study.[157] Given that this study was the first attempt at this institution to carefully review the relationship between MELD score and post-operative hemostasis, there was no evidence-based algorithm to treat factors based upon the MELD score. As more contributions to this area of research are provided, an investigation of an evidence-based algorithm may be warranted.

4.6   CONCLUSION

Pre-operative hepatic and renal dysfunction appears to have immediate and long lasting hemostatic effects on VAD patients. MELD score was a predictor of post operative blood product administration, chest tube drainage and bleeding adverse events regardless of the VAD implanted. VAD patients with high pre-operative MELD scores exhibited significantly different temporal trends of thrombin generation and platelet counts, as well as protracted fibrinolysis. Though the rate of adverse events decreased markedly after the first 2 days of implantation, the sub-clinical effects of a high pre-operative MELD score on the hemostatic system appeared to be persistent.

5.0   REAL TIME VISUALIZATION OF PLATELET DEPOSITION UNDER FLOW ONTO CLINICALLY-RELEVANT OPAQUE SURFACES

5.1   INTRODUCTION

Many cardiovascular devices such as vascular grafts, stents, and heart valves are susceptible to the risk of device thrombosis and thromboembolic events.[158] A large portion of biomaterial research has been devoted to investigating materials to reduce the thrombogenicity of cardiac devices. Materials such as poly(ethylene glycol) (PEG), biomimetic phosphorylcholine-based surfaces, sulfobetaines, covalently bonded albumin and functional heparin-immobilized materials have been studied extensively as coatings for blood contacting devices to reduce platelet adhesion. Deible et al effectively masked the thrombogenic surface of denuded human placental arteries by covalently attaching PEG-diisocyanate to the exposed surface proteins.[159] The coated arteries had decreased platelet deposition compared to similar arteries exposed to a non-reactive PEG solution. Ye et al reported on the reduction of platelet deposition and bulk-phase platelet activation of silinated 2- methacryloyloxyethyl phosphorylcholine (MPC)- or sulfobetaine - coated $TiAl_6V_4$ compared to uncoated $TiAl_6V_4$.[88] Eberhart et al immobilized albumin through the addition of alkyl groups onto 4 and 5 mm polyetherpolyurethane tubes.[160] The coated tubes showed less thrombogenicity in a canine vascular graft model than non-coated tubes. An oft-used technique for covalent heparin immobilization is the end-point immobilization

method, in which a reactive aldehyde group is exposed on the heparin chain and conjugated to a primary amine on the substrate. This technique was used by Lin et al on a polytetrafluoroethylene small diameter graft and evaluated for platelet deposition and graft patency using a baboon femoral artery graft model.[161] Reduced platelet deposition was found on the coated grafts compared to uncoated at 1 and 4 hrs post implant, and coated graft patency was improved at 4 wks compared to the uncoated grafts.

As described in Section 1.1, among long-term cardiovascular devices, continuous flow VADs are particularly difficult to reduce the risk of thrombosis and thromboembolism due to a combination of fluid dynamics, length of expected support, patient population and small blood volume to surface area ratio.

While the importance of patient selection and pre-operative risk factors continues to be studied (Chapter 4), these investigations are most likely to affect post-operative medical management of anticoagulation. Moreover, consistent anticoagulation has shown to be difficult even in patients without the thrombogenic environment of mechanical circulatory support.[4,10,49] In light of these difficulties, the optimization of the blood contacting material in the pump is an area where small improvements could greatly enhance the biocompatibility performance of VADs. However, A remarkable number of VAD developers use highly polished $TiAl_6V_4$ (e.g. Heartmate II, Jarvik 2000, HeartWare HVAD) as the blood – contacting material despite only moderate hemocompatibility.[82,83,162,163]

A method for accessing time dependent, flow induced platelet adhesion and thrombosis formation on clinically relevant surfaces could improve material evaluation of VADs during design and improve material selection. Since opaque materials are often used in VADs, traditional methods for real time platelet deposition are not applicable. A method for real time

visualization and characterization of platelet deposition onto opaque materials under physiologically–relevant conditions was developed. This was accomplished through the use of a parallel plate flow chamber perfused with a whole blood analog of fluorescently labeled donor platelets with transparent hemoglobin–depleted red blood cells (RBC ghosts) and observed with long working distance epifluorescence microscopy. Real-time platelet deposition onto polished $TiAl_6V_4$ along with several alternative continuous flow VAD materials was then observed and recorded using this novel approach.

5.2   MATERIALS AND METHODS

5.2.1   Platelet collection and fluorescent labeling

Fresh whole blood was collected from healthy donors who had refrained from taking any anti-platelet agents 14 days prior to collection. Platelet-rich-plasma (PRP) was collected by centrifuging citrated blood (0.5 mL Vacutainer tubes, [0.105M] citrate, BD, Franklin Lakes, NJ, USA) at 250xg for 15 min. Platelets were fluorescently labeled by the addition of quinacrine dihydrochloride (0.5 μM final concentration, Sigma-Aldrich, St. Louis, MO, USA) to the PRP.

5.2.2   RBC ghost cell preparation and characterization

Units of packed RBCs (type O-, Valley Biomedical Products & Services, Inc., Winchester, VA, USA) were converted into RBC ghosts through the modification of established protocols.[164-167] Briefly, the RBCs were rinsed and centrifuged (2000xg, 15 min) three times with phosphate

buffered saline without Ca^{2+} or Mg^{2+} (PBS, VWR International LLC., Radnor, PA, USA) and then suspended in PBS at a 50% hematocrit. On ice, the RBC suspension was added 1:10 to a lysing solution composed of 4mM $MgSO_4$, 5X concentrated PBS, and acetic acid (Sigma-Aldrich Co. LLC.) in distilled water with a final osmolality of 40 mOsm and pH of 5.0-5.2. After 5 min, osmolality and pH were increased to physiologic norms (300 mOsm and 7.8, respectively) by the addition of 0.3 mL of 5X concentrated PBS and 2µL of 1M Tris buffer (Thermo Fisher Scientific Inc., Pittsburgh, PA, USA) per mL of cell suspension and incubated on ice for 8 hrs. The cells were then resealed by incubation at 37°C for 1 hr. The suspension was centrifuged at 25400xg for 30 min and the supernatant was discarded. The cells were washed 3 times with PBS (25400xg for 30 min) and stored in PBS with 1 mL/L gentamicin (Thermo Fisher Scientific). The resultant RBC ghosts were observed to be translucent.

Prior to RBC ghost cell creation, an aliquot of native RBCs was set aside for comparative rheological testing. The viscosity of RBC ghosts in human plasma was measured using a cone and plate viscometer (Brookfield Digital Rheometer, Model DV-III, Brookfield Engineering Laboratories, Inc., Stoughton, MA, USA) and compared to native RBCs. The elongation index under various wall shear rates for RBC ghosts and native RBCs was measured using a CSS Optical Rheology System (Linkam Scientific Instruments Ltd., Tadworth, Surrey, UK) and analyzed using ImageJ imaging software (NIH). The elongation index was calculated as (L−W)/(L+W) where L and W are the major and minor axes of the ellipse, respectively.

Additionally, the translucence of the RBC ghosts was verified by replacing the test material on the parallel plate flow chamber with a microscope slide that was pre-loaded with immobilized 5.5 µm beads that fluoresce at the same wavelength as quinacrine dihydrochloride (Fluorescent Yellow Particle Slide; Spherotec, Inc., Lake Forrest IL). The RBC ghosts were

perfused through the parallel plate without quinacrine dihydrochloride - labeled PRPs, so that the only fluorescent signal was the beads on the far wall of the chamber.

5.2.3   Test materials

Six materials or coatings were analyzed: $TiAl_6V_4$ (LaunchPoint Technologies Inc., Goleta, CA, USA), methacryloyloxyethyl phosphorylcholine polymer – coated $TiAl_6V_4$ (MPC-$TiAl_6V_4$), silicon carbide (SiC; CoorsTek, Inc., Golden, CO, USA) alumina (Al_2O_3; LaunchPoint Technologies Inc.), yttria partially stabilized zirconia (YZTP; CoorsTek), and Zirconia Toughened Alumina (ZTA; CoorsTek). MPC-$TiAl_6V_4$ was synthesized using established protocols and graciously donated by Dr. Sang-Ho Ye.[88] The materials evaluated were selected for their physical characteristics, which were generally compatible with use as blood contacting materials in a rotary VAD (see Appendix B). All samples were cleaned with Simple Green (Thermo Fisher Scientific Inc.) and Tergazyme (Alconox, Inc., White Plains, NY, USA) and then sonicated three times with distilled water prior to testing to remove the majority of contaminates. This protocol was based on the cleaning methods used for rotary VADs undergoing preclinical testing.[168]

5.2.4   Parallel plate flow chamber

Several flow chamber designs were tested for compatibility with real-time visualization (see Appendix A). The final parallel plate flow chamber design was similar to that described by Kent et al.[169] The top plate was clear acrylic with angled nylon inflow and outflow luer connectors, and the bottom plate was the interchangeable test material. A simple clamping mechanism held

91

the plates together, with a silicone gasket outlining the channel width and length (5 x 8 mm). Aluminum shim stock was placed between the plates to provide a precisely defined channel height of 0.076 mm (**Figure 5.1**). The flow within this chamber was assumed to be one-dimensional laminar parallel plate flow.[83,169]
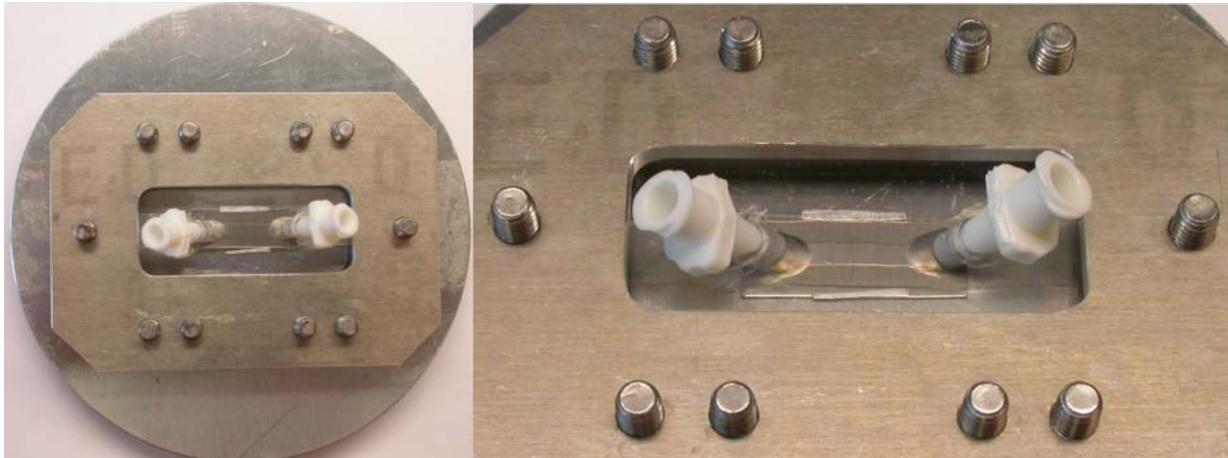
Figure 5.1: Image of the final design of the parallel plate flow chamber. The chamber was clamped between the metal circle and rectangle by screws. Thin aluminum shim stock can be seen along the length of either side of the silicone gasket to ensure precise chamber height.

5.2.5   Blood analog perfusion and image acquisition

The experimental flow path is presented in **Figure 5.2**. All non-test surfaces were pacified by incubation with 1% bovine serum albumin (BSA, microbiological grade powder; MP Biomedicals, LLC, Solon, OH, USA) in PBS for 20 min and rinsed with sterile normal saline prior to perfusion. Quinacrine dihydrochloride - labeled PRP was mixed with RBC ghosts for an end hematocrit of 25%. This suspension was collected into a 20 mL polystyrene syringe (BD Biosciences) and pulled through the parallel plate flow chamber by a syringe pump (Harvard

Apparatus, Holliston, Massachusetts, USA) for 5 min at flow rates of 0.118 and 0.295 mL/min (wall shear rates of 400 sec^{-1} and 1000 sec^{-1} respectively). Platelet adhesion was visualized at approximately 4 mm from the inlet leur, in real time, using an inverted epifluorescence microscope (Olympus IX FLA, Olympus Corporation, Shinjuku, Tokyo, Japan) with a 40x super long working distance objective (PlanFL, phase contrast, working distance 6.5mm - 8.3mm, numerical aperture 0.55, and acceptable coverslip thicknesses of 0-2.6mm; Olympus Corporation) and a 103W HBO short arc mercury lamb light source (OSRAM GmbH, Munich,Germany). Images were acquired every 0.4 sec for 5 min beginning at 1 min after the start of perfusion using a CCD camera (PCO-TECH Inc., Romulus, Michigan, USA).
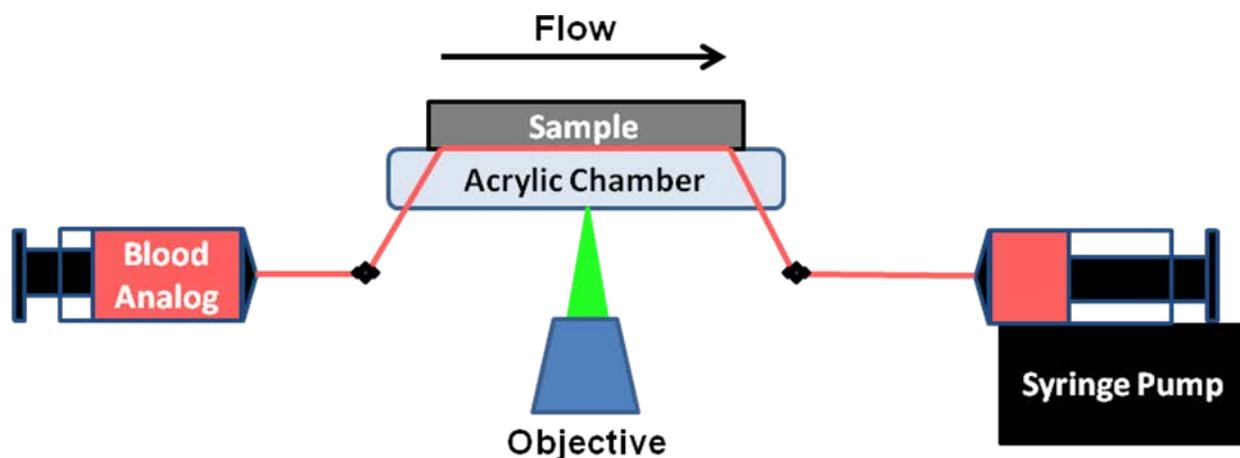
Figure 5.2: Experimental set-up. The virtually transparent blood analog and long working distance objective allowed for real time visualization of adherent fluorescent platelets through the flow path onto the opaque test surface. The blood suspension was perfused through the chamber across the sample for 5 minutes, and real time images were acquired 4mm from the inlet by a CCD camera.

Images were analyzed for the percent of the surface covered by deposited platelets using a custom designed MatLab program (MathWorks, Inc., Natick, MA, USA). Briefly, the images were converted from grayscale to binary (**Figure 5.3 A** and **B**, respectively). All pixels that were

93

brighter than a predetermined threshold were rendered white (platelets) whereas all pixels below that threshold were rendered black. The percent area of white pixels was considered to be equivalent to the percent area of platelet surface coverage. To visually determine the accuracy of the analysis the outline of the original image was overlaid onto the original image (**Figure 5.3 C**).
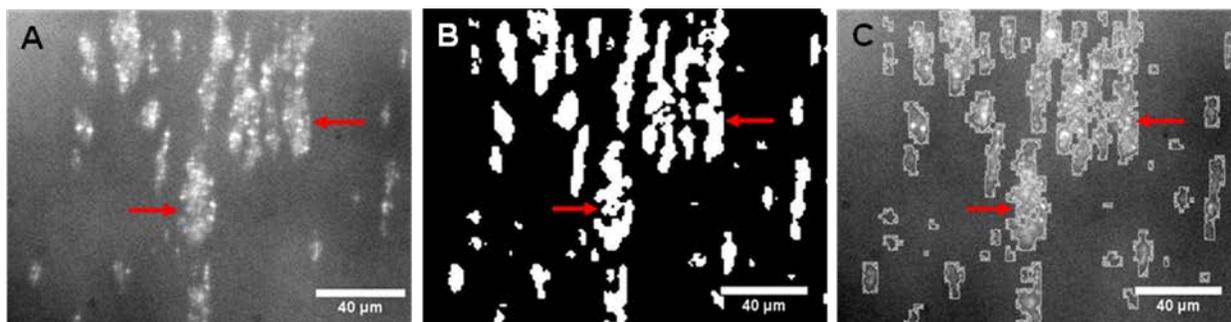
Figure 5.3: Pictorial representation of image analysis and platelet surface coverage calculation. Images were obtained after 5 minutes of perfusion with SiC. (A) Original fluorescent image. (B) Binary image rendered by the MatLab program. (C) Original fluorescent image overlaid with the outline of the binary image.

5.2.6 Scanning electron microscopy

Following perfusion, samples were gently rinsed with PBS and incubated with glutaraldehyde (2.5% in PBS; Sigma-Aldrich) for 10 min. Next, the materials were washed 3x with PBS and dehydrated in consecutive stages of increasing ethanol (Sigma-Aldrich) concentrations. The samples were then chemically dried with hexamethyldisilazane (Thermo Fisher). Finally, the samples were coated with gold-palladium (Hummer VI Sputtering System, TechnicsWest, Inc., San Jose, California, USA) and scanning electron micrographs (SEMs) were obtained (Model JSM6330F, JEOL, Tokyo, Japan).

5.2.7 Flow cytometry

Bulk phase activation of the platelets following the addition of RBC ghosts was measured by flow cytometry using previously described methods.[148] Briefly, PRP was collected from healthy donors using the method described above and separated into two aliquots. RBC ghosts were added to one of the aliquots such that the final hematocrit of the solution was 25%, and sterile saline was added at the same volume to the other aliquot. Each aliquot was then incubated in buffer solution (Tyrode's solution with 1% BSA, Electron Microscopy Science, Hatfield, PA, USA) with fluorescein isothiocyanate – conjugated mouse anti–human CD42b (CD42b, clone LG.3A10; AbD Serotec, Raleigh, NC, USA) and either recombinant phycoerythrin–conjugated (RPE) mouse anti-human CD62P or RPE-conjugated isotype- matched control antibody (CD62P and Mouse IgG$_1$, clones Psel.KO.2.5 and W3/25, respectively; both from AbD Serotec) in the dark for 20 min. The cells were washed with Tryrode's solution with 1% BSA and 0.106 M sodium citrate dehydrate (Thermo Fisher), centrifuged, and the pellet isolated. The cells were re-suspended in 1% paraformaldehyde (Sigma-Aldrich) and stored at 4° C (<24 hr) until analyzed. CD42b+ events (>5000) were collected on a 3-color FACScan (BD Biosciences) and analyzed with WINList software (Verity Software House, Topsham, ME).

5.2.8 Statistical analyses

All data are presented as mean ± standard error of the mean. Rheological data were analyzed by ANOVA. Flow cytometric data were analyzed by Student's T test. SPSS v20 (IBM Corp, Armonk, NY) was used for all statistical analyses.

5.3   RESULTS

5.3.1   RBC ghost cell rheology

To verify that RBC ghosts behaved in flow as native RBCs, the rheological properties of RBC ghosts were examined by comparing their viscosity as a function of shear rate to that of native RBCs. **Figure 5.4 A** depicts the viscosity response of native and ghost RBCs in plasma under shear. No difference between the two curves was found (P=0.61). Similarly, there was no difference in the elongation index of native RBCs when compared to RBC ghosts (**Figure 5.4 B**; P=0.41). This was further confirmed qualitatively (**Figure 5.5 A**). The translucence of the RBC ghosts was also verified qualitatively through the use of immobilized fluorescent yellow beads (**Figure 5B**). Additionally, there was no difference in bulk phase platelet activation between PRP and PRP mixed with RBC ghosts (8.7 ± 0.9% and 7.3 ± 0.9%, respectively; P=0.13).
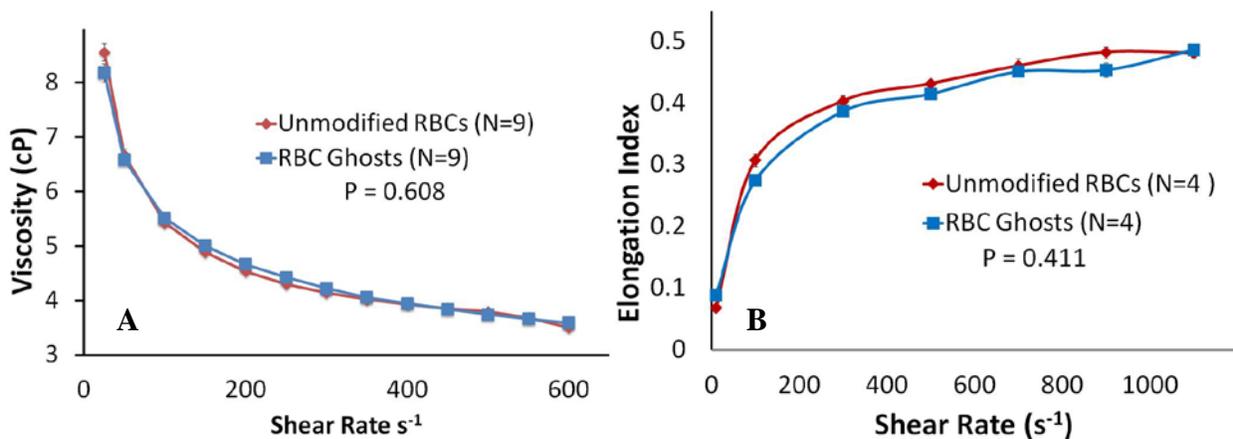
Figure 5.4: Rheological comparison of unmodified red blood cells and ghost red blood cells at varying wall shear rates. (A) Viscosity. (B) Elongation Index. Data are presented as mean ± standard error of the mean. The hematocrit for all samples for both studies was 24%. RBC, red blood cell.
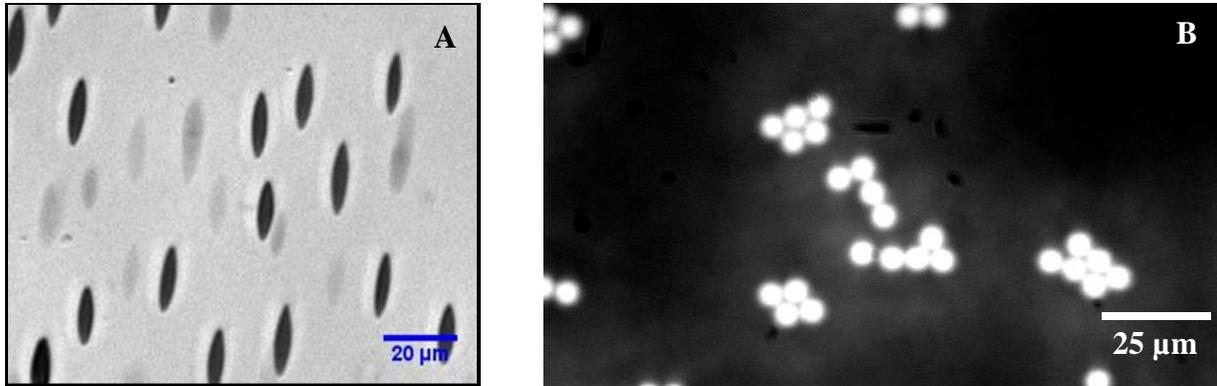
Figure 5.5:Qualitative comparison of unmodified RBCs and RBC ghosts. (A) Unmodified (dark) and ghost (light) RBCs during elongation index studies. (B) Parallel plate flow chamber filled with RBC ghosts to test translucence. Fluorescent beads immobilized on a glass slide was used as the test material to ensure visualization of the far wall of the chamber through the RBC ghosts. RBC, red blood cell.

5.3.2 Acute platelet adhesion onto test surfaces

Representative fluorescent images of platelet adhesion to the 6 opaque test surfaces after 5 min of perfusion at wall shear rates of 400 sec^{-1} and 1000 sec^{-1} are shown in **Figure 5.6**. These results were verified qualitatively through SEM images (**Figure 5.7**). On the videos acquired during these studies, the thrombi grew in elliptical patterns in the direction of flow over time. Embolization occurred infrequently, but was present during the experiments. Sequential photographs acquired along the flow path following some of the experiments suggested that the platelets uniformly reacted with the test materials and were not diffusion-limited from deposited platelets at the inlet of the chamber (**Figure 5.8**).
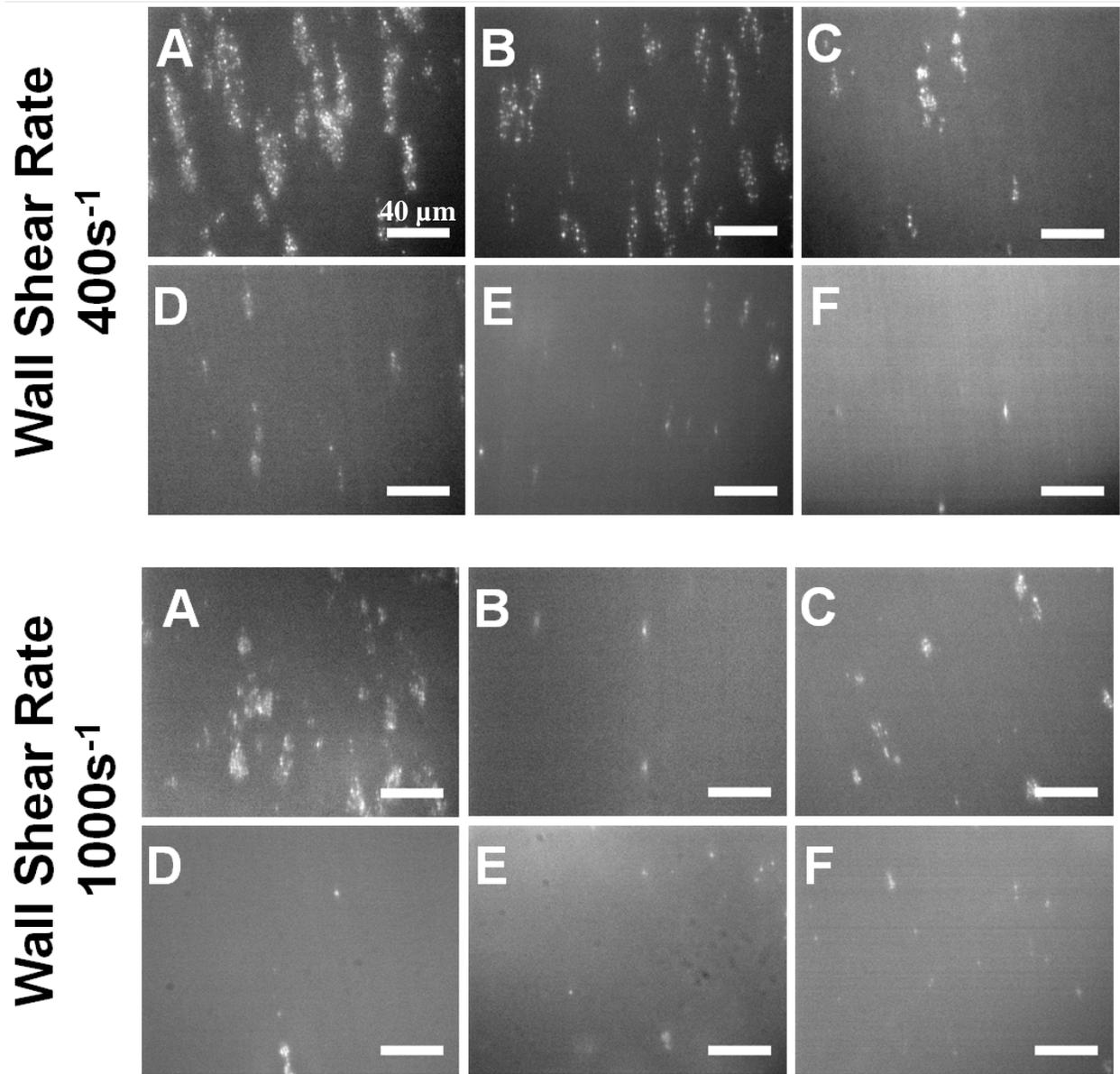
Figure 5.6: Representative fluorescent images of platelets adhered to test surfaces after 5 minutes of perfusion. (A) TiAl$_6$V$_4$. (B) SiC. (C) Al2O3. (D) YZTP. (E) ZTA. (F) MPC.
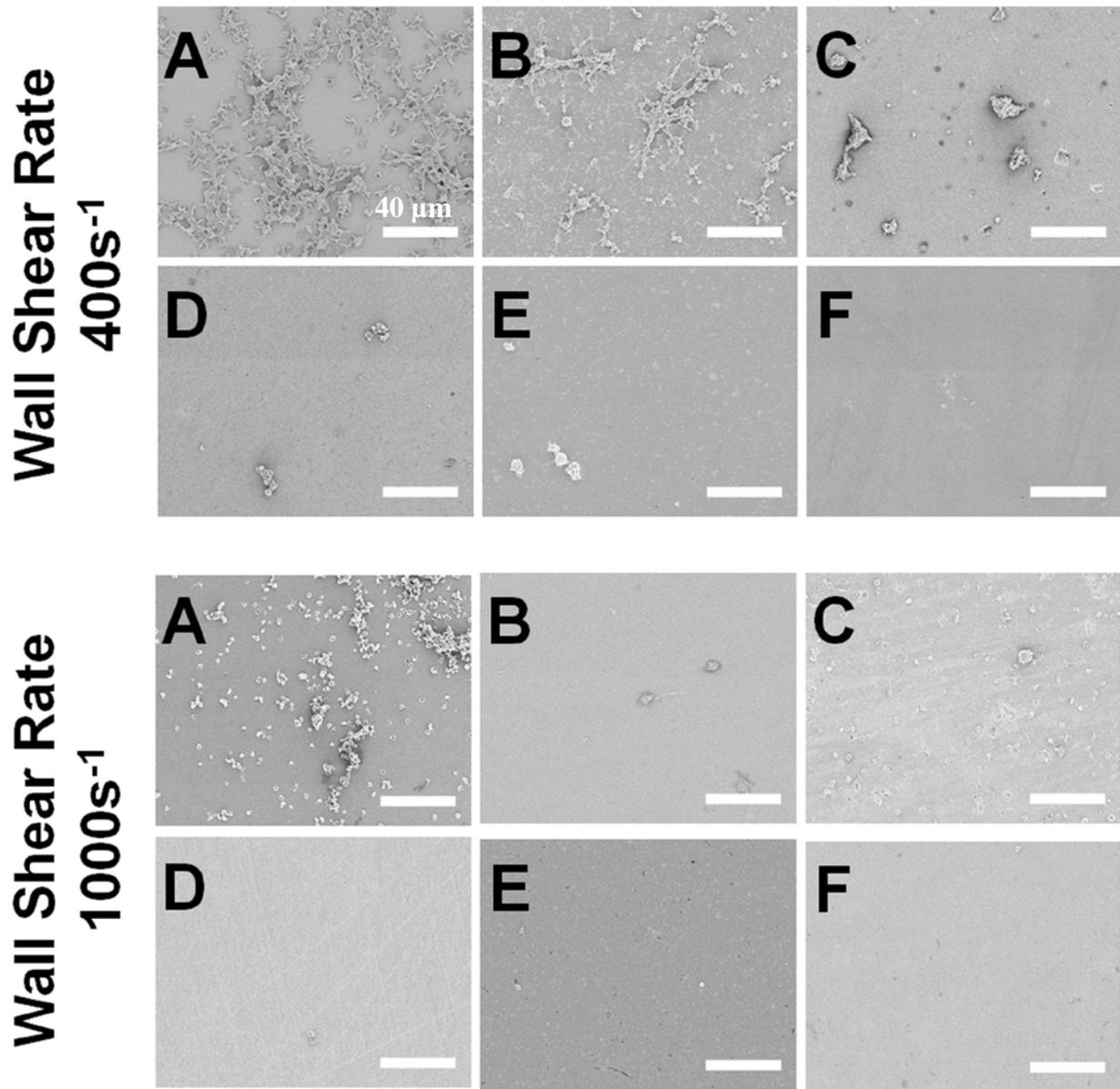
Figure 5.7: Representative SEM micrographs of platelets adhered to test surfaces after 5 minutes of perfusion. (A) TiAl$_6$V$_4$. (B) SiC. (C) Al2O3. (D) YZTP. (E) ZTA. (F) MPC.
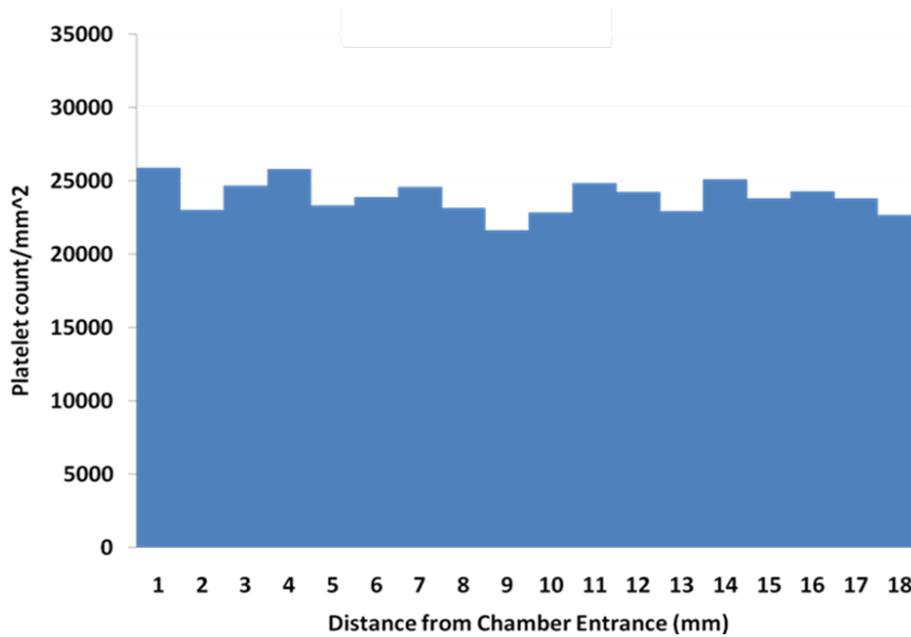
Figure 5.8: Consistent platelet coverage along the length of the parallel plate flow path as determined by sequential epifluorescent photographs following a 5 min perfusion with TiAl$_6$V$_4$.

5.4   DISCUSSION

Previous methods for examining platelet deposition required that the material be transparent, utilized end point analysis, or used PRP instead of blood to perfuse over the surfaces.[170-173] Many cardiac devices require structural and mechanical properties that are not able to be met with transparent materials. Additionally, the number of materials with known thrombogenicity is greatly reduced if opaque materials are not able to be properly evaluated. When end point analysis is used to evaluate these opaque surfaces, much of the information between timepoints is lost, as real time interactions of platelet deposition and possible embolization are not available to the investigator. Observations in these end point systems often involve disruption of the test environment, and increasing the number of observations during a single test may introduce

errors. PRP may be used to provide a clear testing solution and allow for real time observations of platelet-surface interactions, but the test environment may have a reduced relationship to *in vivo* performance, limiting the usefulness of the characterization.

The use of RBC ghosts mixed with PRP allows for a more physiologically–relevant analysis of platelet deposition. Studies utilizing only PRP as the test fluid were not able to mimic the near-wall gradient of platelets caused by interactions with native RBCs during blood flow. RBCs migrate to the center of the flow path, pushing platelets towards the edges and increasing their density near the wall.[165] Models of platelet adhesion suggest that adhesion is dependent on near-wall interactions with RBCs.[174] Another model suggests that near-wall platelet-platelet interactions exhibit longer contact time and total contact area than platelet collisions occurring far from the wall.[175,176] This phenomenon has also been reported with *in vitro* flow systems, where the platelet gradient near the test walls enhances the interactions of the platelets with the test surface and increases deposition.[177,178]

The axial migration of RBCs that promotes platelet transportation away from the center of vessels is due to unique abilities of RBCs to deform and aggregate, producing a shear-thinning effect.[179,180] **(Figure 5.4**) A similar transport phenomenon was assumed between RBC ghosts and platelets due to the similar viscosity and elongation index curves between RBC ghosts and native RBCs. The optically clear RBC ghosts were substituted for native RBCs in order to maintain this phenomenon of an increased platelet surface gradient near the chamber walls.

The parallel plate flow chamber design was employed due to its ability to provide well-developed laminar flow as specified wall shear rates while allowing one side to be interchangeable.[83,181] Tubular flow systems have been used successfully in literature for platelet studies; however, the capillaries are typically transparent or use end-point

analysis.[182,183] Annular flow systems have also been used, with a common variation being the cylinder-in-cylinder. However, these also rely on end-point analysis for determination of platelet deposition.[184] Milner et al have used a spinning disk in PRP to study platelet deposition onto different surfaces.[185,186] The spinning disk technique is attractive as the wall shear rate increases along the radius of each interchangeable disk, allowing for a range of wall shear rates to be tested on a surface during a single experiment. However, this method relies on end-point analysis of the surfaces and the use of PRP as the test fluid. Similarly, cone and plate viscometers have been used for platelet testing with opaque surfaces but also rely on end-point analysis.[187,188] Additionally, Szarvas et al compared the parallel plate flow chamber to the cone-and-plate method and found surface – specific deposition of platelets was best evaluated with the parallel plate flow chamber.[189] They also found that bulk phase aggregation of platelets occurred more readily in the cone-and-plate method, which may introduce error in surface deposition experiments. Zwaginga et al agreed with these observations.[190]

Schaub et al developed a novel technique using a fiber optic bundle attached to an epifluorescent microscope for investigation of the biocompatibility of common mechanical circulatory assist surfaces and vascular graft materials in vitro.[83] This bundle could be inserted through a diaphragm into the flow path of whole blood, allowing the researcher to observe fluorescently labelled platelet deposition temporally on the surface of opaque materials. The investigators looked at several materials such as $TiAl_6V_4$, low temperature isotropic carbon, diamond – like carbon coating on Ti (DLC), polycrystalline carbon coating (PCD) and electrolytically treated titanium alloy (TiO). The polymeric materials tested were used primarily for blood conduits such as expanded polytetraflouroethylene (ePTFE), denucleated ePTFE, woven Dacron and collagen impregnated knitted Dacron (HEM). Using a parallel plate flow

chamber, the investigators were able to observe platelet deposition at 60 s intervals for 5 min, though with limited resolution and field of view. Additionally, this technique requires the observer to disrupt the flow for each observation, which may introduce errors in subsequent timepoints.

5.5   LIMITATIONS

One limitation to this study is that it was an acute *in vitro* analysis. The test materials were subjected to blood analog perfusion for five min, whereas the tested materials would be implanted for much longer periods of time (months to years). However, when determining an alternative material for in vivo testing it would be more ideal to select a surface that has very little platelet surface coverage after 5 min compared to surfaces that promote the formation of large thrombi within the same period of time. Another limitation to this study is that we used a hematocrit of only 25%. Although this is lower than the average hematocrit of healthy individuals, this blood composition is typical for patients implanted with VADs.[191] Another limitation is that this was a 2-dimensional analysis. We were not able to effectively measure thrombus formation in the Z direction, which reduced the information we were able to obtain on each experiment. However, we assumed that any thrombus growth in the Z direction would be the result of platelet-platelet interactions and would be minimally affected by the properties of the test material.

5.6   CONCLUSIONS

Determining the *in vitro* thrombogenicity of surfaces is an important step in developing and selecting new materials for use in blood-wetted devices. A method was developed for the analysis of time- and flow- dependent platelet adhesion on opaque surfaces in real time. This method allows for an increased number of biomaterials to be examined in vitro under physiologically–relevant conditions. An improved understanding and characterization of acute thrombogenicity of opaque materials may encourage innovation in the utilization of alternative materials in cardiac device design.

6.0   CONTINUED RESEARCH AND FUTURE DIRECTIONS

The studies presented in the previous sections add to the scientific knowledge of the body's immunological and hemostatic response to VAD implantation. This information also lays the groundwork for additional research that will continue to advance the field. The following are research opportunities outside of the objectives of this dissertation that have become available as a result of the work contained herein.

6.1   IMMUNOLOGICAL RESPONSES TO VAD IMPLANTATION

6.1.1   Impact of VAD support on granulocyte activation, dysfunction and apoptosis

As stated previously, inspiration for this research came, in part, from a series of in vitro studies from Shive et al. revealing an increase in apoptosis and dysfunction among granulocytes and monocytes exposed to high fluid shear stresses.[106,107,192] The first paper in the series revealed that bacteria has a stronger ability to adhere to artificial surfaces (specifically segmented polyurethane (PEUU)) under high fluid shear stresses than polymorphonucleocytes (PMNs).[192] The study went on to show a decrease in the ability of PMNs pre-exposed to high fluid shear stresses to produce reactive oxygen species (ROS) when stimulated. (**Table 6.A**) Though the PMNs pre-exposed to high shear stresses exhibited a diminished ability to produce

ROS upon stimulation. Interestingly, the shear stresses investigated were designed to be physiologically relevant and possibly far below the super-physiologic shear forces exhibited by VADs. The authors suggest that an inverse relationship may exist between PMN stimulation dysfunction and shear stress exposure.

Table 6.A: ROS released from PMNs before and after exposure to shear flow. From Shive et al. [192]

Stimulus-Induced Superoxide (SO) Release (nm SO/10^6 cells) by Fresh and Preexposed* PMNs on PEUU-A′

Stimulus	Fresh Incubation Time (min)				Preexposed Incubation Time (min)			
	5	30	60	120	5	30	60	120
None	2.4 ± 0.6	7.1 ± 1.6	12.4 ± 2.4	15.3 ± 1.8	3.9 ± 0.3	6.1 ± 1.1	7.4 ± 1.2	10.2 ± 1.6
Bacteria	2.4 ± 0.4	12.5 ± 1.5[b,f]	15.4 ± 1.5	16.8 ± 1.3	3.7 ± 0.9	9.9 ± 1.6[b]	14.4 ± 1.4[e]	14.0 ± 2.2
PMA[a]	9.5 ± 2.6	19.6 ± 2.4[c]	28.7 ± 2.3[d]	36.8 ± 4.1	9.0 ± 2.4	14.9 ± 1.3[d]	22.7 ± 2.3[c]	30.7 ± 2.1[d]

Data are expressed as mean ± SEM; $n \geq 5$.
Significant differences:
   [a]All time points: $p < .05$ or $p < .001$ compared to no stimulus; $p < .05$ or $p < .01$ compared to bacteria.
   [b]$p < .0001$ compared to previous time point.
   [c]$p < .01$ compared to previous time point.
   [d]$p < .05$ compared to previous time point.
   [e]$p < .01$ compared to exposed PMNs, no stimulus.
   [f]$p < .05$ compared to fresh PMNs, no stimulus.
*PMNs were exposed to PEUU-A′ under shear stress (0–18 dynes/cm^2) at 37°C for 60 min. Nonadherent PMNs were removed and incubated on either PEUU-A′ alone, PEUU-A′ with preseeded *Staphylococcus epidermidis*, or incubated on PEUU-A′ and stimulated with PMA. Fresh cells were not exposed to shear stress.

The inability of neutrophils to remain adherent to PEUU under shear forces prompted further investigation from this same research group. As a result, Shive et al found that neutrophils adhered to PEUU underwent shear-dependent apoptosis. (**Figure 6.1**) In an elegant study, the authors report nearly total apoptosis of adherent neutrophils at relatively low shear stresses, with the neutrophils exhibiting a more pronounced apoptotic response to shear than to standard chemical induction. The authors hypothesized that the artificial surfaces found in cardiac devices may induce apoptosis among neutrophils, decreasing the population of innate immune cells available to defend against invasion from microbes. Since neutrophils make up the

vast majority of the immune system's initial response to microbe infiltration, apoptosis of these

cells may leave the host at a much higher risk of infection.
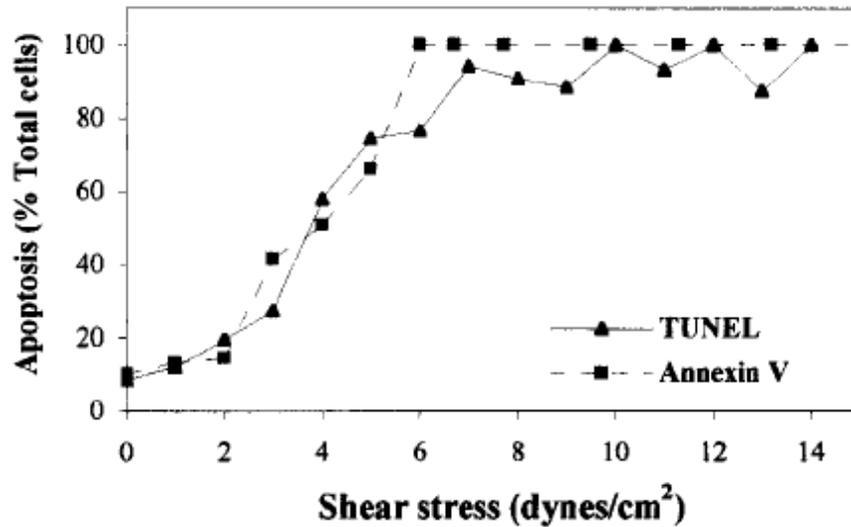
Figure 6.1: Shear-dependent apoptosis of neutrophils adhered to PEUU. From Shive et al. [107]

Similarly, a third report by Shive et al investigated the effect of fluid shear stress on

monocyte adhesion and apoptosis.[106] The authors reported a shear-dependent apoptotic

response among adherent monocytes comparable to but weaker than the response displayed by

neutrophils. Again the authors hypothesized that apoptotic reduction of the number of available

monocytes may expose the host to an increased risk of infection.
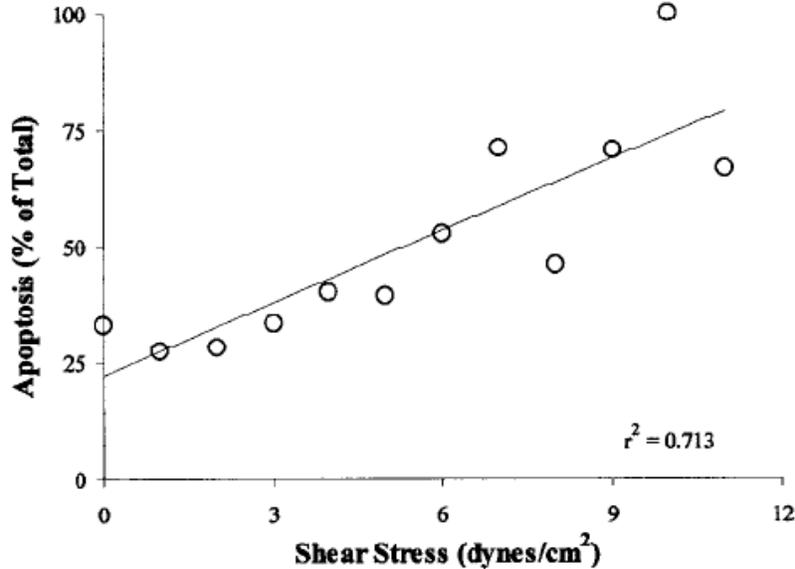
Figure 6.2: Shear-dependent apoptosis of monocytes adhered to PEUU. From Shive et al. [106]

As state previously, expression of MAC-1 has been reported to be a modulator of granulocyte apoptosis. MAC-1 expression on granulocytes was not reported by Shive et al, nor was it investigated in rotary VAD patients prior to the studies described in Section 3.0. The elevated levels of MAC-1 expression found in HeartMate II patients (and to a lesser extent, HeartWare and Thoratec pneumatic) suggest that these patients will likely also have an elevated percentage of apoptotic granulocytes. Interestingly, among the leukocyte-derived microparticles described by Diehl et al, many expressed MAC-1.[136] Although the specific leukocyte origins of the microparticles were not reported, these may be the apoptotic remnants of activated circulating granulocytes.

The first report by Shive et al suggests that granulocyte dysfunction may also be increased following VAD implantation.[192] The elevated levels of MAC-1 expression found on HeartMate II patients were not associated with infection, and were therefore assumed to be

expressed in error by cell to other stimuli. Similarly, circulating granulocytes may also be induced to release their ROS contents through interactions with the VAD surface or shear stresses in the pump. Studies involving cardiopulmonary bypass have reported a decreased ROS response by granulocytes to stimuli.[193] Further studies into granulocyte dysfunction could include an investigation of granulocyte ROS response before and after VAD implantation.

In addition to the granulocyte data presented in Section 3.0, monocyte expression of MAC-1 in VAD patients following implantation was also measured, though with limited success. **Figure 6.3** shows the long- and short-term expression of MAC-1 in VAD patients. Though the overall trend appears to be reduction in monocyte activation following VAD support, no differences could be found either with respect to time or by device implanted. One possible reason for this was that the available monocyte population for each patient slowly disappeared following implantation. It was common for implanted patients to have less than 300 monocytes per 100 µL of blood as determined by FSC, SSC and expression of CD14 by flow cytometry (suggested analysis is at least 2000 cells). There are two probable explanations for the disappearing monocytes. The first cause could be that monocytes were lost during the processing of the flow cytometry samples. Monocytes are notoriously difficult to handle as they are known to adhere to most surfaces, and would be even stickier if they were activated from the presence of the VAD. Many of the monocytes may have simply stuck to the sides of the blood collection tubes and the polystyrene tubes used for flow cytometry analysis. Another possibility is that the monocyte population decreased over time due to shear-induced apoptosis, similar to that described by the in vitro studies by Shive et al.[106] Other studies have shown monocyte activation following VAD implantation, though these were conducted

with patients implanted with previous-generation devices.[57] This possibility may also help to explain the trend towards a reduction in monocyte expression of MAC-1, as the activated monocytes may have been quickly removed from circulation and were slow to return to a normal population. Unfortunately, in the hands of this author, the number of events available for analysis was too small and the data was had too high of a variance to make an definitive statements, but this topic may be of interest to in future studies.
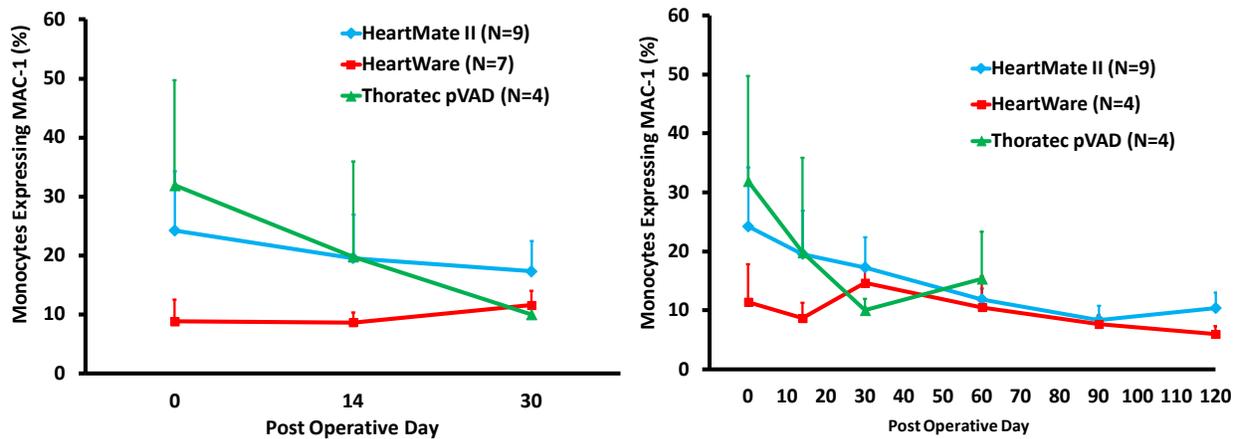
Figure 6.3: Macrophage antigen-1 (MAC-1) expression on circulating monocytes in a subset of ventricular assist device patients following implantation. (A) MAC-1 expression in all three devices evaluated to 1 month post-implant. (B) MAC-1 expression in HMII and HW patients to postoperative day 120, and PVAD to day 60. Data presented as mean plus standard error of the mean. The "0" on the abscissa indicates preoperative values. HMII, HeartMate II; HW, HeartWare; PVAD, Thoratec pneumatic VAD.

6.2   THROMBOSIS AND HEMOSTASIS FOLLOWING VAD IMPLANTATION

A striking result among the data presented in Section 4.0 was the overwhelming influence of pre-operative hepatic health on post-operative blood product consumption and bleeding

complications. This author had hypothesized that the type of device would be the determining factor for bleeding and thrombosis experienced by patients following implantation. The different flow fields, blood-contacting materials and shear rates between pulsatile and continuous flow VADs were expected to produce different adverse event rates as well as different concentrations of plasma indicators of thrombosis. Moreover, these differences between VAD types had already been found to have contributed to the immunological differences presented in Section 3.0. Instead, patient-related factors proved to have a great influence on the immediate post-operative clinical course of the patient. Utilization of the health assessment scores for patients as a predictor of bleeding may be an important tool for proper post-operative treatment of VAD patients.

Future studies building off of the data presented here could measure the circulating levels of various liver-dependent coagulation factors temporally in VAD patients following implantation. The main aim of the study would be to correlate pre-operative measures of liver health (e.g. MELD score) with post-operative coagulation factor levels and bleed product consumption. Coagulation proteins synthesized in the liver and therefore candidates for measurement would be factors I (fibrinogen), II, V, VII, IX, X and XI, as well as proteins C and S, and antithrombin. One variation of this study would be to measure the coagulation factors a frequent timepoints throughout the peri-operative period to determine the average time required to for each factor to reach hemostasis. While the administration of factor-rich products may artificially inflate some of the values, these products appear to be only minimally effective at correcting hemostatic imbalance in the face of hepatic dysfunction.

Another variation on this study would be to measure these same factors at much later timepoints such as at 1, 3 and 6 months of support. The rationale for this approach builds upon a

study by Yang et al that investigated changes to measures of hepatic health (including MELD score) after VAD implantation.[146] The authors found some signs of worsening liver function (such as hyperbilirubinemia) at 30 days post-implantation, and these values did not improve until 3 to 6 months after implant. (**Table 6.B**) A similar trend may exist among clotting factors.

Table 6.B: Dynamics of patient variables before and after VAD implantation. From Yang et al. [146]

Variables[a]	Pre-VAD	30 days on-VAD	p-value[b]	Late on-VAD	p-value[c]
Albumin, mg/dl	3.5 ± 0.6	3.4 ± 0.5	0.0001	3.9 ± 0.7	<0.0001
Total protein, mg/dl	6.4 ± 1.3	6.7 ± 1.0	0.0759	7.3 ± 1.1	<0.0001
AST, IU/liter	75 ± 191	34 ± 35	0.0021	40 ± 98	0.0742
ALT, IU/liter	89 ± 245	27 ± 24	0.0003	34 ± 67	0.0057
Alkaline phosphatase, IU/liter	94.6 ± 52.9	156.9 ± 217.9	<0.0001	120.5 ± 88.3	<0.0001
Bilirubin, mg/dl					
Total	1.7 ± 1.2	2.2 ± 6.1	0.4472	1.0 ± 0.9	<0.0001
Direct	0.6 ± 0.6	1.0 ± 3.2	0.3631	0.3 ± 0.5	<0.0001
White blood cell count, $10^3/\mu L$	9.4 ± 3.7	10.1 ± 4.2	0.0254	8.5 ± 3.5	0.0029
Hemoglobin, g/dl	11.2 ± 1.9	10.2 ± 1.5	<0.0001	11.3 ± 1.9	0.5760
Hematocrit, %	33.9 ± 5.4	32.3 ± 4.5	<0.0001	35.1 ± 5.6	0.0508
Platelet count, $10^3/\mu L$	197 ± 84	285 ± 113	<0.0001	230 ± 88	0.0027
International normalized ratio	1.36 ± 0.40	1.67 ± 0.69	<0.0001	1.53 ± 0.56	<0.0001
Pulsatile HM	1.42 ± 0.46	1.38 ± 0.54	0.7254	1.34 ± 0.46	0.2401
HM II	1.28 ± 0.30	1.98 ± 0.70	<0.0001	1.82 ± 0.58	<0.0001
Blood urea nitrogen, mg/dl	38 ± 20	23 ± 15	<0.0001	24 ± 13	<0.0001
Creatinine, mg/dl	1.6 ± 0.6	1.3 ± 0.7	<0.0001	1.3 ± 0.6	<0.0001
Sodium, mg/dl	133 ± 5	137 ± 3	<0.0001	137 ± 3	<0.0001
Potassium, mg/dl	4.2 ± 0.5	4.2 ± 0.5	0.1203	4.3 ± 0.7	0.0547
MELD	14.7 ± 5.4	14.7 ± 5.4	0.7615	13.5 ± 4.9	0.0294
MELD-XI	15.8 ± 5.6	14.0 ± 5.4	<0.0001	13.3 ± 3.9	<0.0001

ALT, alanine aminotransferase; AST, aspartate aminotransferase; HM, HeartMate; HMII, HeartMate II; MELD, Model of End-stage Liver Disease (MELD); MELD-XI, Model of End-stage Liver Disease eXcluding INR.
[a]Values are shown as mean ± standard deviation.
[b]p-value for comparison pre-VAD vs on-VAD 30 days.
[c]p-value for comparison pre-VAD vs late on-VAD.

Despite the relative homogeneity of bleeding and thrombosis responses between VADs found in Section 4.0, device design may still be a significant contributing factor to a VADs overall thrombogenicity. Determination of this thrombogenicity in patients may only be possible at much further timepoints than those presented in recent literature. If liver dysfunction remains persistent in VAD patients at 2 to 3 months post-implantation as suggested by Yang et al, then

any attempt at measuring indices of thrombosis between implanted devices before this time may be masked by patient-related effects.[146] Interestingly, differences in D-dimer levels among the patients presented in Section 4.0 did not become significant until 25 and 55 days post-implant, with trends suggesting that the HeartMate II would continue to have elevated values over the other pumps. (**Figure 4.4**) Studies with longer periods between implantation and assessment timepoints may help to reveal thrombotic differences between pump designs by allowing the patient-related effects enough time to subside. A combination of long-term measurements of coagulation factors combined with longitudinal assessment of VAD thrombogenicity may eventually allow clinicians to understand the transition from patient-dominant effects to pump-dominant effects. This information may then allow clinicians to alter anticoagulation and anti-platelet regimens to match the source of hemostatic imbalance.

6.3   REAL-TIME VISUALIZATION OF PLATELET DEPOSITION ONTO OPAQUE SURFACES UNDER FLOW

The suspension composed of red blood cell ghosts and platelet rich plasma described in Section 5.0 proved to be an acceptable blood analog for use in platelet deposition studies. Section 5.3.1 described the similarity in rheological properties between the unmodified and ghost red blood cells. Several studies have found an increase in the amount of circulating leukocyte- and platelet-derived microparticles in patients implanted with continuous-flow VADs.[136,194] (**Figure 6.4**) Other investigators have suggested that microparticles encourage a pro-thrombotic state in the cardiac patients through exposure of phosphatidylserine surfaces and tissue factor expression.[195,196] In order to further improve on the blood analog solution as a model of a

113

VAD patient's native blood composition, the addition of leukocyte- and platelet-derived microparticles could be added to enhance the reactivity of the platelets with the artificial surfaces. Creation of the microparticles and determination of microparticle concentration could be performed using established protocols. The microparticles could be added to the suspension immediately prior to the perfusion, or it could be joined to the perfusion solution through a Y connection proximal to the flow chamber. The influence of microparticles on platelet deposition could be studied by keeping the test material constant and varying the microparticle concentration in the blood analog (between no microparticles (control) and low, medium and high concentrations derived from literature).
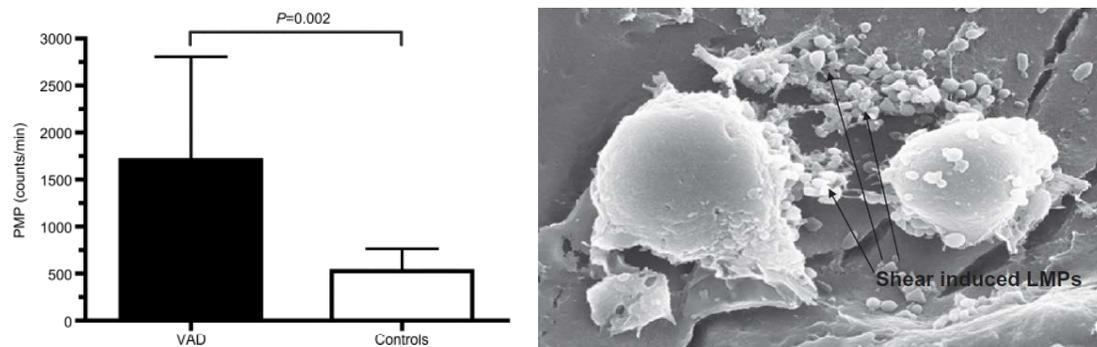
Figure 6.4: (Left) Increase in platelet-derived microparticles between VAD patients and heart failure controls. From Deihl et al.[136] (Right) Example of leukocyte-derived microparticles following 6 hours of in vitro human blood circulation with the VentrAssist LVAD. From Chan et al.[194] PMP, platelet-derived microparticles; LMP, leukocyte-derived microparticles.

Many cardiac devices are composed of assembled or mated components which inevitably creates crevices along the flow path. These crevices may become a nidus for thrombus formation through flow disruption or stagnation. Application of the method described in Section 5.0 to a step or crevice could help to better understand thrombus dynamics around this common

geometry in cardiac devices. To help visualize the development of the thrombus over time, the red blood cell ghost and platelet rich plasmas suspension could be divided into three aliquots, with each aliquot labeled with a dye with different spectral characteristics. Each aliquot could then be successively perfused over the crevice or step. Rotation of the microscope filter set could allow tracking of platelet deposition from the current dye as well as tracking of differently labeled dyes from earlier in the experiment. This experiment may be able to help provide information on the progression of thrombus formation. Periodic collection of the effluent and subsequent analysis with flow cytometry may allow for mapping of the composition of the emboli and provide information on the dynamics of platelet embolization.

7.0 FINAL CONCLUSIONS

Ventricular Assist Devices (VADs) have become an established treatment for advanced heart failure, prolonging the life of patients when used as a bridge to transplantation or as destination therapy. VAD support is challenging due to the amount of surface area exposed to blood and the intended length of time for support, representing one of the most difficult environments in which to place a medical device. Even though device enhancements and increased experience among implanting institutions has improved the overall quality of life for patients support by VADs, these patients remain vulnerable to biological complications present during the infancy of this technology.

Infection remains an ongoing risk during VAD support, regardless of the length of support. While there are many factors that influence a patient's risk for infection, few studies have reported on the impact of VAD implantation on leukocyte function and number, and many of these studies involved previous generation devices.

A series of studies with HeartMate XVE patients focused on selective reductions in adaptive immune cell populations following implantation. Ankersmit et al found a significant and specific decrease in CD4+ T cells.[101] Subsequent reports revealed that the CD4+ T cell depletion may have caused non-specific B cell hyperactivity in these patients. The effects of this immune state were found to be longer transplant wait times and hospital stays, both of which increase health risks and costs to the patient.

The Ankersmit et al study was used as template to study the effect of implantation of the currently-utilized HeartMate II rotary LVAD on circulating T cells.[101] HeartMate II patients exhibited similar pre-operative levels of circulating adaptive immune cells as well as CD4/CD8 T cell ratio. However, HeartMate II patients did not exhibit the same selective reduction in CD4 T cells as was found in HeartMate XVE patients. When extended to 4 months after implantation, no differences were found in CD4 or CD8 T cell levels. Even though there appeared to be a different response in adaptive immune cells between implantation of the HeartMate XVE and the HeartMate II, the HeartMate II patients in this study still experienced a substantial risk to infection. Sensitization following HeartMate II implantation also remained a problem.

Given the vastly different flow patterns, shear stresses and blood contacting surfaces of the two VADs, it was not surprising that the two sets of patients responded differently following implantation. The unregulated pseudo-endothelialization of the surfaces of the pulsatile HeartMate XVE combined with longer contact time between this bioactive surface and circulating blood components may have contributed to a reduction in circulating CD4 T cell numbers by selective apoptosis. In contrast, the polished titanium of the rotary HeartMate II resists cellular adhesion and prolonged leukocyte interactions. Despite these differences, the HeartMate II patients continued to be plagued by similar infection and sensitization outcomes found in earlier generation devices such as the HeartMate XVE. This research suggests that there may still be immunological compromise among current-generation VAD patients, but these alterations may be influenced more by the response of innate immune cells following implantation rather than the adaptive immune system.

There is a paucity of research presented on the response of circulating leukocytes following VAD implantation. Many studies understandably focus on the occurrence of infections

in VAD patients, with information like location, severity, frequency and outcomes; however, these studies largely ignore investigating the underlying cellular impact of VAD support. The cause for infection was often assumed to be the existence of a percutaneous driveline providing a pathway for infectious agent migration. Few studies presented temporal immune cell data in VAD patients, and even fewer investigated the response of the innate immune system following VAD support.

This research found that the systemic immunological response to VAD placement, either through surgical insult or the presence of the device, to be substantial and more pronounced than other cardiac surgeries. The sharp rise in circulating leukocytes presented in this research has been presented in other reports of valve replacement surgeries or cardiopulmonary bypass support, but the average time for resolution of this spike was much shorter than was found in VAD patients.

Additionally, the type of device implanted may influence post-operative immune response experienced by the patient. Granulocyte activation, as measured by expression of macrophage antigen-1, was significantly higher in HeartMate II patients than those supported with either a HeartWare or Thoratec pneumatic LVAD, and lasted for a longer period of time than levels reported for cardiopulmonary bypass circuits. Expression of macrophage antigen-1 mediates extravasation of the circulating granulocytes into surrounding tissue beds, reducing the number available for immune defense and promoting edema. Expression of macrophage antigen-1 can also be a precursor to apoptosis, further reducing infection resistance. This may help to explain the similar occurrence of infection events between the HeartMate II and Thoratec pneumatic LVAD patients even though the HeartMate II has a substantially smaller driveline exit site. In contrast, HeartWare patients exhibited little granulocyte activation and significantly less

infection events than either the HeartMate II or the Thoratec pneumatic LVAD. This research suggests that circulating immune cell activation and infection risk may be influenced by VAD design, though the principle variables and factors involved have not yet been determined.

VAD patients also remain at considerable risk for bleeding and thromboembolic complications. VAD support is typically reserved for some of the very sickest patients, often with pre-operative conditions predisposing to coagulopathies. Investigation into pre-operative indices that could predict post-operative bleeding and thromboembolic complications could be of benefit to clinicians to improve patient selection and post-implant patient hemostasis and anticoagulation management. Recent studies have demonstrated a correlation between the Model for End-Stage Liver Disease (MELD) score with peri-operative bleeding and post-operative morbidity and mortality. High MELD scores may indicate multi-organ failure and hepatic congestion. Liver impairment may in turn lead to hemostatic imbalance and disregulation.

This research found that pre-operative hepatic and renal dysfunction appears to have immediate and long lasting hemostatic effects on patients implanted with the HeartMate II, HeartWare or Thoratec pneumatic LVADs. MELD score was a positive predictor of post-operative blood product administration, chest tube drainage and bleeding adverse events regardless of the VAD implanted. When multivariate linear regression analysis was performed on total blood product administration, MELD score was a significant pre-operative predictor along with age and mean pulmonary artery pressure. VAD patients with high pre-operative MELD scores exhibited significantly different temporal trends of thrombin generation and platelet counts, as well as protracted fibrinolysis. Though the rate of adverse events decreased markedly after the first 2 days of implantation, the sub-clinical effects of a high pre-operative MELD score on the hemostatic system appeared to be persistent, though the manifestation of this

influence is still to be determined. Surprisingly, the type of VAD implanted during this study was not a significant factor in any of the peri-operative bleeding measurements despite very different surgical implantation techniques and VAD hemodynamic profiles. Similarly, no difference was found between devices among the hemostatic markers followed except for higher D-dimer concentrations in HeartMate II patients at further timepoints, which may reflect ongoing fibrinolysis at the unique textured inflow cannula.

Heavy reliance on anticoagulation medications to balance hemostasis in VAD patients is a common and imperfect solution to prevention of thromboembolic complications. Prolonged therapeutic anticoagulation is often difficult, and patients that fall outside of the therapeutic range are often at great risk for hemorrhagic or thromboembolic stroke. The utilization of surfaces other than titanium as the blood contacting surfaces of circulatory support devices may improve the hemocompatibility performance of these devices, possibly decreasing the necessity of anticoagulation and anti-platelet agents and improving outcomes. Since many potential device materials are opaque, development of an in vitro method for assessing these materials could be of considerable value to VAD designers.

Prior methods for examining platelet deposition required that the material be transparent, utilized end point analysis, or used platelet rich plasma instead of blood to perfuse over the surfaces. End point analysis may produce misleading results due to the limited information provided, and platelet rich plasma had a reduced near-wall platelet gradient compared to whole blood. This research produced a method for the analysis of time- and flow- dependent platelet adhesion on opaque surfaces in real time using a physiologically-relevant blood analog solution. The blood analog solution was composed of optically transparent red blood cell ghosts and fluorescently dyed platelet rich plasma. The red blood cell ghosts exhibited rheological

properties similar to unmodified red blood cells. A parallel plate flow chamber was developed that allowed for visualization of the surface of the opaque test materials through the flow path using an inverted microscope with a long working distance objective. This method produced videos of platelet deposition onto a variety of opaque test materials such as $TiAl_6V_4$, zirconia-toughened alumina, yttria partially stabilized zirconia, alumina, silicon carbide and methacryloyloxyethyl phosphorylcholine polymer – coated $TiAl_6V_4$ at wall shear rates of 400 and 1000 s^{-1}. The final images of these videos were confirmed through scanning electron micrographs. This novel method for observing platelet deposition allows for an increased number of biomaterials to be examined in vitro under physiologically–relevant conditions. Assessment and utilization of less-thrombogenic materials as the blood contacting surfaces of cardiac devices (such as VADs) could greatly improve the performance of these devices in the patient. Since many cardiac devices are metallic, this newly developed method for assessment of platelet deposition could encourage innovation in material selection.

This body of research presented above may impact the VAD community through a variety of pathways. Hopefully these chapters will spark further investigations on immunological changes in VAD patients. Future research on immune cell responses to VAD implantation may focus on the innate immune cells and shift away from the adaptive system. The author does not suggest that VADs do not impact the adaptive system; rather, by underlining the uniqueness of the HeartMate XVE LVAD, this research should encourage the formation of new theories and paradigms to investigate in currently-utilized devices. These new paradigms may feature a renewed appreciation for alterations in innate immune cells exposed to artificial surfaces and super-physiological shear rates. Further research into these alterations may influence future VAD design to prevent infection as leukocyte responses appear to be device-specific.

121

This research may impact future clinical research and practice by highlighting the importance of pre-operative hepatic health of the VAD patient on post-implant hemostasis. While the association of hepatic dysfunction with morbidity and mortality among VAD patients has been presented previously, this research investigated the influence of hepatic dysfunction on blood product consumption and circulating biomarkers of hemostasis in current generation VADs. This research may help to encourage referring physicians to consider VAD support in advanced heart failure patients prior to the onset of hepatic congestion. Clinicians may be able to better predict the blood product requirements and anticipated coagulopathies for VAD patients and develop therapies to reduce these requirements prior to surgery. Also of note for clinicians is that the pre-operative hepatic health of the patient was a much stronger predictor of blood product consumption than the type of device implanted. This suggests that any perceived hemocompatibility advantages between VAD designs may not be realized until later in the support period.

The ability to assess platelet deposition onto opaque materials in real time under varying shear conditions may impact future material design and selection for cardiac devices as well as encourage further research of platelet interactions with artificial surfaces. This novel method may help to promote innovation among cardiac device developers as new materials may be assessed in vitro for thrombogenicity. The in vitro assessments may also help to improve resource efficiency during device development as many previous device designers had to rely on unreliable end-point analysis experiments or risk catastrophe in expensive pre-clinical animal studies. This novel method has been successfully used to identify four materials with better biocompatibility performance than the oft-used $TiAl_6V_4$ as a blood contacting surface, while another surface that was superior to $TiAl_6V_4$ by end-point analysis may actually be much worse

as it encourages platelet build-up and embolization. Further application of this assessment method may be to investigate the influence of steps and crevices on thrombus formation on opaque surfaces, such as those found along the seams of joining components of VADs.

APPENDIX A

PARALLEL PLATE CHAMBER DESIGN RATIONALE AND HISTORY

A.1   INTRODUCTION

As discussed in Chapter 5, the parallel plate flow chamber design was employed due to its ability to provide accurate control of instantaneous flow conditions while allowing one side of the chamber to be interchangeable (as opposed to tubular and annular flow chambers). Several chamber designs in the literature were attractive, most notably the Poiseuille flow from the design by Chung et al that allowed for a wide, uniform distribution of wall shear forces (**Figure 1, left**); however problems with this design were the crevices present from the way samples were held in the flow field and possible recirculation in the temporary reservoir above the inlet opening.[181]   Both of these problems would possibly introduce increased activation of the platelets through stagnation or recirculation zones. These recirculation zones could increase the local concentration of platelet activating agents released from alpha and dense granules from deposited platelets. Instead, the design of the parallel plate chamber was similar to that used by Schaub et al (**Figure 1, right**), except without the ports for introducing the fiber optic bundle (Schaub et al).[83] However, this chamber design contained a small step where a gasket was necessary to seal the chamber where the material and the chamber meet, both at the inlet and

outlet. The effects of this step on the assessment of the materials may be limited by decreasing the size of the step as much as possible and by examining the surface of the test materials far enough away from the entrance that any flow disruption has diminished and laminar flow may be assumed.
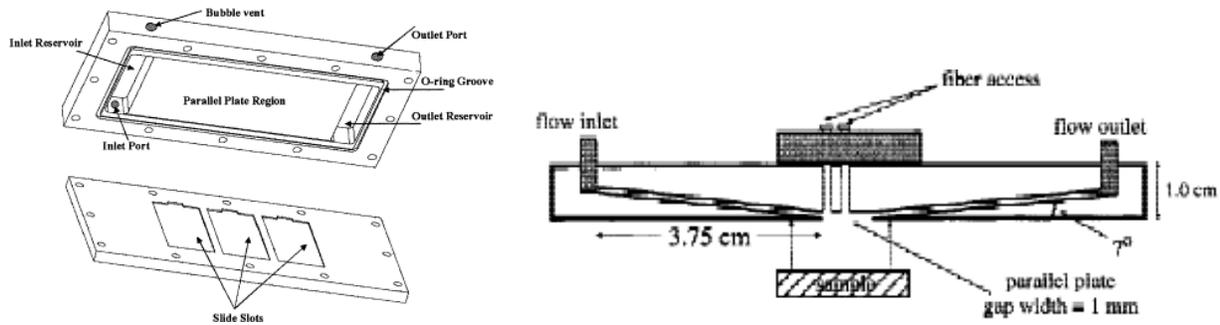
Figure 7.1: The flow chambers used by Chung et al (left) and Schaub et al (right) [83,181]

Numerically, the design of the flow chamber can be reduced to the three parameters of plate shear stress, Reynolds number and entrance length [197], which are defined as:

Equation 1: Wall Shear Stress

$$\tau_w = \frac{6\mu Q}{w h^2}$$

Equation 2: Reynolds Number

$$Re = \frac{v_{avg}\,\rho h}{\mu} = \frac{\tau_w \rho h^2}{6\mu^2}$$

Equation 3: Entrance Length

$$L_{ent} = 0.04h\,Re = 0.04\,\frac{\tau_w \rho h^3}{6\mu^2}$$

125

Limiting the height of the flow chamber will decrease the Re and the entrance length effects while making the height too small may cause excessive shear stress and shear rates. The wall shear rates selected for testing were 400 and 1000 s^{-1} based on approximations for the range of shear rates platelets may be expected to experience in blood-wetted medical devices. These formulas were used to set the flow rate on the syringe pump used in the studies and to calculate the amount of blood needed for a 5 min perfusion.

A.2   FLOW CHAMBER DESIGNS

A.2.1 Polycarbonate

The first generation flow chamber was designed by Dr. Trevor Snyder at the University of Pittsburgh and was tested by the author (F**igure 2**). The flow chambers were three separate polycarbonate pieces glued together to form the inflow track for the fluid, one side of the parallel plate, and the outflow track for the fluid. The other side of the parallel plate consisted of the interchangeable test materials. The three glued pieces formed a gradual widening flow path towards inlet and outlet openings at the test surface, while a silicon gasket was used to define the height and width of the flow path over the test material. Polycarbonate was chosen as the plate material due to its transparency and observations of its resistance to platelet deposition during other biocompatibility assessments within the laboratory.

Several problems became apparent with this design during initial testing. All of the flow chambers failed at the glued interlocking edges before significant data was collected, resulting in leaking and breaking apart (**Figure 3**).   The machining costs for repairing or replacing the

chambers were high and the lead time was several weeks for any repairs, so any problems with the chambers caused substantial delays with testing. The flow path of each chamber had many seams and cracks due to unavoidable imperfections in machining and difficulties with assembly. The silicon gasket was able to define the width and length of the blood flow path as designed, but the height of the flow path was not well controlled. Further modifications were necessary to control the flow path height as this was a critical variable for determining wall shear rate. The polycarbonate was also found to be highly autofluorescent, especially in the wavelengths most commonly used in yellow-fluorescent platelet dyes (such as quinacrine dihydrochloride).This autofluorescence made real-time visualization of thrombus growth impossible. The first efforts in the biocompatibility characterization of opaque blood-contacting materials (such as titanium) consisted of measuring platelet activation after contact with the material by collecting the effluent and observing platelet adhesion at the end of each test through microscopy (end-point analysis). No useful data was obtained through these experiments.

Figure 7.2: The first generation polycarbonate parallel plate flow chamber clamped onto TiAl6V4 (bottom). A simple C-clamp provided the clamping pressure, and a silicon gasket was used to define the flow path width. Flow path height was not well controlled.

Figure 7.3: The first generation polycarbonate parallel plate flow chamber following repair after breaking. Notice the rough edges of the flow path as well as the apparent leaks at the chamber junctions.

A.2.2 Polydimethylsiloxane

The failure of the polycarbonate chambers prompted the investigation of simpler and more efficient designs. The second generation of flow chambers utilized polydimethylsiloxane (PDMS) as the chamber material due to the reduced cost and effort of fabrication (using a mold instead of machining) and the material properties of the PDMS (allowing for self-sealing of the chamber instead of using a gasket) (**Figure 4**). Similar to the polycarbonate design, these chambers also focused on effluent collection and end-of-study microscopy to measure platelet activation and deposition as the thickness of the PDMS did not allow for visualization of the sample surface while in the flow chamber during testing. However, the PDMS was much easier to manipulate, eliminating the rough edges found in the polycarbonate chamber and removing the gasket which caused a "step" at the inlet and outlet of the flow path.
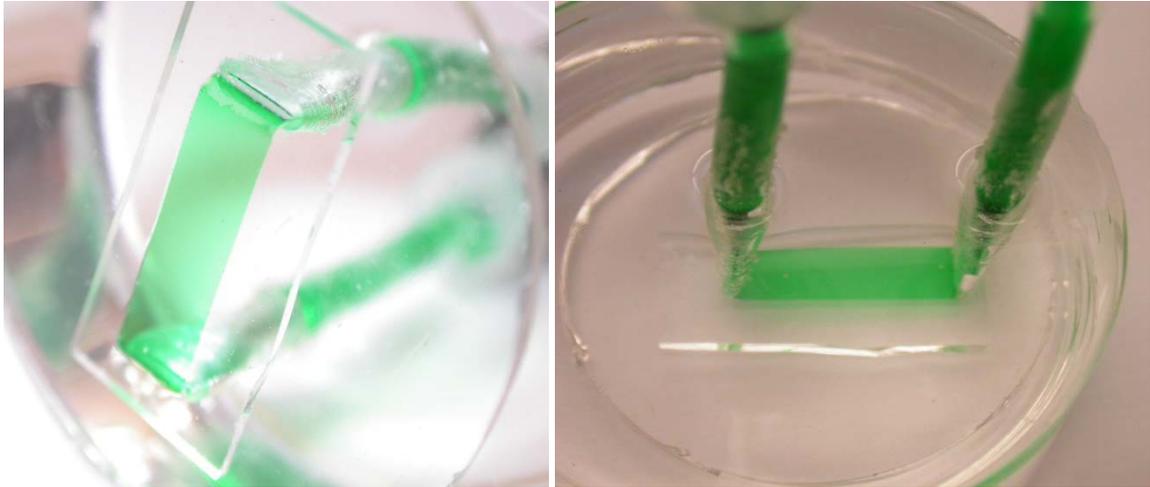
Figure 7.4: Second generation parallel plate flow chambers made of PDMS. The inlet and outlet was constructed of silicon i.v. tubing and the rest of the surfaces were PDMS. In these pictures, glass was used as the test material and water with green dye was used to illustrate the flow path.

Blood-perfusion studies performed with these prototypes suggested that real-time or periodic visualization of platelet deposition on the test surface during perfusion could be possible. Unsuccessful attempts were made to visualize the surface of the test materials through the PDMS due to the thickness of the chambers. To accommodate visualization, a third generation flow chamber was made with less PDMS (to make it thinner) and the inlet and outlet angles were made more horizontal with regards to the flow path so as to provide a viewing window for the microscope objective. These improvements, combined with modifications to the perfusion protocol and blood (quinacrine dihydrochloride – dyed PRP combined with RBC ghost cells, discussed in Chapter 5) allowed for visualization of platelet deposition during testing.

The second and third generation flow chambers were fabricated by curing PDMS around a mold of the flow path. To precisely control the height and width of the flow channel 0.2" strips of very flat brass or aluminum alloy shim stock were bent at two places, 0.7" apart, with 3/32" ID Tygon tubing shoved over each end of the strip. The height of the flow channel was

determined by the thickness of the shim stock used in the mold. In order to reduce the blood volume necessary for these studies , 0.015", 0.010" and 0.005" –thick shim stock was used. The shim and tubing apparatus was attached to a flat metal disc with a very thin layer of weak glue and compressed using a rare-earth magnet and metal rods (**Figure 5**). After drying, excess glue was removed from the edges of the shim and the mold was placed in a polystyrene dish. Silgard 184 PDMS (Corning) was poured into the dish, degassed and cured using a vacuum oven (**Figure 6**). After curing, the chamber was removed from the dish and the round metal disc was carefully removed to reveal the shim strip in the PDMS. The shim strip was cut and each half was pulled out of the PDMS, leaving the tubing partially embedded as the inlet and outlet ports for the chamber. The tubing was further secured to the PDMS by application of silicone glue at the intersections of the tubing PDMS. The resultant flow chambers had a smooth, continuous flow path that gradually transitioned the flow path from circular tubing to rectangular parallel plate and then back to circular tubing without apparent steps or crevices and with precise channel dimensions (**Figure 7**).

Figure 7.5: Flow chamber mold prior to encapsulation in PDMS. The brass shim strip will produce the blood flow path and is glued to the stainless steel round shim disc on the bottom. The mold is pictured on top of the rare-earth magnet, used to stabilize the mold in the polystyrene dish as the PDMS is poured.
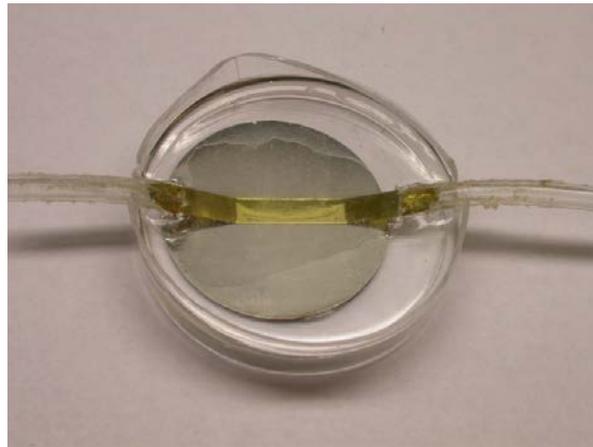
Figure 7.6: PDMS chamber in the polystyrene dish after curing in a vacuum oven. When removed from the dish, the round steel shim on the bottom easily breaks from the brass shim strip and is removed from the chamber. The brass is then cut and pulled from each end, leaving the tubing and flow path behind.
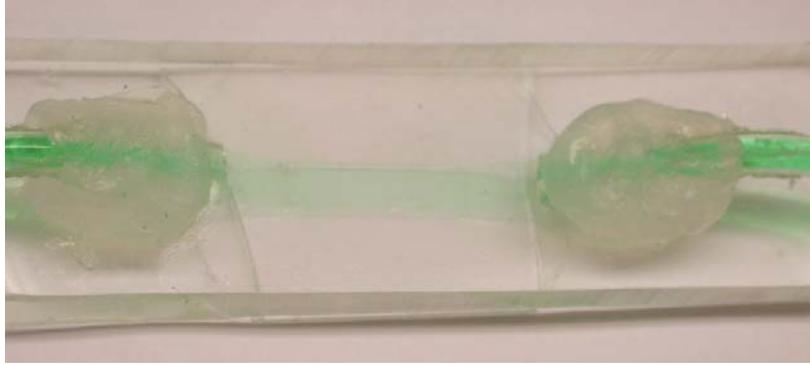
Figure 7.7: A finished PDMS parallel plate flow chamber. The chamber is viewed from the top with a glass microscope slide used as the material sample on the bottom. Excess PDMS around the edges of the chamber has been trimmed to fit the microscope stage insert described below. The large mounds of clear polymer where the tubing intersects the PDMS is silicon glue applied to provide additional mechanical support to the tubing. The flow path for this picture is visible through the use of a green dye.

An inverted epifluorescent microscope was used for the real time visualization of platelets through the PDMS chambers. Since the chambers would have to be in an inverted position on the microscope, a robust clamping mechanism was necessary. Two different clamping mechanisms were tested for sealing the PDMS chambers to the test materials. The first mechanism consisted of a grooved acrylic plate (which fit as an insert in the stage of the inverted microscope) with two side clamps along the edge of the fluid flow path of the chamber. (**Figure 8**) The side clamps allowed for a viewing window for the microscope. This clamping mechanism was not successful in maintaining a seal during the flow experiments due to the flexibility of the PDMS chambers; once the apparatus was inverted on the microscope, both the inlet and outlet portions of the flow chamber would bend slightly downwards and break the seals along the inlet and outlet of the fluid path. It was also difficult to attain equal distribution of force on the flexible chambers, and bulging could be seen between the two clamps. These problems were corrected with the second clamping mechanism, which consisted of the same acrylic plate but

used a solid bar with a window cut out as the clamp. (**Figure 9**) The bar distributed the clamping force more evenly on the chamber, and was able to provide a more reliable seal than the side clamps.
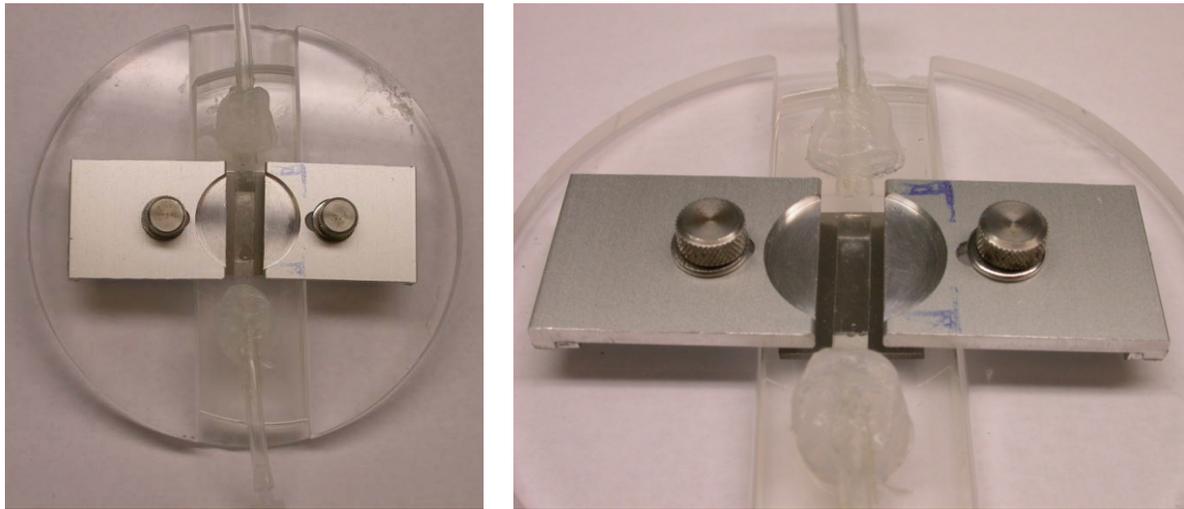
Figure 7.8: Side clamps for the PDMS flow chambers to help maintain a seal with the sample material when overturned on the inverted epifluorescent microscope. The clear base holding the clamps is the microscope state insert. The semi-circle on each clamp allows the microscope objective closer access to the PDMS chamber and a shorter working distance to the material sample surface (titanium is the material sample in these pictures).
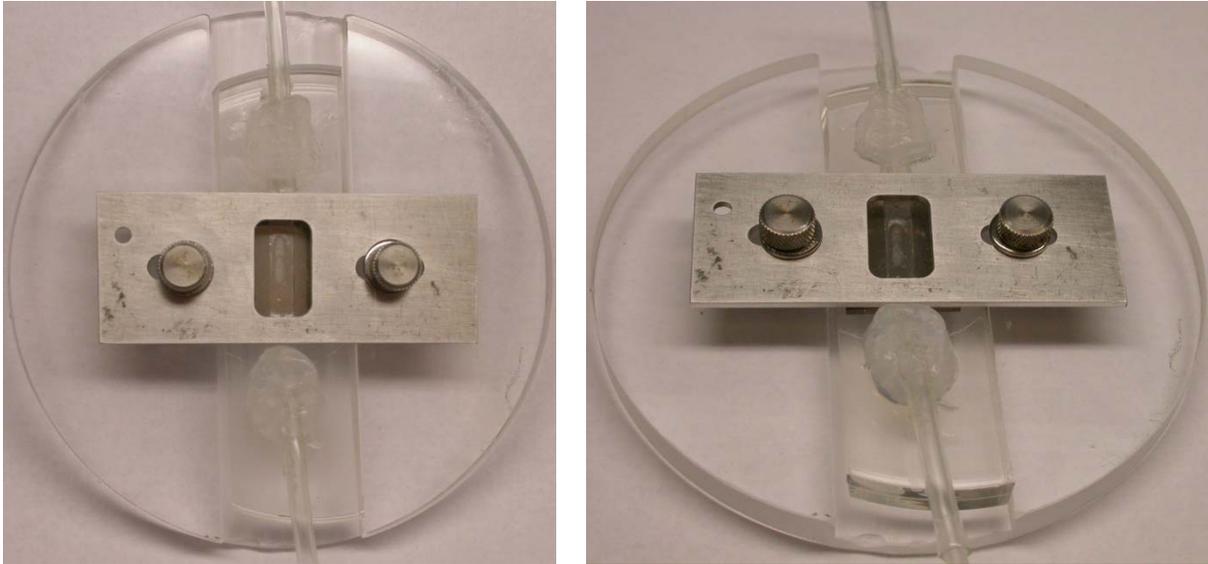
Figure 7.9: A plate clamping mechanism for sealing the PDMS chambers. The plate provided a larger area of force and possibly provided a more uniform pressure distribution and robust seal. The plate was made of stainless steel and the clear base was a microscope stage insert. The test material in the picture was titanium.

Visualization of platelet deposition on the near wall of the chamber revealed that unmodified PDMS was moderately thrombogenic (**Figure 10**). Platelet activation caused by the PDMS could introduce significant error into the system through the release of agonists from activated platelets (such as adenosine diphosphate). In order to mask the surface and make it less thrombogenic, the chamber (without the sample material) was incubated in 4% bovine serum albumin dissolved in PBS for 15 min and then washed with PBS to remove excess protein. When platelet perfusion studies were repeated, there was a marked decrease in the amount of platelets deposited on the surface of the PDMS (**Figure 10**). The albumin coating appeared to reduce the platelet deposition on the non-test surfaces such that any potential error from the non-test surfaces was effectively pacified. This albumin incubation step was then used in all further flow chamber experiments and is briefly described in Section 5.2.5.
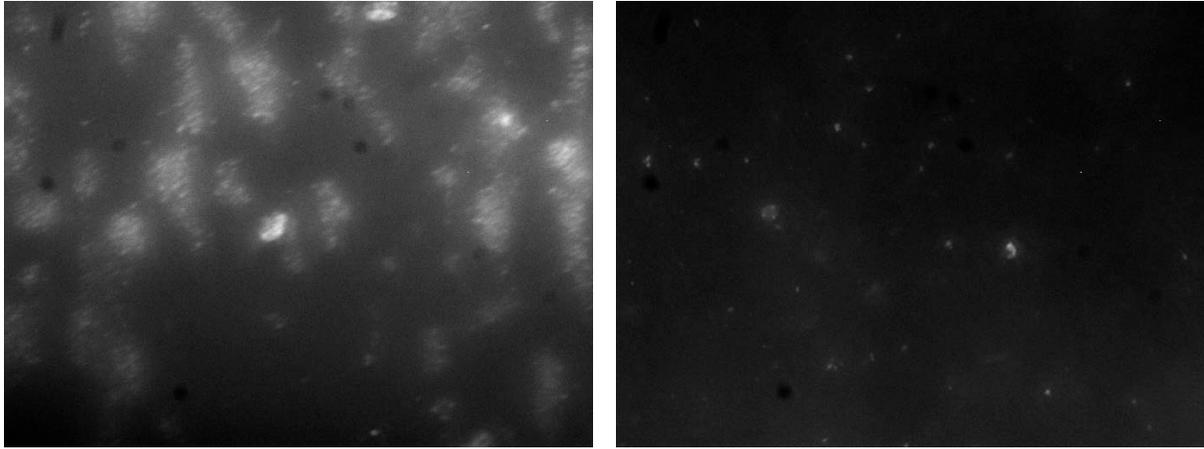
Figure 7.10: The near wall surface of the PDMS parallel plate flow chamber after 5 min of perfusion with quinacrine dihydrochloride labeled whole blood at 1000 s^{-1}. The near wall surface consisted of the unmodified PDMS chamber (left) or the PDMS chamber incubated with 4% BSA for 15 min and rinsed with PBS prior to blood contact. Microscope magnification was 600X for both images.

Using the bar clamp apparatus, real-time visualization of platelets onto opaque surfaces with the incorporation of ghost red blood cells was first performed with this third generation PDMS flow chamber design. However, there were several problems that became apparent during experiments. Although the bar clamp provided a more reliable seal between the PDMS chamber and the test material, the seal would still fail during some experiments and introduce air bubbles into the flow path. The air bubbles would either stop the fluid flow (if the seal was broken at the outlet port) or would wipe away all platelets on the surface of the material (if the seal was broken at the inlet port). Similar to the polycarbonate chambers, the length and width of the fluid path was well defined but the height of the path could not be determined. The clamping pressures needed to produce a reliable seal would compress the PDMS and may have changed the chamber height.

A.2.3 Glass and acrylic

A collaboration with Daniel McKeel produced a flow chamber design that consisted of side ports into reservoirs on either side of a channel that when filled, will produce a laminar flow across the channel (**Figure 11**). This chamber was similar to that described by Chung et al to maximize the area of laminar flow over the test samples and minimize jetting.[181] The incorporation of the glass cover slip created a clear, thin window into the flow path.
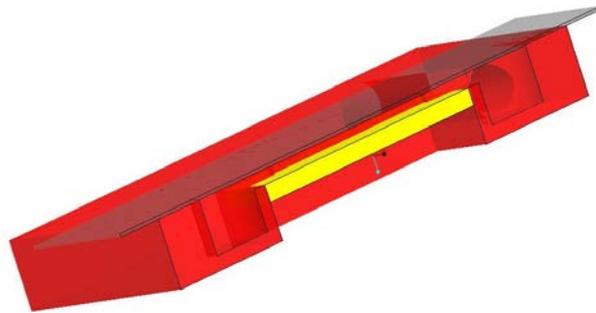
Figure 7.11: Longitudinal cross-section of the glass and acrylic chamber design. The red surfaces are acrylic, the light blue rectangle is a glass cover slip, and the yellow block is the material test sample. Part of the acrylic block and cover slip area are transparent in order to show one of the inlet ports; the other port has been cut off but would exit towards the reader.

Though the chamber was successful at producing laminar flow across the test material, several problems with this design excluded it from use. The most serious problem was that the fluid gap through the plates was large, necessitating a very large volume of blood relative to the previous chamber designs. This was a result of precision limitations with the milling equipment available. The smallest gap height achieved was 0.1", which is an order of magnitude larger than the PDMS channels. In order to perfuse this chamber at the highest wall shear rates (1000 s^{-1})

for 5 minutes, it would require approximately 1.6 L; in contrast, a PDMS chamber with gap height 0.01" under the same conditions would require 16 mL.

Another limitation with this design was the difficulty in controlling the glue that attaches the glass cover slip to the acrylic (**Figure 12**). The edges of the glue were very uneven and allowed blood to stagnate between cracks. This made the chamber a possible source of thrombosis and increased the error in the system. Ultimately these problems led to abandoning the design.

Figure 7.12: Blood perfusion studies with the acrylic chamber. Left: blood leaking into imperfections in the glue between the acrylic chamber and the glass cover slip. Right: a sample material being exposed to flowing blood in the acrylic chamber.

APPENDIX B

CANDIDATE MATERIALS SELECTION AND PRELIMINARY TESTING

B.1 MATERIALS AQUIRED FOR TESTING

As discussed in Chapter 5, several materials were tested as alternatives to Ti6Al4V as the blood-contacting surfaces in cardiovascular devices. Each material tested was FDA approved for medical implantation, and each material had physical properties amenable to use within a continuous flow VAD (similar to TiAl6V4) while providing advantages such as improved fabrication techniques (e.g. ability to be injection-molded). Prior to parallel plate flow chamber development (Appendix A), several preliminary tests of biocompatibility of these materials were performed. The results of these preliminary tests are presented below.

1. TiAl$_6$V$_4$ (LaunchPoint Technologies Inc., Goleta, CA, USA)

2. Alumina (Al$_2$O$_3$; LaunchPoint Technologies Inc.)

3. Zirconia Toughened Alumina (ZTA; CoorsTek, Inc., Golden, CO, USA)

4. Yttria Tetragonal Zirconia Polycrystal (YTZP; CoorsTek)

5. Magnesia partially stabilized Zirconia (DuraZ ^{TM}; CoorsTek)

6. Polyetheretherketone (PEEK)

7. 30% Carbon Fiber PEEK (CF-PEEK)

8. Implantable Grade Polyetherketoneketone (PEKK)

9. Silicon Carbide (SiC; CoorsTek, Inc., Golden, CO, USA)

10. Silinated methacryloyloxyethyl phosphorylcholine polymer – coated $TiAl_6V_4$ (SiMPC; generously provided by Dr. William Wagner's Lab using established protocols [88])

11. Poly(MPC)-co-methacryl acidpolymer coating on $TiAl_6V_4$ (PMA; generously provided by Dr. William Wagner's Lab using established protocols [198])

Unfortunately not all of the materials collected were able to be tested using the parallel plate flow chamber due to unforeseen autofluorescence at the wavelength necessary for visualization of quinacrine dihydrochloride – labelled platelets. The samples that autofluoresced were PEEK, CF-PEEK and PEKK. Additionally, the DuraZ samples were too short to fit the flow path of the parallel plate chambers and could not be included in the experiments.

B.2   COMPARATIVE CLOTTING TIME ASSAY

B.2.1   Introduction

As stated earlier, a variety of materials may fulfill the mechanical and processing requirements to be employed in mechanical circulatory support devices as an alternative to the commonly utilized $TiAl_6V_4$. Novel materials or coatings may retain the attractive physical characteristics of $TiAl_6V_4$ while improving the biocompatibility of the blood contacting surface. In vitro biocompatibility testing of novel materials or coatings at the pre-clinical stage of device development allows for easier implementation and testing. Additionally, the ovine model is often chosen for adult and pediatric VAD evaluation and therefore ovine blood should be considered for use during in vitro biocompatibility testing. The following was a first-level evaluation of the

139

hemocompatibility of several alternative materials compared with $TiAl_6V_4$ using a standard blood clotting time assay with ovine and human blood.

B.2.2 Methods

Briefly, test materials were washed in Tergazyme ®for > 20 min, washed in Simple Green ® for >20 min, rinsed with DI wather 5 times and rinsed 3 times in physiological saline solution. Each material was placed into an empty 5 ml no-additive Vacutainer ^{TM} (BD) tube. Human or sheep blood was collected in sodium citrate tubes (1:10) following radial (human) or jugular (ovine) venipuncture; the first 3 ml was discarded to reduce activation of the coagulation system from the venipuncture. Fresh citrated human or sheep whole blood was added to each Vacutainer tubes (4 ml), re-calcified with 4 nM CaCl (final concentration), capped and placed on a hematology rocker at room temperature. An additional empty Vacutainer tube was included on the rocker as a negative control. The SiC material was not able to be tested as these samples did not fit within the Vacutainer tubes. The SiMPC and PMA samples were smaller than the other materials and were tested separately against a $TiAl_6V_4$ sample of the same size. Each material tested had similar surface roughness (~8 Ra) and blood volume to surface area ratio (0.90 ± 0.05 cm²/mL for SiMPC, PMA, and the size-matched $TiAl_6V_4$; 1.4 ± 0.10 cm²/mL for all other samples). The time to clot was recorded in seconds, starting at the addition of the CaCl and stopping at near – complete coagulation of the blood by visual inspection. Each test was normalized by the clotting time of the negative control sample to reduce between – subject variability of blood collection; this was especially necessary for the sheep samples due to their excitability during blood collection. The normalized data was analyzed using a two – tailed t-test against $TiAl_6V_4$, with significance at $p<0.05$

B.2.3   Results and Discussion

The PEEK and PEKK samples exhibited significantly longer clotting times than $TiAl_6V_4$ in both human and sheep blood (**Figures 1 and 2**); sheep blood also exhibited significantly longer clotting times for the CF-PEEK than $TiAl_6V_4$ (**Figure 2**). Though most of the ceramic samples produced longer clotting times than $TiAl_6V_4$, none of these differences were significant. Additionally, both SiMPC and PMA had longer clotting times than $TiAl_6V_4$ in ovine blood (**Figure 3**).
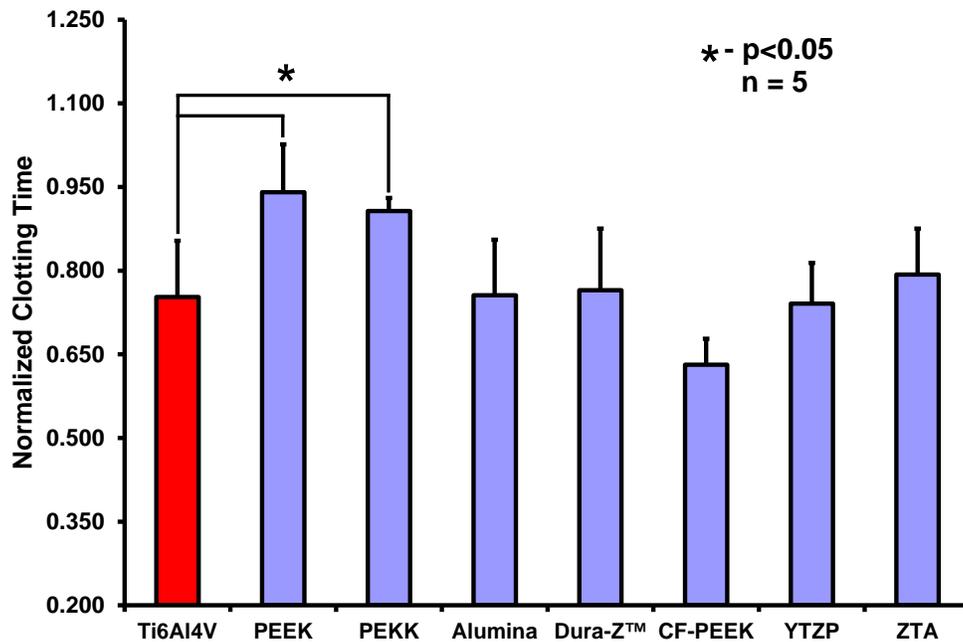
Figure 7.13: Clotting time results using re-calcified human blood and compared to $TiAl_6V_4$.
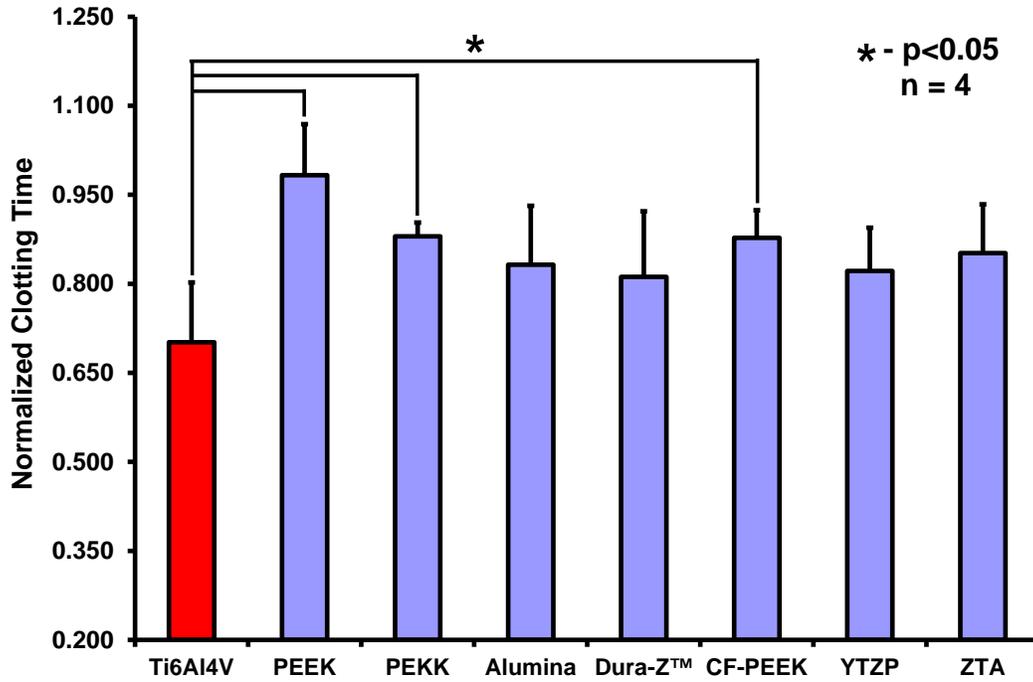
Figure 7.14: Blood clotting-time results using re-calcified sheep blood and compared to TiAl$_6$V$_4$.
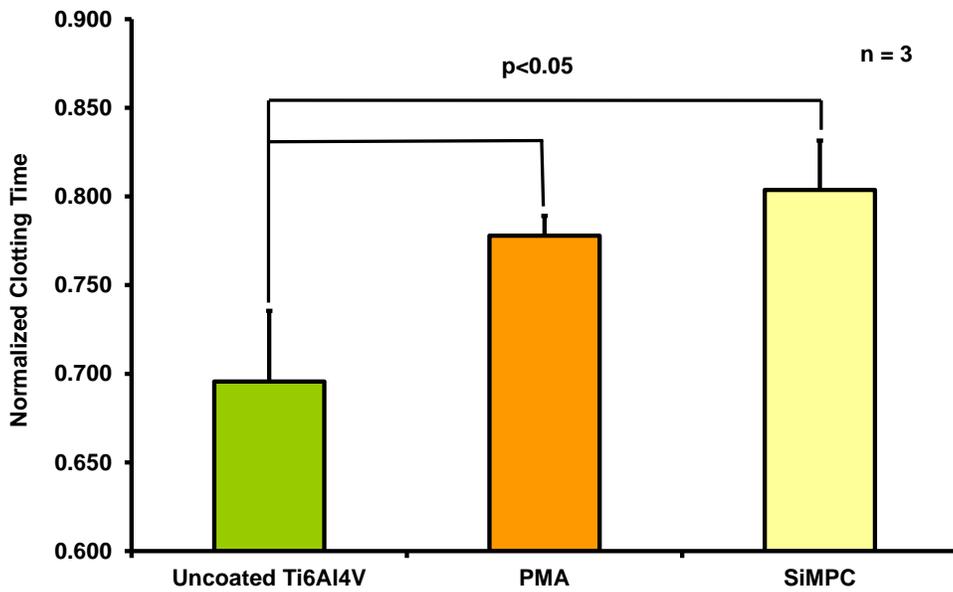
Figure 7.15: Clotting-time results using re-calcified sheep blood and compared to uncoated Ti6Al4V.

The application of a standardized blood clotting time assay to alternative VAD blood contacting materials provided a first level analysis of the biocompatibility of these materials. While this method may not be as controlled as an experiment as the parallel plate flow studies, the combination of several different types of flow within the tubes (including both turbulent and stagnant areas) and a relatively high blood volume to surface area ratio provides a very challenging environment for the materials. Sheep and human blood produced similar results, with PEEK and PEKK exhibiting a significantly longer blood clotting time. The longer clotting times for PEEK and PEKK suggest a possible improved biocompatibility over $TiAl_6V_4$. Similarities between the sheep and human results provide encouragement that pre-clinical biocompatibility testing in sheep will yield relevant predictive information on the performance of cardiac devices in humans.

BIBLIOGRAPHY

1. Argenziano M, Oz MC, Rose EA. The continuing evolution of mechanical ventricular assistance. Curr Probl Surg 1997;34:317-86.

2. Goldstein DJ, Oz MC, Rose EA. Implantable left ventricular assist devices. N Engl J Med 1998;339:1522-33.

3. Guy TS. Evolution and current status of the total artificial heart: the search continues. ASAIO J 1998;44:28-33.

4. Miller LW, Pagani FD, Russell SD, John R, Boyle AJ, Aaronson KD, et al. Use of a continuous-flow device in patients awaiting heart transplantation. N Engl J Med 2007;357:885-96.

5. Wagner WR, Schaub RD, Sorensen EN, Snyder TA, Wilhelm CR, Winowich S, et al. Blood biocompatibility analysis in the setting of ventricular assist devices. J Biomater Sci Polym Ed 2000;11:1239-59.

6. Kirklin JK, Naftel DC, Kormos RL, Stevenson LW, Pagani FD, Miller MA, et al. Fifth INTERMACS annual report: risk factor analysis from more than 6,000 mechanical circulatory support patients. J Heart Lung Transplant 2013;32:141-56.

7. Goldstein DJ. Worldwide experience with the MicroMed DeBakey Ventricular Assist Device as a bridge to transplantation. Circulation 2003;108 Suppl 1:II272-7.

8. Rose EA, Gelijns AC, Moskowitz AJ, Heitjan DF, Stevenson LW, Dembitsky W, et al. Long-term mechanical left ventricular assistance for end-stage heart failure. N Engl J Med 2001;345:1435-43.

9. INTERMACS. Manual of Operations, Version 3.0. Available at http://www.uab.edu/medicine/intermacs/manual-of-operations 2013.

10. Kirklin J. INTERMACS Annual Report 2008. International Society of Heart and Lung Transplantation, 28th Annual Meeting and Scientific Sessions: INTERMACS, 2008.

11. Kormos R, Kirklin J, Naftel DC, Young JB, Acker MA, Jessup M, et al. Early Neurological Adverse Events (NAE) after Pulsatile VAD Implantation in 455 Patients: Incidence, Severity and Outcome. J Heart Lung Transplant 2009;28:S129.

12. Slaughter MS, Tsui SS, El-Banayosy A, Sun BC, Kormos RL, Mueller DK, et al. Results of a multicenter clinical trial with the Thoratec Implantable Ventricular Assist Device. J Thorac Cardiovasc Surg 2007;133:1573-80.

13. Pagani FD, Miller LW, Russell SD, Aaronson KD, John R, Boyle AJ, et al. Extended mechanical circulatory support with a continuous-flow rotary left ventricular assist device. J Am Coll Cardiol 2009;54:312-21.

14. Starling RC, Naka Y, Boyle AJ, Gonzalez-Stawinski G, John R, Jorde U, et al. Results of the post-U.S. Food and Drug Administration-approval study with a continuous flow left ventricular assist device as a bridge to heart transplantation: a prospective study using the INTERMACS (Interagency Registry for Mechanically Assisted Circulatory Support). J Am Coll Cardiol 2011;57:1890-8.

15. Slaughter MS, Rogers JG, Milano CA, Russell SD, Conte JV, Feldman D, et al. Advanced heart failure treated with continuous-flow left ventricular assist device. N Engl J Med 2009;361:2241-51.

16. John R, Kamdar F, Liao K, Colvin-Adams M, Boyle A, Joyce L. Improved survival and decreasing incidence of adverse events with the HeartMate II left ventricular assist device as bridge-to-transplant therapy. Ann Thorac Surg 2008;86:1227-34; discussion 1234-5.

17. Starling RC, Moazami N, Silvestry SC, Ewald G, Rogers JG, Milano CA, et al. Unexpected abrupt increase in left ventricular assist device thrombosis. N Engl J Med 2013;370:33-40.

18. Meyer AL, Malehsa D, Bara C, Budde U, Slaughter MS, Haverich A, et al. Acquired von Willebrand syndrome in patients with an axial flow left ventricular assist device. Circ Heart Fail 2010;3:675-81.

19. Esmore D, Kaye D, Spratt P, Larbalestier R, Ruygrok P, Tsui S, et al. A prospective, multicenter trial of the VentrAssist left ventricular assist device for bridge to transplant: safety and efficacy. J Heart Lung Transplant 2008;27:579-88.

20. Strueber M, O'Driscoll G, Jansz P, Khaghani A, Levy WC, Wieselthaler GM. Multicenter evaluation of an intrapericardial left ventricular assist system. J Am Coll Cardiol 2011;57:1375-82.

21. Slaughter MS, Pagani FD, McGee EC, Birks EJ, Cotts WG, Gregoric I, et al. HeartWare ventricular assist system for bridge to transplant: combined results of the bridge to transplant and continued access protocol trial. J Heart Lung Transplant 2013;32:675-83.

22. Wu L, Weng YG, Dong NG, Krabatsch T, Stepanenko A, Hennig E, et al. Outcomes of HeartWare Ventricular Assist System support in 141 patients: a single-centre experience. Eur J Cardiothorac Surg 2013;44:139-45.

23. Dell'Aquila AM, Schneider SR, Schlarb D, Redwan B, Sindermann JR, Ellger B, et al. Initial clinical experience with the HeartWare left ventricular assist system: a single-center report. Ann Thorac Surg 2013;95:170-7.

24. Eckman PM, John R. Bleeding and thrombosis in patients with continuous-flow ventricular assist devices. Circulation 2012;125:3038-47.

25. Long JW, Kfoury AG, Slaughter MS, Silver M, Milano C, Rogers J, et al. Long-term destination therapy with the HeartMate XVE left ventricular assist device: improved outcomes since the REMATCH study. Congest Heart Fail 2005;11:133-8.

26. Rogers JG, Butler J, Lansman SL, Gass A, Portner PM, Pasque MK, et al. Chronic mechanical circulatory support for inotrope-dependent heart failure patients who are not transplant candidates: results of the INTrEPID Trial. J Am Coll Cardiol 2007;50:741-7.

27. Witt BJ, Gami AS, Ballman KV, Brown RD, Jr., Meverden RA, Jacobsen SJ, et al. The incidence of ischemic stroke in chronic heart failure: a meta-analysis. J Card Fail 2007;13:489-96.

28. Lazar RM, Shapiro PA, Jaski BE, Parides MK, Bourge RC, Watson JT, et al. Neurological events during long-term mechanical circulatory support for heart failure: the Randomized Evaluation of Mechanical Assistance for the Treatment of Congestive Heart Failure (REMATCH) experience. Circulation 2004;109:2423-7.

29. Deng MC, Edwards LB, Hertz MI, Rowe AW, Keck BM, Kormos R, et al. Mechanical circulatory support device database of the International Society for Heart and Lung Transplantation: third annual report--2005. J Heart Lung Transplant 2005;24:1182-7.

30. Mussivand T. Neurological dysfunction associated with mechanical circulatory support: complications that still need attention. Artif Organs 2008;32:831-4.

31. Mussivand T. Mechanical circulatory support devices: is it time to focus on the complications, instead of building another new pump? Artif Organs 2008;32:1-4.

32. Sefton MV, Gemmell CH, Gorbet MB. What really is blood compatibility? J Biomater Sci Polym Ed 2000;11:1165-82.

33. Hoffman AS, Cohn D, Hanson SR, Harker LA, Horbett TA, Ratner BD, et al. Application of radiation-grafted hydrogels as blood-contacting biomaterials. Radiation Physics and Chemistry (1977) 1983;22:267-283.

34.   Gorbet MB, Sefton MV. Biomaterial-associated thrombosis: roles of coagulation factors, complement, platelets and leukocytes. Biomaterials 2004;25:5681-703.

35.   Lowe GD. Virchow's triad revisited: abnormal flow. Pathophysiol Haemost Thromb 2003;33:455-7.

36.   Basmadjian D, Sefton MV, Baldwin SA. Coagulation on biomaterials in flowing blood: some theoretical considerations. Biomaterials 1997;18:1511-22.

37.   Gemmell CH, Ramirez SM, Yeo EL, Sefton MV. Platelet activation in whole blood by artificial surfaces: identification of platelet-derived microparticles and activated platelet binding to leukocytes as material-induced activation events. J Lab Clin Med 1995;125:276-87.

38.   Gemmell CH, Yeo EL, Sefton MV. Flow cytometric analysis of material-induced platelet activation in a canine model: elevated microparticle levels and reduced platelet life span. J Biomed Mater Res 1997;37:176-81.

39.   Sefton MV, Sawyer A, Gorbet M, Black JP, Cheng E, Gemmell C, et al. Does surface chemistry affect thrombogenicity of surface modified polymers? J Biomed Mater Res 2001;55:447-59.

40.   Vroman L. Effect of absorbed proteins on the wettability of hydrophilic and hydrophobic solids. Nature 1962;196:476-7.

41.   Jackson SP. The growing complexity of platelet aggregation. Blood 2007;109:5087-95.

42.   Savage B, Saldivar E, Ruggeri ZM. Initiation of platelet adhesion by arrest onto fibrinogen or translocation on von Willebrand factor. Cell 1996;84:289-97.

43.   Nesbitt WS, Westein E, Tovar-Lopez FJ, Tolouei E, Mitchell A, Fu J, et al. A shear gradient-dependent platelet aggregation mechanism drives thrombus formation. Nat Med 2009;15:665-73.

44.   Livingston ER, Fisher CA, Bibidakis EJ, Pathak AS, Todd BA, Furukawa S, et al. Increased activation of the coagulation and fibrinolytic systems leads to hemorrhagic complications during left ventricular assist implantation. Circulation 1996;94:II227-34.

45.   Meuris B, Arnout J, Vlasselaers D, Schetz M, Meyns B. Long-term management of an implantable left ventricular assist device using low molecular weight heparin and antiplatelet therapy: a possible alternative to oral anticoagulants. Artif Organs 2007;31:402-5.

147

46. Sandner SE, Zimpfer D, Zrunek P, Steinlechner B, Rajek A, Schima H, et al. Low molecular weight heparin as an alternative to unfractionated heparin in the immediate postoperative period after left ventricular assist device implantation. Artif Organs 2008;32:819-22.

47. Spanier T, Oz M, Levin H, Weinberg A, Stamatis K, Stern D, et al. Activation of coagulation and fibrinolytic pathways in patients with left ventricular assist devices. J Thorac Cardiovasc Surg 1996;112:1090-7.

48. Joshi A, Magder LS, Kon Z, Kallam S, Kwon M, Sangrampurkar R, et al. Association between prothrombin activation fragment (F1.2), cerebral ischemia (S-100beta) and international normalized ratio (INR) in patients with ventricular assisted devices. Interact Cardiovasc Thorac Surg 2007;6:323-7.

49. Butchart EG, Payne N, Li HH, Buchan K, Mandana K, Grunkemeier GL. Better anticoagulation control improves survival after valve replacement. J Thorac Cardiovasc Surg 2002;123:715-23.

50. Wilhelm CR, Ristich J, Knepper LE, Holubkov R, Wisniewski SR, Kormos RL, et al. Measurement of hemostatic indexes in conjunction with transcranial doppler sonography in patients with ventricular assist devices. Stroke 1999;30:2554-61.

51. Koster A, Loebe M, Hansen R, Potapov EV, Noon GP, Kuppe H, et al. Alterations in coagulation after implantation of a pulsatile Novacor LVAD and the axial flow MicroMed DeBakey LVAD. Ann Thorac Surg 2000;70:533-7.

52. Himmelreich G, Ullmann H, Riess H, Rosch R, Loebe M, Schiessler A, et al. Pathophysiologic role of contact activation in bleeding followed by thromboembolic complications after implantation of a ventricular assist device. ASAIO J 1995;41:M790-4.

53. Dewald O, Schmitz C, Diem H, Goehring P, Vetter HO, Roell W, et al. Platelet activation markers in patients with heart assist device. Artif Organs 2005;29:292-9.

54. Wang IW, Kottke-Marchant K, Vargo RL, McCarthy PM. Hemostatic profiles of HeartMate ventricular assist device recipients. ASAIO J 1995;41:M782-7.

55. Etz C, Welp H, Rothenburger M, Tjan TD, Wenzelburger F, Schmidt C, et al. Analysis of platelet function during left ventricular support with the Incor and Excor system. Heart Surg Forum 2004;7:E423-7.

56. Majeed F, Kop WJ, Poston RS, Kallam S, Mehra MR. Prospective, observational study of antiplatelet and coagulation biomarkers as predictors of thromboembolic events after implantation of ventricular assist devices. Nat Clin Pract Cardiovasc Med 2009;6:147-57.

57.   Wilhelm CR, Ristich J, Kormos RL, Wagner WR. Monocyte tissue factor expression and ongoing complement generation in ventricular assist device patients. Ann Thorac Surg 1998;65:1071-6.

58.   Haj-Yahia S, Birks EJ, Rogers P, Bowles C, Hipkins M, George R, et al. Midterm experience with the Jarvik 2000 axial flow left ventricular assist device. J Thorac Cardiovasc Surg 2007;134:199-203.

59.   Pae WE, Connell JM, Boehmer JP, Korfer R, El-Banayosy A, Hetzer R, et al. Neurologic events with a totally implantable left ventricular assist device: European LionHeart Clinical Utility Baseline Study (CUBS). J Heart Lung Transplant 2007;26:1-8.

60.   Breet NJ, van Werkum JW, Bouman HJ, Kelder JC, Ruven HJ, Bal ET, et al. Comparison of platelet function tests in predicting clinical outcome in patients undergoing coronary stent implantation. JAMA;303:754-62.

61.   Damani SB, Topol EJ. The Case for Routine Genotyping in Dual-Antiplatelet Therapy. J Am Coll Cardiol;56:109-111.

62.   Gurbel PA, Tantry US, Shuldiner AR, Kereiakes DJ. Genotyping One Piece of the Puzzle to Personalize Antiplatelet Therapy. J Am Coll Cardiol;56:112-116.

63.   Diamond SL. Systems biology to predict blood function. J Thromb Haemost 2009;7 Suppl 1:177-80.

64.   Kitano H. Systems biology: a brief overview. Science 2002;295:1662-4.

65.   Vodovotz Y, Csete M, Bartels J, Chang S, An G. Translational systems biology of inflammation. PLoS Comput Biol 2008;4:e1-14.

66.   Sakariassen KS, Muggli R, Baumgartner HR. Measurements of platelet interaction with components of the vessel wall in flowing blood. Methods Enzymol 1989;169:37-70.

67.   Deutsch S, Tarbell JM, Manning KB, Rosenberg G, Fontaine AA. Experimental fluid mechanics of pulsatile artificial blood pumps. Annual Review of Fluid Mechanics 2006;38:65-86.

68.   Hochareon P, Manning KB, Fontaine AA, Tarbell JM, Deutsch S. Fluid dynamic analysis of the 50 cc Penn State artificial heart under physiological operating conditions using particle image velocimetry. J Biomech Eng 2004;126:585-93.

69.   Wu ZJ, Antaki JF, Burgreen GW, Butler KC, Thomas DC, Griffith BP. Fluid dynamic characterization of operating conditions for continuous flow blood pumps. ASAIO J 1999;45:442-9.

70. Leverett LB, Hellums JD, Alfrey CP, Lynch EC. Red blood cell damage by shear stress. Biophys J 1972;12:257-73.

71. Kameneva MV, Burgreen GW, Kono K, Repko B, Antaki JF, Umezu M. Effects of turbulent stresses upon mechanical hemolysis: experimental and computational analysis. ASAIO J 2004;50:418-23.

72. Behbahani M, Behr M, Hormes M, Steinseifer U, Arora D, Coronado O, et al. A review of computational fluid dynamics analysis of blood pumps. European Journal of Applied Mathematics 2009;20:363-397.

73. Antaki JF, Ghattas O, Burgreen GW, He B. Computational flow optimization of rotary blood pump components. Artif Organs 1995;19:608-15.

74. Burgreen GW, Antaki JF, Griffith BP. A design improvement strategy for axial blood pumps using computational fluid dynamics. ASAIO J 1996;42:M354-60.

75. Burgreen GW, Antaki JF, Wu ZJ, Holmes AJ. Computational fluid dynamics as a development tool for rotary blood pumps. Artif Organs 2001;25:336-40.

76. Kim NJ, Diao C, Ahn KH, Lee SJ, Kameneva MV, Antaki JF. Parametric study of blade tip clearance, flow rate, and impeller speed on blood damage in rotary blood pump. Artif Organs 2009;33:468-74.

77. Farrar DJ, Litwak P, Lawson JH, Ward RS, White KA, Robinson AJ, et al. In vivo evaluations of a new thromboresistant polyurethane for artificial heart blood pumps. J Thorac Cardiovasc Surg 1988;95:191-200.

78. Menconi MJ, Pockwinse S, Owen TA, Dasse KA, Stein GS, Lian JB. Properties of blood-contacting surfaces of clinically implanted cardiac assist devices: gene expression, matrix composition, and ultrastructural characterization of cellular linings. J Cell Biochem 1995;57:557-73.

79. Frazier OH, Baldwin RT, Eskin SG, Duncan JM. Immunochemical identification of human endothelial cells on the lining of a ventricular assist device. Tex Heart Inst J 1993;20:78-82.

80. Rafii S, Oz MC, Seldomridge JA, Ferris B, Asch AS, Nachman RL, et al. Characterization of hematopoietic cells arising on the textured surface of left ventricular assist devices. Ann Thorac Surg 1995;60:1627-32.

81. Slater JP, Rose EA, Levin HR, Frazier OH, Roberts JK, Weinberg AD, et al. Low thromboembolic risk without anticoagulation using advanced-design left ventricular assist devices. Ann Thorac Surg 1996;62:1321-7; discussion 1328.

82. Sin DC, Kei HL, Miao X. Surface coatings for ventricular assist devices. Expert Rev Med Devices 2009;6:51-60.

83. Schaub RD, Kameneva MV, Borovetz HS, Wagner WR. Assessing acute platelet adhesion on opaque metallic and polymeric biomaterials with fiber optic microscopy. J Biomed Mater Res 2000;49:460-8.

84. Ishihara K, Fukumoto K, Iwasaki Y, Nakabayashi N. Modification of polysulfone with phospholipid polymer for improvement of the blood compatibility. Part 2. Protein adsorption and platelet adhesion. Biomaterials 1999;20:1553-9.

85. Ishihara K, Fukumoto K, Iwasaki Y, Nakabayashi N. Modification of polysulfone with phospholipid polymer for improvement of the blood compatibility. Part 1. Surface characterization. Biomaterials 1999;20:1545-51.

86. Ye SH, Johnson CA, Jr., Woolley JR, Snyder TA, Gamble LJ, Wagner WR. Covalent surface modification of a titanium alloy with a phosphorylcholine-containing copolymer for reduced thrombogenicity in cardiovascular devices. J Biomed Mater Res A 2008.

87. Snyder TA, Tsukui H, Kihara S, Akimoto T, Litwak KN, Kameneva MV, et al. Preclinical biocompatibility assessment of the EVAHEART ventricular assist device: coating comparison and platelet activation. J Biomed Mater Res A 2007;81:85-92.

88. Ye SH, Johnson CA, Jr., Woolley JR, Oh HI, Gamble LJ, Ishihara K, et al. Surface modification of a titanium alloy with a phospholipid polymer prepared by a plasma-induced grafting technique to improve surface thromboresistance. Colloids Surf B Biointerfaces 2009;74:96-102.

89. Hansson KM, Tosatti S, Isaksson J, Wettero J, Textor M, Lindahl TL, et al. Whole blood coagulation on protein adsorption-resistant PEG and peptide functionalised PEG-coated titanium surfaces. Biomaterials 2005;26:861-72.

90. Bluestein D, Chandran KB, Manning KB. Towards non-thrombogenic performance of blood recirculating devices. Ann Biomed Eng;38:1236-56.

91. Goodman PD, Barlow ET, Crapo PM, Mohammad SF, Solen KA. Computational model of device-induced thrombosis and thromboembolism. Ann Biomed Eng 2005;33:780-97.

92. Goubergrits L. Numerical modeling of blood damage: current status, challenges and future prospects. Expert Rev Med Devices 2006;3:527-31.

93. Xenos M, Girdhar G, Alemu Y, Jesty J, Slepian M, Einav S, et al. Device Thrombogenicity Emulator (DTE) - Design optimization methodology for cardiovascular devices: A study in two bileaflet MHV designs. J Biomech.

94. Dowling RD, Etoch SW, Stevens KA, Johnson AC, Gray LA, Jr. Current status of the AbioCor implantable replacement heart. Ann Thorac Surg 2001;71:S147-9; discussion S183-4.

95. Dowling RD, Gray LA, Jr., Etoch SW, Laks H, Marelli D, Samuels L, et al. Initial experience with the AbioCor implantable replacement heart system. J Thorac Cardiovasc Surg 2004;127:131-41.

96. Hund SJ, Antaki JF. An extended convection diffusion model for red blood cell-enhanced transport of thrombocytes and leukocytes. Phys Med Biol 2009;54:6415-35.

97. Sorensen EN, Burgreen GW, Wagner WR, Antaki JF. Computational simulation of platelet deposition and activation: I. Model development and properties. Ann Biomed Eng 1999;27:436-48.

98. Antaki JF, Ricci MR, Verkaik JE, Snyder ST, Maul TM, Kim J, et al. PediaFlow Maglev Ventricular Assist Device: A Prescriptive Design Approach. Cardiovasc Eng;1:104-121.

99. Tsukui H, Abla A, Teuteberg JJ, McNamara DM, Mathier MA, Cadaret LM, et al. Cerebrovascular accidents in patients with a ventricular assist device. J Thorac Cardiovasc Surg 2007;134:114-23.

100. Ankersmit HJ, Tugulea S, Spanier T, Weinberg AD, Artrip JH, Burke EM, et al. Activation-induced T-cell death and immune dysfunction after implantation of left-ventricular assist device. Lancet 1999;354:550-5.

101. Ankersmit HJ, Edwards NM, Schuster M, John R, Kocher A, Rose EA, et al. Quantitative changes in T-cell populations after left ventricular assist device implantation: relationship to T-cell apoptosis and soluble CD95. Circulation 1999;100:II211-5.

102. Schuster M, Kocher A, John R, Hoffman M, Ankersmit J, Lietz K, et al. B-cell activation and allosensitization after left ventricular assist device implantation is due to T-cell activation and CD40 ligand expression. Hum Immunol 2002;63:211-20.

103. Drakos SG, Kfoury AG, Kotter JR, Reid BB, Clayson SE, Selzman CH, et al. Prior human leukocyte antigen-allosensitization and left ventricular assist device type affect degree of post-implantation human leukocyte antigen-allosensitization. J Heart Lung Transplant 2009;28:838-42.

104. Schnizlein-Bick CT, Mandy FF, O'Gorman MR, Paxton H, Nicholson JK, Hultin LE, et al. Use of CD45 gating in three and four-color flow cytometric immunophenotyping: guideline from the National Institute of Allergy and Infectious Diseases, Division of AIDS. Cytometry 2002;50:46-52.

105. Simon D, Fischer S, Grossman A, Downer C, Hota B, Heroux A, et al. Left ventricular assist device-related infection: treatment and outcome. Clin Infect Dis 2005;40:1108-15.

152

106. Shive MS, Brodbeck WG, Colton E, Anderson JM. Shear stress and material surface effects on adherent human monocyte apoptosis. J Biomed Mater Res 2002;60:148-58.

107. Shive MS, Salloum ML, Anderson JM. Shear stress-induced apoptosis of adherent neutrophils: a mechanism for persistence of cardiovascular device infections. Proc Natl Acad Sci U S A 2000;97:6710-5.

108. Itescu S, Tung TC, Burke EM, Weinberg A, Moazami N, Artrip JH, et al. Preformed IgG antibodies against major histocompatibility complex class II antigens are major risk factors for high-grade cellular rejection in recipients of heart transplantation. Circulation 1998;98:786-93.

109. Moazami N, Itescu S, Williams MR, Argenziano M, Weinberg A, Oz MC. Platelet transfusions are associated with the development of anti-major histocompatibility complex class I antibodies in patients with left ventricular assist support. J Heart Lung Transplant 1998;17:876-80.

110. Rudensky B, Yinnon AM, Shutin O, Broide E, Wiener-Well Y, Bitran D, et al. The cellular immunological responses of patients undergoing coronary artery bypass grafting compared with those of patients undergoing valve replacement. Eur J Cardiothorac Surg 2010;37:1056-62.

111. Franke A, Lante W, Kurig E, Zoller LG, Weinhold C, Markewitz A. Hyporesponsiveness of T cell subsets after cardiac surgery: a product of altered cell function or merely a result of absolute cell count changes in peripheral blood? Eur J Cardiothorac Surg 2006;30:64-71.

112. Bartal I, Melamed R, Greenfeld K, Atzil S, Glasner A, Domankevich V, et al. Immune perturbations in patients along the perioperative period: alterations in cell surface markers and leukocyte subtypes before and after surgery. Brain Behav Immun 2010;24:376-86.

113. Gambichler T, Tigges C, Burkert B, Hoxtermann S, Altmeyer P, Kreuter A. Absolute count of T and B lymphocyte subsets is decreased in systemic sclerosis. Eur J Med Res 2010;15:44-6.

114. Rose EA, Levin HR, Oz MC, Frazier OH, Macmanus Q, Burton NA, et al. Artificial circulatory support with textured interior surfaces. A counterintuitive approach to minimizing thromboembolism. Circulation 1994;90:II87-91.

115. Spanier TB, Chen JM, Oz MC, Stern DM, Rose EA, Schmidt AM. Time-dependent cellular population of textured-surface left ventricular assist devices contributes to the development of a biphasic systemic procoagulant response. J Thorac Cardiovasc Surg 1999;118:404-13.

116. Dasse KA, Chipman SD, Sherman CN, Levine AH, Frazier OH. Clinical experience with textured blood contacting surfaces in ventricular assist devices. ASAIO Trans 1987;33:418-25.

117. Stringham JC, Bull DA, Fuller TC, Kfoury AG, Taylor DO, Renlund DG, et al. Avoidance of cellular blood product transfusions in LVAD recipients does not prevent HLA allosensitization. J Heart Lung Transplant 1999;18:160-5.

118. McKenna DH, Jr., Eastlund T, Segall M, Noreen HJ, Park S. HLA alloimmunization in patients requiring ventricular assist device support. J Heart Lung Transplant 2002;21:1218-24.

119. John R, Lietz K, Schuster M, Naka Y, Rao V, Mancini DM, et al. Immunologic sensitization in recipients of left ventricular assist devices. J Thorac Cardiovasc Surg 2003;125:578-91.

120. George I, Colley P, Russo MJ, Martens TP, Burke E, Oz MC, et al. Association of device surface and biomaterials with immunologic sensitization after mechanical support. J Thorac Cardiovasc Surg 2008;135:1372-9.

121. Arnaoutakis GJ, George TJ, Kilic A, Weiss ES, Russell SD, Conte JV, et al. Effect of sensitization in US heart transplant recipients bridged with a ventricular assist device: update in a modern cohort. J Thorac Cardiovasc Surg 2011;142:1236-45, 1245 e1.

122. Massad MG, Cook DJ, Schmitt SK, Smedira NG, McCarthy JF, Vargo RL, et al. Factors influencing HLA sensitization in implantable LVAD recipients. Ann Thorac Surg 1997;64:1120-5.

123. Holman WL, Park SJ, Long JW, Weinberg A, Gupta L, Tierney AR, et al. Infection in permanent circulatory support: experience from the REMATCH trial. J Heart Lung Transplant 2004;23:1359-65.

124. Sharma V, Deo SV, Stulak JM, Durham LA, 3rd, Daly RC, Park SJ, et al. Driveline infections in left ventricular assist devices: implications for destination therapy. Ann Thorac Surg 2012;94:1381-6.

125. Schaffer JM, Allen JG, Weiss ES, Arnaoutakis GJ, Patel ND, Russell SD, et al. Infectious complications after pulsatile-flow and continuous-flow left ventricular assist device implantation. J Heart Lung Transplant 2011;30:164-74.

126. Deng MC, Erren M, Tjan TD, Tamminga N, Werntze B, Zimmermann P, et al. Left ventricular assist system support is associated with persistent inflammation and temporary immunosuppression. Thorac Cardiovasc Surg 1999;47 Suppl 2:326-31.

127. Klotz S, Vahlhaus C, Riehl C, Reitz C, Sindermann JR, Scheld HH. Pre-operative prediction of post-VAD implant mortality using easily accessible clinical parameters. J Heart Lung Transplant 2010;29:45-52.

128. Donnenberg VS, Donnenberg AD. Identification, rare-event detection and analysis of dendritic cell subsets in broncho-alveolar lavage fluid and peripheral blood by flow cytometry. Front Biosci 2003;8:s1175-80.

129. Holman WL, Kirklin JK, Naftel DC, Kormos RL, Desvign-Nickens P, Camacho MT, et al. Infection after implantation of pulsatile mechanical circulatory support devices. J Thorac Cardiovasc Surg 2010;139:1632-1636 e2.

130. Holman WL, Pamboukian SV, McGiffin DC, Tallaj JA, Cadeiras M, Kirklin JK. Device related infections: are we making progress? J Card Surg 2010;25:478-83.

131. Gordon RJ, Weinberg AD, Pagani FD, Slaughter MS, Pappas PS, Naka Y, et al. Prospective, multicenter study of ventricular assist device infections. Circulation 2013;127:691-702.

132. Galinanes M, Watson C, Trivedi U, Chambers DJ, Young CP, Venn GE. Differential patterns of neutrophil adhesion molecules during cardiopulmonary bypass in humans. Circulation 1996;94:II364-9.

133. Takala A, Jousela I, Jansson SE, Olkkola KT, Takkunen O, Orpana A, et al. Markers of systemic inflammation predicting organ failure in community-acquired septic shock. Clin Sci (Lond) 1999;97:529-38.

134. Rinder CS, Fontes M, Mathew JP, Rinder HM, Smith BR. Neutrophil CD11b upregulation during cardiopulmonary bypass is associated with postoperative renal injury. Ann Thorac Surg 2003;75:899-905.

135. Yamazaki S, Inamori S, Nakatani T, Suga M. Activated protein C attenuates cardiopulmonary bypass-induced acute lung injury through the regulation of neutrophil activation. J Thorac Cardiovasc Surg 2011;141:1246-52.

136. Diehl P, Aleker M, Helbing T, Sossong V, Beyersdorf F, Olschewski M, et al. Enhanced microparticles in ventricular assist device patients predict platelet, leukocyte and endothelial cell activation. Interact Cardiovasc Thorac Surg 2010;11:133-7.

137. Loebe M, Koster A, Sanger S, Potapov EV, Kuppe H, Noon GP, et al. Inflammatory response after implantation of a left ventricular assist device: comparison between the axial flow MicroMed DeBakey VAD and the pulsatile Novacor device. Asaio J 2001;47:272-4.

138. Asimakopoulos G, Taylor KM. Effects of cardiopulmonary bypass on leukocyte and endothelial adhesion molecules. Ann Thorac Surg 1998;66:2135-44.

139.   Takala AJ, Jousela IT, Takkunen OS, Jansson SE, Kyosola KT, Olkkola KT, et al. Time course of beta 2-integrin CD11b/CD18 (Mac-1, alpha M beta 2) upregulation on neutrophils and monocytes after coronary artery bypass grafting. CD11b upregulation after CABG surgery. Scand J Thorac Cardiovasc Surg 1996;30:141-8.

140.   Walzog B, Jeblonski F, Zakrzewicz A, Gaehtgens P. Beta2 integrins (CD11/CD18) promote apoptosis of human neutrophils. FASEB J 1997;11:1177-86.

141.   Nagpal AD, Larsen BK, Smedira NG, Soltesz EG. Endoscopic tunneling of HeartMate II left ventricular assist device driveline. J Thorac Cardiovasc Surg 2013;145:297-8.

142.   Schaffer JM, Arnaoutakis GJ, Allen JG, Weiss ES, Patel ND, Russell SD, et al. Bleeding complications and blood product utilization with left ventricular assist device implantation. Ann Thorac Surg 2011;91:740-7; discussion 747-9.

143.   Matthews JC, Pagani FD, Haft JW, Koelling TM, Naftel DC, Aaronson KD. Model for end-stage liver disease score predicts left ventricular assist device operative transfusion requirements, morbidity, and mortality. Circulation 2010;121:214-20.

144.   Bonde P, Ku NC, Genovese EA, Bermudez CA, Bhama JK, Ciarleglio MM, et al. Model for end-stage liver disease score predicts adverse events related to ventricular assist device therapy. Ann Thorac Surg 2012;93:1541-7; discussion 1547-8.

145.   Deo SV, Daly RC, Altarabsheh SE, Hasin T, Zhao Y, Shah IK, et al. Predictive value of the model for end-stage liver disease score in patients undergoing left ventricular assist device implantation. ASAIO J 2012;59:57-62.

146.   Yang JA, Kato TS, Shulman BP, Takayama H, Farr M, Jorde UP, et al. Liver dysfunction as a predictor of outcomes in patients with advanced heart failure requiring ventricular assist device support: Use of the Model of End-stage Liver Disease (MELD) and MELD eXcluding INR (MELD-XI) scoring system. J Heart Lung Transplant 2012;31:601-10.

147.   Snyder TA, Watach MJ, Litwak KN, Wagner WR. Platelet activation, aggregation, and life span in calves implanted with axial flow ventricular assist devices. Ann Thorac Surg 2002;73:1933-8.

148.   Johnson CA, Jr., Snyder TA, Woolley JR, Wagner WR. Flow cytometric assays for quantifying activated ovine platelets. Artif Organs 2008;32:136-45.

149.   Malinchoc M, Kamath PS, Gordon FD, Peine CJ, Rank J, ter Borg PC. A model to predict poor survival in patients undergoing transjugular intrahepatic portosystemic shunts. Hepatology 2000;31:864-71.

150.   Kamath PS, Wiesner RH, Malinchoc M, Kremers W, Therneau TM, Kosberg CL, et al. A model to predict survival in patients with end-stage liver disease. Hepatology 2001;33:464-70.

151.   Teh SH, Nagorney DM, Stevens SR, Offord KP, Therneau TM, Plevak DJ, et al. Risk factors for mortality after surgery in patients with cirrhosis. Gastroenterology 2007;132:1261-9.

152.   Northup PG, Wanamaker RC, Lee VD, Adams RB, Berg CL. Model for End-Stage Liver Disease (MELD) predicts nontransplant surgical mortality in patients with cirrhosis. Ann Surg 2005;242:244-51.

153.   Chokshi A, Cheema FH, Schaefle KJ, Jiang J, Collado E, Shahzad K, et al. Hepatic dysfunction and survival after orthotopic heart transplantation: application of the MELD scoring system for outcome prediction. J Heart Lung Transplant 2012;31:591-600.

154.   Northup PG, Sundaram V, Fallon MB, Reddy KR, Balogun RA, Sanyal AJ, et al. Hypercoagulation and thrombophilia in liver disease. J Thromb Haemost 2008;6:2-9.

155.   Solomon C, Hagl C, Rahe-Meyer N. Time course of haemostatic effects of fibrinogen concentrate administration in aortic surgery. Br J Anaesth 2013;110:947-56.

156.   John R, Panch S, Hrabe J, Wei P, Solovey A, Joyce L, et al. Activation of endothelial and coagulation systems in left ventricular assist device recipients. Ann Thorac Surg 2009;88:1171-9.

157.   Aaronson KD, Slaughter MS, Miller LW, McGee EC, Cotts WG, Acker MA, et al. Use of an intrapericardial, continuous-flow, centrifugal pump in patients awaiting heart transplantation. Circulation 2012;125:3191-200.

158.   Li S, Henry JJ. Nonthrombogenic approaches to cardiovascular bioengineering. Annu Rev Biomed Eng 2011;13:451-75.

159.   Deible CR, Beckman EJ, Russell AJ, Wagner WR. Creating molecular barriers to acute platelet deposition on damaged arteries with reactive polyethylene glycol. J Biomed Mater Res 1998;41:251-6.

160.   Eberhart RC, Munro MS, Frautschi JR, Lubin M, Clubb FJ, Jr., Miller CW, et al. Influence of endogenous albumin binding on blood-material interactions. Ann N Y Acad Sci 1987;516:78-95.

161.   Lin PH, Chen C, Bush RL, Yao Q, Lumsden AB, Hanson SR. Small-caliber heparin-coated ePTFE grafts reduce platelet deposition and neointimal hyperplasia in a baboon model. J Vasc Surg 2004;39:1322-8.

162.   Riedel N, Smith B, Williams J, Popat K. Improved thrombogenicity on oxygen etched Ti6Al4V surfaces. Mater Sci Engr: C 2012;32:1196-203.

163. Walkowiak-Przybylo M, Klimek L, Okroj W, Jakubowski W, Chwilka M, Czajka A, et al. Adhesion, activation, and aggregation of blood platelets and biofilm formation on the surfaces of titanium alloys Ti6Al4V and Ti6Al7Nb. J Biomed Mater Res A 2012;100:768-75.

164. Schwoch G, Passow H. Preparation and properties of human erythrocyte ghosts. Mol Cell Biochem 1973;2:197-218.

165. Aarts PA, van den Broek SA, Prins GW, Kuiken GD, Sixma JJ, Heethaar RM. Blood platelets are concentrated near the wall and red blood cells, in the center in flowing blood. Arteriosclerosis 1988;8:819-24.

166. Goldsmith HL, Bell DN, Braovac S, Steinberg A, McIntosh F. Physical and chemical effects of red cells in the shear-induced aggregation of human platelets. Biophys J 1995;69:1584-95.

167. Bozzo J, Tonda R, Hernandez MR, Alemany M, Galan AM, Ordinas A, et al. Comparison of the effects of human erythrocyte ghosts and intact erythrocytes on platelet interactions with subendothelium in flowing blood. Biorheology 2001;38:429-37.

168. Johnson CA, Jr., Vandenberghe S, Daly AR, Woolley JR, Snyder ST, Verkaik JE, et al. Biocompatibility assessment of the first generation PediaFlow pediatric ventricular assist device. Artif Organs 2011;35:9-21.

169. Kent NJ, Basabe-Desmonts L, Meade G, MacCraith BD, Corcoran BG, Kenny D, et al. Microfluidic device to study arterial shear-mediated platelet-surface interactions in whole blood: reduced sample volumes and well-characterised protein surfaces. Biomed Microdevices 2010;12:987-1000.

170. Godo MN, Sefton MV. Characterization of transient platelet contacts on a polyvinyl alcohol hydrogel by video microscopy. Biomaterials 1999;20:1117-26.

171. Deible CR, Petrosko P, Johnson PC, Beckman EJ, Russell AJ, Wagner WR. Molecular barriers to biomaterial thrombosis by modification of surface proteins with polyethylene glycol. Biomaterials 1999;20:101-9.

172. Lei L, Li C, Yang P, Huang N. Photo-immobilized heparin micropatterns on Ti–O surface: preparation, characterization, and evaluation in vitro. J Mater Sci 2011;46:6772-82.

173. Otto M, Franzen A, Hansen T, Kirkpatrick CJ. Modification of human platelet adhesion on biomaterial surfaces by protein preadsorption under static and flow conditions. J Mater Sci Mater Med 2004;15:35-42.

174. Tokarev AA, Butylin AA, Ataullakhanov FI. Platelet adhesion from shear blood flow is controlled by near-wall rebounding collisions with erythrocytes. Biophys J 2011;100:799-808.

175. Mody NA, King MR. Platelet adhesive dynamics. Part I: characterization of platelet hydrodynamic collisions and wall effects. Biophys J 2008;95:2539-55.

176. Mody NA, King MR. Platelet adhesive dynamics. Part II: high shear-induced transient aggregation via GPIbalpha-vWF-GPIbalpha bridging. Biophys J 2008;95:2556-74.

177. Goldsmith HL, Spain S. Margination of leukocytes in blood flow through small tubes. Microvasc Res 1984;27:204-22.

178. Xu C, Wootton DM. Platelet near-wall excess in porcine whole blood in artery-sized tubes under steady and pulsatile flow conditions. Biorheology 2004;41:113-25.

179. Kim S, Ong PK, Yalcin O, Intaglietta M, Johnson PC. The cell-free layer in microvascular blood flow. Biorheology 2009;46:181-9.

180. Sherwood JM, Dusting J, Kaliviotis E, Balabani S. The effect of red blood cell aggregation on velocity and cell-depleted layer characteristics of blood in a bifurcating microchannel. Biomicrofluidics 2012;6:24119.

181. Chung BJ, Robertson AM, Peters DG. The numerical design of a parallel plate flow chamber for investigation of endothelial cell response to shear stress. Computers & Structures 2003;81:535-546.

182. Roald HE, Barstad RM, Bakken IJ, Roald B, Lyberg T, Sakariassen KS. Initial interactions of platelets and plasma proteins in flowing non-anticoagulated human blood with the artificial surfaces Dacron and PTFE. Blood Coagul Fibrinolysis 1994;5:355-63.

183. Chen C, Ofenloch JC, Yianni YP, Hanson SR, Lumsden AB. Phosphorylcholine coating of ePTFE reduces platelet deposition and neointimal hyperplasia in arteriovenous grafts. J Surg Res 1998;77:119-25.

184. Anderson GH, Hellums JD, Moake J, Alfrey CP, Jr. Platelet response to shear stress: changes in serotonin uptake, serotonin release, and ADP induced aggregation. Thromb Res 1978;13:1039-47.

185. Milner KR, Snyder AJ, Siedlecki CA. Sub-micron texturing for reducing platelet adhesion to polyurethane biomaterials. J Biomed Mater Res A 2006;76:561-70.

186. Wang IW, Anderson JM, Marchant RE. Staphylococcus epidermidis adhesion to hydrophobic biomedical polymer is mediated by platelets. J Infect Dis 1993;167:329-36.

187. Varon D, Dardik R, Shenkman B, Kotev-Emeth S, Farzame N, Tamarin I, et al. A new method for quantitative analysis of whole blood platelet interaction with extracellular matrix under flow conditions. Thromb Res 1997;85:283-94.

188. Spectre G, Brill A, Gural A, Shenkman B, Touretsky N, Mosseri E, et al. A new point-of-care method for monitoring anti-platelet therapy: application of the cone and plate(let) analyzer. Platelets 2005;16:293-9.

189. Szarvas M, Oparaugo P, Udvardy ML, Toth J, Szanto T, Daroczi L, et al. Differential platelet deposition onto collagen in cone-and-plate and parallel plate flow chambers. Platelets 2006;17:185-90.

190. Zwaginga JJ, Sakariassen KS, Nash G, King MR, Heemskerk JW, Frojmovic M, et al. Flow-based assays for global assessment of hemostasis. Part 2: current methods and considerations for the future. J Thromb Haemost 2006;4:2716-7.

191. Woolley JR, Teuteberg JJ, Bermudez CA, Bhama JK, Lockard KL, Kormos R, et al. Temporal leukocyte numbers and granulocyte activation in pulsatile and rotary ventricular assist device patients. Artif Organs 2013;in press.

192. Shive MS, Hasan SM, Anderson JM. Shear stress effects on bacterial adhesion, leukocyte adhesion, and leukocyte oxidative capacity on a polyetherurethane. J Biomed Mater Res 1999;46:511-9.

193. Pavelkova M, Kubala L, Ciz M, Pavlik P, Wagner R, Slavik J, et al. Blood phagocyte activation during open heart surgery with cardiopulmonary bypass. Physiol Res 2006;55:165-73.

194. Chan CH, Hilton A, Foster G, Hawkins KM, Badiei N, Thornton CA. The evaluation of leukocytes in response to the in vitro testing of ventricular assist devices. Artif Organs 2013;37:793-801.

195. Morel O, Toti F, Hugel B, Bakouboula B, Camoin-Jau L, Dignat-George F, et al. Procoagulant microparticles: disrupting the vascular homeostasis equation? Arterioscler Thromb Vasc Biol 2006;26:2594-604.

196. Polgar J, Matuskova J, Wagner DD. The P-selectin, tissue factor, coagulation triad. J Thromb Haemost 2005;3:1590-6.

197. Nauman EA, Risic KJ, Keaveny TM, Satcher RL. Quantitative assessment of steady and pulsatile flow fields in a parallel plate flow chamber. Ann Biomed Eng 1999;27:194-9.

198. Ye SH, Johnson CA, Jr., Woolley JR, Snyder TA, Gamble LJ, Wagner WR. Covalent surface modification of a titanium alloy with a phosphorylcholine-containing copolymer for reduced thrombogenicity in cardiovascular devices. J Biomed Mater Res A 2009;91:18-28.